INFORMATION TO USERS

This manuscript has been reproduced from the microfilm master. UMI films the text directly from the original or copy submitted. Thus, some thesis and dissertation copies are in typewriter face, while others may be from any type of computer printer.

The quality of this reproduction is dependent upon the quality of the copy submitted. Broken or indistinct print, colored or poor quality illustrations and photographs, print bleedthrough, substandard margins, and improper alignment can adversely affect reproduction.

In the unlikely event that the author did not send UMI a complete manuscript and there are missing pages, these will be noted. Also, if unauthorized copyright material had to be removed, a note will indicate the deletion.

Oversize materials (e.g., maps, drawings, charts) are reproduced by sectioning the original, beginning at the upper left-hand corner and continuing from left to right in equal sections with small overlaps.

Photographs included in the original manuscript have been reproduced xerographically in this copy. Higher quality 6" x 9" black and white photographic prints are available for any photographs or illustrations appearing in this copy for an additional charge. Contact UMI directly to order.

Bell & Howell Information and Learning
300 North Zeeb Road, Ann Arbor, MI 48106-1346 USA

UMI®
800-521-0600

Mapping the Substrate for Brain Stimulation Reward: New Approaches to an Old Problem

Andreas Arvanitogiannis

A Thesis

in

The Department

of

Psychology

Presented in Partial Fulfillment of the Requirements
for the Degree of Doctor of Philosophy at
Concordia University
Montréal, Québec, Canada

November 1997

National Library of Canada
Acquisitions and Bibliographic Services
395 Wellington Street
Ottawa ON K1A 0N4
Canada

Bibliothèque nationale du Canada
Acquisitions et services bibliographiques
395, rue Wellington
Ottawa ON K1A 0N4
Canada

Your file Votre référence

Our file Notre référence

0-612-40304-1

Canada

ABSTRACT

Mapping the Substrate for Brain Stimulation Reward:
New Approaches to an Old Problem

Andreas Arvanitogiannis, Ph.D.
Concordia University, 1998

A major goal for research on brain stimulation reward (BSR) is the identification of the directly-activated ("first-stage") neurons subserving the powerfully rewarding effect produced by electrical stimulation of the medial forebrain bundle (MFB). This objective was addressed by combining immunohistochemical, lesion, and behavioral methods. Immunohistochemical staining of the immediate early gene product, Fos, was used to visualize neurons activated by rewarding stimulation of the lateral hypothalamic (LH) level of the MFB. Production of Fos protein was increased ipsilateral to the stimulation electrode in subjects that had previously self-stimulated. Among the caudal diencephalic, midbrain and hindbrain structures with pronounced increases in Fos-like immunoreactivity ipsilateral to the site of stimulation were the arcuate nucleus, ventral tegmental area (VTA), central gray, pedunculopontine area (PPTg), parabrachial nucleus, and locus coeruleus. Among the forebrain structures showing a greater density of labeled neurons ipsilateral to the stimulating electrode were the septum, bed nucleus of the stria terminalis (BST), medial preoptic area (MPO), substantia innominata (SI), lateral preoptic area (LPO), and LH. Several of these structures, the VTA, PPTg, LPO, SI, and LH, have

been implicated in MFB self-stimulation by the results of pharmacological, psychophysical, electrophysiological, and lesion studies. To complement previous lesion studies implicating the LPO, SI, and LH in BSR, changes in self-stimulation of the LH and VTA were assessed following excitotoxic lesions of more medial structures, including the MPO and BST. Damage centered in the MPO had little or no effect on the rewarding efficacy of more caudal stimulation. Thus, neurons with cell bodies in the medial portion of the basal forebrain may make a smaller contribution to the rewarding effect of MFB stimulation than neurons in the lateral portion. To further probe the role that basal forebrain neurons play in self-stimulation I describe and test an extension of the matching law to relate behavioral performance to the intensity and rate of reinforcement. Analyzing performance in this three-dimensional space provides a means of distinguishing lesion-induced changes that are due to damage in the first-stage neurons and/or their efferents from changes that result from damage in neurons that modulate the rewarding effect of the stimulation.

ACKNOWLEDGMENTS

It has been a privilege to do graduate work at the Center for Studies in Behavioral Neurobiology. During the years of research that culminated in this thesis, I have enjoyed the counsel and support of a number of outstanding individuals. To Peter Shizgal, my thesis advisor, I am especially indebted for giving me generously of his time and knowledge. With his enthusiasm for scholarly work and his considerable skills as a scientist and writer, he has provided a model for my own aspirations and has raised my own standards in many ways. Best of all, perhaps, he set an example of how to combine the experimental and theoretical analysis of core problems in behavioral neuroscience. My writing reflects his influence and ideas which I have assimilated over the years. I also owe an enormous debt to Jane Stewart for having exposed me to the varied fascinations of psychological theory and research and for giving me ample encouragement and advice. Through her effectiveness at conveying the richness of behavioral and neurobiological approaches to psychology, she broadened and deepened my perspective in all dimensions. To Barbara Woodside I owe a debt of thanks for a careful reading of the thesis and for much useful criticism, and advice. She provided essential help and support throughout the preparation of this thesis. Shimon Amir, Zalman Amit, Kent Conover, Jim Pfaus, and Roy Wise gave me ideas, advice, and invaluable conversation. Shimmy, in particular, has been an unfailing source of inspiration and positive reinforcement. To the members

of the Shizgal lab (Kent Conover, Stephanie Fulton, Peter Marinelli, Keiji Oda, Luigi Riscaldino) go my thanks for the provision of an atmosphere conductive to bringing this work to fruition. Luigi assisted me in a competent and cheerful manner with some of the experiments reported in this thesis. Bill Mundl designed the hardware and Steve Cabilio the software used to run the experiments described in Chapter 4 and I am grateful to them for all the time and trouble they have taken. My thanks also go to many fellow students who provided humor and perspective when they were needed. Finally, my greatest debt is to Cecilia Flores, whose extensive personal and intellectual contributions defy adequate description and whose constant support, encouragement and indulgence made everything not only possible but also worthwhile. She has stimulated and inspired me in all my endeavors and continues to do so every day.

I am grateful for financial support from Concordia University, the "Fonds pour la Formation de Chercheurs at l'Aide à la Recherche" (FCAR), and the Hellenic Scholarships Foundation.

DEDICATION

This thesis is dedicated to my father Spiros, my mother Yianna, and my brother Alexis for supporting me in innumerable ways through an extended career as a student. Without their love and generosity this thesis would still be a dream.

TABLE OF CONTENTS

LIST OF FIGURES

LIST OF TABLES

INTRODUCTION

As an earthquake in physiological psychology, the discovery that electrical stimulation of certain brain regions is powerfully rewarding and is self-administered vigorously by laboratory rats measured right at the top of the Richter scale (Olds & Milner, 1954). The shocks rippled through the popular press that reported on this discovery with hype and hyperbole. "It may prove the key to human behavior," trumpeted *The Montreal Star* (Macfarlane, 1954). By virtue of the slippery slope, reports went as far as to even fuel fears that brain stimulation reward (BSR) could be used as an agent for social control (Valenstein, 1973). Much of this is amusing, at least in retrospect, but is also understandable. Indeed, no matter how often one has witnessed the phenomenon of BSR, it is impossible not to retain a sense of amazement that electrical stimulation can produce so immediate and so profound an effect. A rat will press a lever for it, to the point of starvation or exhaustion, and will cross a shock grid to get it (Frank & Stutz, 1984; Olds, 1958; Routtenberg & Lindy, 1965). It appears that the stimulation electrode injects a meaningful signal into the neural circuitry mediating goal-directed behavior, a signal that can act as a highly attractive goal object.

In time the aftershocks subsided and the dust settled but BSR did not lose its luster. BSR has become a model system for the study of goal-directed

behavior and how the brain generates it. To understand why this is so, consider, first, that electrical stimulation is easily controlled. The parameters of the stimulation translate directly into neurophysiologically meaningful variables. For example, the pulse frequency determines how many times each axon within the radius of effective excitation fires, while the current determines the radius of effective excitation. Consider, now, the task of linking BSR to the activity of identified neurons. The first step towards accomplishing this task is to identify the neural elements in the immediate vicinity of the electrode tip whose direct activation gives rise to the rewarding effect of the stimulation. This effect has been related to the rewarding effects of naturally-occurring goal objects (Hoebel, 1969; Shizgal & Conover, 1996) as well as to the rewarding effects of dependence-inducing drugs (Wise, 1996). Thus, identifying the neural substrate for BSR is likely to advance our understanding of the neural mechanisms involved in adaptive goal selection and the undermining of adaptive choice by dependence-inducing drugs.

The initial strategy employed to investigate the BSR system was to map the brain sites that support self-stimulation. Stimulation of numerous regions evokes BSR (Olds & Olds, 1963). Of these stimulation of the medial forebrain bundle (MFB) is particularly effective and an easy site at which to shape self-stimulation behavior. Accordingly, finding the directly-stimulated stage ("first-stage") of MFB self-stimulation has been the focus of intensive research. For decades, psychophysical techniques have been used to define quantitative characteristics of the first-stage neurons (Gallistel, Shizgal, &

Yeomans, 1981; Shizgal & Murray, 1989; Yeomans, 1988). The success of the psychophysical approach in sketching a portrait of the neurons in question is beyond dispute. Still, the precise identity of the first stage substrate for MFB self-stimulation continues to challenge and frustrate those who seek to answer it. Simply posed, the question is: What is the location, morphology, and neurochemistry of the first stage neurons?

Sophisticated anatomical techniques and behavioral ideas are now emerging, which define the directions for future research in answering this question. The time may be ripe, therefore, to complement current approaches with new concepts and tools. It is in this spirit that the experiments presented in this thesis were undertaken. I will present a combination of new and promising lines of experimentation geared toward localizing the somata of the directly-stimulated neurons subserving BSR.

For the sake of clarity, this thesis is organized into four chapters. Chapter 1 contains an overview of BSR fundamentals that set the stage for the experiments described hereinafter. In chapter 2, I introduce data from studies conducted to assess the expression of the immediate early gene, *c-fos*, to visualize neurons activated by rewarding stimulation. In chapter 3, I show by means of excitotoxic lesions that neurons residing in the medial portion of the basal forebrain, in contrast to those in the lateral portion, are probably not major contributors to the rewarding effect of MFB stimulation. Chapter 4 describes a new method for testing lesion effects. This method has the

potential to disambiguate the interpretation of lesion experiments by revealing the stage of BSR processing affected by the lesions. Key experiments to validate the new method are also presented.

CHAPTER 1

BSR FUNDAMENTALS

Researchers face a daunting challenge when searching for the directly-stimulated neurons that subserve BSR. The MFB is a heterogeneous structure comprising at least 50 discrete ascending and descending fiber systems (Nieuwenhuys, Geeraedts, & Veening, 1982). Thus, a stimulation electrode aimed at the MFB activates a number of fibers varying in caliber, origin, and termination, only a subset of which are actually responsible for self-stimulation. A number of approaches have been used to distinguish reward-related from other stimulated neurons. In the first part of this chapter, I will briefly describe these approaches and survey some key findings regarding the characterization of the BSR substrate. Such characterization would not be complete without an understanding of the nature of the electrically evoked signal carried by the first-stage neurons. In the final section of this chapter I will consider data that are richly suggestive about the function of the directly stimulated substrate for BSR.

1.1. MAPPING OF THE SUBSTRATE UNDERLYING BSR

1.1.1. The Psychophysical Approach

1.1.1.1. Portrait of the First Stage Substrate for BSR

The electrophysiological and anatomical characteristics of the neurons responsible for the rewarding effect of the stimulation can be inferred from psychophysically derived trade-off functions; functions that describe the relationship between two stimulus parameters producing the same level of behavior.

The refractory periods and conduction velocities of the first stage neurons are inferred from the results of double (C-T) pulse experiments, in which the number of pulse pairs required for criterial behavior is traded-off against the intrapair intervals (Yeomans, 1975; Yeomans, 1979). To infer refractory periods, both the C (conditioning) and the T (test) pulses are delivered through the same electrode. The C pulse evokes an action potential in a population of axons around the electrode. If the T pulse is delivered while the axons are still refractory from the C pulse, then the T pulse does not evoke an action potential. The T pulse evokes an action potential only when the C-T interval is longer than the refractory periods of the stimulated axons. The ability of the T pulse to elicit a second action potential can be inferred behaviorally by determining the number of pulse pairs required for criterial behavior at various C-T intervals.

Conduction velocity and axonal trajectory is inferred from the behavioral adaptation of the collision technique which consists of delivering the two pulses through separate electrodes implanted at sites supporting self-stimulation (Bielajew & Shizgal, 1982; Shizgal, Bielajew, Corbett, Skelton, & Yeomans, 1980; Shizgal & Murray, 1994). In this case, both the C and T pulses evoke action potentials traveling toward (antidromic) and away (orthodromic) from the cell body. In the axons stimulated by both electrodes, at short C-T intervals the orthodromic and antidromic potentials evoked from the pulse pair meet and cancel each other. Thus, at short C-T intervals only one of the orthodromic potentials contributes to the behavioral output. However, if the C-T interval is sufficiently long, the orthodromic potentials evoked from both the C and the T pulse contribute to the rewarding effect. By trading-off the number of pulse pairs required for criterial behavior against the C-T interval one can determine the 'collision interval', that is, the range of C-T intervals over which stimulation effectiveness increases. The collision interval is equal to the sum of the refractory period and the conduction time between electrodes. The conduction velocity of the axons can be estimated by the interelectrode distance divided by the conduction time between electrodes where conduction time is simply the collision interval less the refractory period (the assumption here is that the two stimulation sites are connected via a straight axonal path). Conduction velocity estimates provide additional clues about axonal caliber and degree of myelination.

The results from double pulse experiments imply that the directly stimulated MFB substrate includes fine, myelinated fibers coursing through the lateral hypothalamus (LH) and the ventral tegmental area (VTA) (Bielajew & Shizgal, 1982; Murray & Shizgal, 1996b; Shizgal et al., 1980). Moreover, Bielajew & Shizgal (1986) used a variation of the collision technique (one of the electrodes served as an anode to produce hyperpolarization block) to show that in at least some of the directly activated fibers subserving MFB reward, the behaviorally relevant direction of conduction is rostro-caudal. The logic behind this experiment is as follows. The anodal block creates a hyperpolarized region along the MFB that should only be able to block the conduction of a reward-relevant signal when it occurs downstream from the site of stimulation. Thus, direction could be inferred by noting which of two electrodes along the anterior-posterior axis of the MFB is more effective at reducing stimulation effectiveness when used as the anode. Anodal block was more effective when the electrode placed in the posterior MFB (the VTA) was used as the anode.

Given what is known about MFB anatomy, the direction experiment suggests that basal forebrain structures are likely sources of the descending reward-relevant axons. The idea that first stage neurons originate in the basal forebrain and give rise to axons that descend through the MFB toward the tegmentum has come to be called the 'descending path' hypothesis of MFB self-stimulation.

1.1.1.2. Portrait of the Reward Integrator

Some of the rules governing postsynaptic integration of the signals carried by the first stage neurons have also been inferred psychophysically. The spatio-temporal integration process has been characterized by trading off pulse frequency, a temporal variable pertaining to the number of times a neuron fires, and current, a spatial variable pertaining to the number of neurons fired by the stimulation (Gallistel, 1978; Gallistel et al., 1981). It has been shown that the stimulating current and the pulse frequency required to produce a criterion level of behavior are reciprocally related. Empirically, when one plots the required pulse frequency against the current on double-logarithmic coordinates, one gets a straight line. This indicates that the number of action potentials fired by the first stage neurons determines the rewarding effect of the stimulation, regardless of the spatio-temporal distribution of impulses within a time window of fixed duration. With a fixed duration of stimulation, the rewarding effect is determined solely by the total number of firings in the population of first stage axons. The neurons that perform the integration process (the "integrator") appear simply to count spikes. This model of spatio-temporal integration has been dubbed "the counter model" (Gallistel, 1978; Gallistel et al., 1981). To illustrate, according to the counter model the rewarding effect produced by, say, firing 100 fibers 200 times is the same as that produced by firing 200 fibers 100 times. If the stimulation electrode had an infinitely small tip and was located within a homogeneous bundle of reward fibers, the counter model could be reduced to

two assumptions. First, the number of stimulated axons would be proportionate to the current and second, the number of action potentials carried by the first stage neurons would be the product of the number of axons fired by the stimulation and the number of pulses in the stimulus train.

An important feature of the temporal integration process emerges from varying the time window within which pulses are delivered (i.e. train duration) and measuring the effect of this manipulation by adjusting the number of pulses in the train so as to maintain a constant level of responding. Presumably, manipulations of train duration can affect the postsynaptic integration of firings by producing different degrees of temporal summation. High temporal summation is produced when a set number of pulses is delivered in a short burst rather than in a long one, because excitatory post-synaptic potentials decay with time. It has been shown in the case of BSR that a long train of widely spaced pulses is less effective than a short train of an equal number of closely spaced pulses (Gallistel, 1978; Shizgal & Matthews, 1977). Thus, temporal integration in BSR is said to be leaky (i.e. works like a leaky bucket). Furthermore, when the train duration is increased progressively, integrator output appears to rise during the first 1-2 s and then to reach asymptote. Thus, a train of stimulation 1-2 s in duration is as rewarding as a much longer train.

1.1.1.3. The function relating integrator input to integrator output

The experiments described thus far were aimed at describing quantitative properties, both of the neurons that transduce the neural activity generated by the stimulation electrode and of the process that integrates in space and time this neural activity. In these experiments, the parameters determining the input to the integrator are systematically varied while the integrator's output is held constant. But, because output is held constant, this strategy cannot provide an answer as to the nature of the transformation that relates the integrator's input to its output. This is an important question because the output of the integration process determines the rewarding effect of the stimulation. Put another way, the question still to be answered is: How does the rewarding effect of the stimulation grow as a function of the firing of the directly activated neurons?

Gallistel & Leon's (1991) answer to this question is that, over a limited domain, the growth function for rewarding MFB stimulation is approximated by a power function with an exponent ranging roughly from 2 to 10. As the firing count at the input to the integrator increases, the integrator output rises initially as a power function till it saturates. What requires emphasis, is that small increases in pulse frequency or current result in disproportionate, often enormous, increases in experienced reward. For example, with an exponent of 10, a doubling in frequency would produce a 1024-fold (2^{10}) increase in reward.

This finding stems from an experiment involving a two lever choice paradigm with independent, concurrent variable interval schedules of reward. According to the matching law relative time allocation is proportional to the relative payoff provided by the two levers, as estimated by the product of the rate of reinforcement and the magnitude of the BSR corresponding to each lever. Thus, $\frac{TA_1}{TA_2} = \frac{M_1}{M_2} \times \frac{R_1}{R_2}$, where TA is time allocation, M is reward magnitude, and R is rate of reinforcement. When time allocation is the same at both levers this equation is reduced to: $\frac{M_1}{M_2} = \frac{R_2}{R_1}$, meaning that at equipreference a given change in the reward magnitude received on one lever is compensated by the same change in the rate at which the rewards are received on the other lever. Thus, the function relating the reward magnitude received on a lever to the strength of the stimulation can be determined at equipreference by trading-off reward magnitude (determined by the strength of the stimulation) against the relative rate of reward.

In Gallistel & Leon's (1991) experiment, rats could allot their time to one of two levers: one that delivered a constant value of brain stimulation at different rates of occurrence (the standard lever) and another that delivered a variable value of brain stimulation at a constant rate (the alternate lever). The experimenters determined the adjustment in the parameters of stimulation (either pulse frequency or current) for the alternate reward required to offset the difference in the rates at which the two rewards were received, so that rats

alloted their time equally between the two levers. The logarithms of the pulse frequencies or current intensities required to produce equal preference were plotted against the logarithm of the rate of the competing (standard) reward. These double logarithmic plots were linear. A linear relation between variables in the logarithmic domain corresponds to a power function relation in the normal domain. Interpreted within the context of the matching law, this finding indicates that the function relating experienced reward to the strength of the stimulation is a power function (over a limited range of stimulation strength).

This conclusion is supported by subsequent experiments based on matching (Mark & Gallistel, 1993; Simmons & Gallistel, 1994). Moreover, these experiments have confirmed the counter model of spatiotemporal integration and the fact that temporal integration saturates with train durations up to 2 s (Mark & Gallistel, 1993).

1.1.2. The Electrophysiological Approach

By means of single-unit recording it is possible to determine whether neurons in a particular region are antidromically activated during rewarding stimulation, and if so, whether the characteristics of their fibers match those derived from psychophysical experiments. Unit recordings from basal forebrain areas have provided support for the descending path hypothesis. Electrophysiological experiments have identified "candidate" cells in the basal forebrain, cells that are antidromically activated by rewarding MFB

stimulation and that exhibit properties matching those derived psychophysically (Murray & Shizgal, 1996c; Rompré & Shizgal, 1986). In a skillfully executed experiment (Shizgal, Schindler, & Rompré, 1989), psychophysical and electrophysiological data were collected using the same subjects, thus ensuring that rewarding stimulation activated the same neurons in both the psychophysical and electrophysiological phases of the experiment.

In hindsight, the usefulness of the electrophysiological approach when used in isolation to identify the first stage neurons is rather limited. For example, in the study by Rompré & Shizgal (1986) about one third of antidromically activated cells, a rather high proportion, had properties according to which they could be classified as candidates for the first stage substrate. Nevertheless, the comparison between the electrophysiological and psychophysical measures serves to sharpen the distinction between the neurons most likely to form part of the directly-stimulated substrate for MFB self-stimulation and poorer candidates. If a neurons is to be considered a candidate for the first stage, then estimates of its electrophysiological characteristics should overlap with the psychophysically-derived estimates.

1.1.3. The Lesioning Approach

Psychophysical data can be used to sketch a portrait of the first stage neurons. Single-unit recording experiments can be used to identify "candidate" cells in the basal forebrain, cells that are antidromically activated

by rewarding MFB stimulation and that exhibit properties matching those derived psychophysically. However, the characteristics of candidate neurons identified by these methods are not necessarily unique to those that carry the reward signal. Lesion experiments are invaluable in establishing which candidate neurons compose part of the reward substrate and which merely resemble the reward-related neurons. A decrease in the magnitude of the rewarding effect following damage to a nucleus containing candidate cells provides evidence needed to link neural elements in the damaged region to the rewarding effect.

Crucial to the proper interpretation of lesion experiments is the dissociation between effects of lesions that alter the rewarding impact of the stimulation and effects that alter the capacity of the subject to perform the rewarded response. Experiments relying on the curve-shift paradigm largely achieve such a dissociation (Edmonds & Gallistel, 1974; Miliaressis, Rompré, Laviolette, Philippe, & Coulombe, 1986; Stellar, Waraczynski, & Wong, 1988). When using this paradigm, a series of stimulation frequencies is tested spanning a range sufficient to drive response rates from minimal to maximal values. Lateral shifts in the rising portion of the rate-frequency curve are considered to reflect changes in the reward effectiveness of the stimulation. For example, a rightward shift is interpreted as a decrease in reward effectiveness because more stimulation is required after the lesion to support a given level of performance. In contrast, changes in asymptotic rates of responding are interpreted as changes in the capacity of the subject to respond.

Under the assumptions of the counter model, the quantitative information that rate-frequency curves provide about postlesion changes in reward effectiveness can be linked to the degree of damage suffered by the first-stage substrate. If the outputs of all the directly stimulated fibers are weighted equally, or vary randomly in weight as a function of the location of the fibers, the counter model allows experimenters to view the percentage change in curve-shift magnitude as an index of the proportion of destruction of the first stage neurons. If a lesion were to destroy 50% of the first stage neurons, the number of pulses required to sustain a given level of behavior would have to be doubled and, thus, the rightward curve-shift would be equal to 0.3 $\log_{10}$ units.

There is ample scientific literature on the effects of lesions on BSR, yet only a handful of experiments were carried out using the curve-shift method to distinguish changes in performance capacity from changes in reward effectiveness. In studies that have employed the curve-shift paradigm to scale the effects of lesions on self-stimulation relatively few long-lasting decreases in reward effectiveness have been observed. Electrolytic lesions of the amygdala (Waraczynski, Ng Cheong-Ton, & Shizgal, 1990), dorsomedial hypothalamus (Waraczynski, Conover, & Shizgal, 1992), and parabrachial region (Waraczynski & Shizgal, 1995), excitotoxic lesions of the nucleus accumbens (Johnson & Stellar, 1994) and lateral hypothalamus (Stellar, Hall, & Waraczynski, 1991), aspiration of the entire forebrain rostral to Bregma (Colle & Wise, 1987), as well as basal forebrain knife cuts (Waraczynski, 1988)

have not resulted in consistent and substantial rightward shifts in rate-frequency curves obtained from MFB sites. The knife cut study (Waraczynski, 1988), in particular, raised serious doubts about the validity of the descending path hypothesis. If axons of the descending path of self-stimulation arise in the basal forebrain, then knife cuts in this area should have degraded the reward value of MFB stimulation. A further setback for the descending path hypothesis comes from a recent publication by Gallistel and his co-workers (Gallistel, Leon, Lim, Sim, & Waraczynski, 1996) who demonstrated that some large electrolytic lesions of the anterior MFB failed to reduce the frequency threshold for self-stimulation of the caudal MFB. If the descending path hypothesis were true, one would expect lesions of the rostral MFB to substantially reduce the rewarding efficacy of self-stimulation obtained from more caudal sites.

In contrast to the above mentioned negative findings, other studies have fulfilled this expectation. A careful look at Waraczynski's (1988) study reveals that some of the transections through the lateral preoptic area (LPOA) attenuated BSR. Likewise, Janas & Stellar (1987) found that some knife cuts in the caudal portion of the LPOA decreased the rewarding efficacy of stimulation at more caudal sites. Additional studies by Murray & Shizgal (1991, 1996a) showed that electrolytic lesions at the border of the LH and the LPOA can diminish self-stimulation of the LH and the VTA, at least in some subjects. Moreover, large excitotoxic lesions encompassing the LPOA, anterior LH, and substantia innominata (SI) produced large, long-lasting decreases in

the reward effectiveness of LH stimulation (Arvanitogiannis, Waraczynski, & Shizgal, 1996b). The fact that lesions in the basal forebrain can be effective at degrading BSR, when taken together with the finding that there is overlap between the electrophysiological and the psychophysical measures expected from first stage neurons, is consistent with the idea that at least some of the first stage neurons originate in the basal forebrain. It would be misleading, however, to claim that there is consensus regarding this conclusion.

The lack of consensus is due, at least in part, to a common and puzzling aspect of results of lesions. Apparently similar or overlapping lesions often produce different effects on BSR in subjects with similarly located electrode tips. For example, inconsistencies are apparent both within and across studies employing anterior MFB lesions. Several methodological considerations important for the interpretation of the results of studies using lesions may be at the heart of these inconsistencies. The first pertains to the sensitivity of the curve-shift method. Sensitivity depends on the resolution with which the rate-frequency curves are sampled. It stands to reason that the smaller the increment separating the tested frequencies, the smaller the displacement that can be discerned.

A second methodological issue concerns the number of currents tested. In most lesion studies only one, arbitrarily chosen, current has been used to determine the rate-frequency curve. However, Murray & Shizgal (1991) observed that the likelihood of detecting a lesion effect is increased when rate-

frequency curves are collected at multiple currents. If reward-related fibers passing close to the electrode tip project from the lesion site, rightward curve shifts should be seen at low currents. However, if the axons projecting from the damaged area course some distance away from the electrode tip, these axons would be recruited only at relatively high currents, and the position of rate-frequency curves obtained at lower currents would be unaltered by the lesion.

A third issue germane to the interpretation of the lesion data concerns the criterion for a meaningful curve shift. According to the counter model changes in rewarding efficacy should provide a scalar measure of the amount of damage done to the population of reward neurons by a lesion. Removing half the reward axons from the field of stimulation ought to produce a 0.3 $\log_{10}$ unit curve shift. In many cases, lesions produce smaller shifts. These effects are usually dismissed and the lesions that produced them are labeled "relative ineffective". The same is said of lesions that produce large but transient effects. The mere occurrence of these effects demands their careful reinterpretation.

The final point I want to raise is that the anatomical localization of the electrode tip provides no information about which fibers near the electrode are excited by the stimulation. The observation that similarly placed lesions produce different effects in self-stimulation obtained from similar sites may simply reflect underlying differences in the field of excitation around the

stimulation electrode. To address this problem a means must be found to visualize the neurons activated by the stimulation. A detailed analysis of the overlap between the pathways damaged by the lesion and the pathways activated by the stimulation should shed some light on the inconsistencies observed in lesion studies.

1.1.4. The Pharmacological Approach

BSR is similar in certain respects to the self-administration of psychomotor stimulants. Both are self-administered in a compulsive fashion and both may activate the same brain circuitry (see, e.g., Wise & Rompré, 1989). In particular, both phenomena are dopamine dependent. Microdialysis and voltametry studies indicate that both psychomotor stimulant reward and BSR elevate dopamine levels in the nucleus accumbens (Blaha & Phillips, 1990; Gratton, Hoffer, & Gerhardt, 1988; Nakahara, Ozaki, Miura, Miura, & Nagatsu, 1989; Pettit & Justice, 1989). But the most compelling evidence suggesting dopaminergic involvement in BSR derives from pharmacological studies. Dopamine receptor blockers increase self-stimulation thresholds (Gallistel, Boytim, Gomita, & Klebanoff, 1982; Gallistel & Freyd, 1987; Stellar, Kelley, & Corbett, 1983), whereas dopamine agonists have the opposite effect (Colle & Wise, 1988; Gallistel & Freyd, 1987; Gallistel & Karras, 1984).

Not surprisingly, it was once thought that direct activation of MFB dopamine fibers initiated rewarding signals in this region. However, psychophysical and electrophysiological findings ruled out this possibility.

Dopamine neurons are not myelinated and their thresholds of activation are above the level of the stimulation parameters commonly used in BSR studies. According to Yeomans (1988), dopamine neurons may contribute to the first stage only when high currents, long pulse durations, and small electrode tip diameters allow their activation. The question then arises: What place does the dopamine system occupy in the neural substrate giving rise to the rewarding effect?

According to the simplest hypothesis, the dopamine neurons are in series with the first stage ones and thus, carry the reward signal (Wise, 1980; Yeomans, 1982). An alternative hypothesis is that the dopamine neurons do not actually relay the reward signal but rather, play a permissive role at some stage of the BSR substrate (Gallistel & Freyd, 1987). One example of a permissive role would be to gate signal processing in the pathway responsible for the rewarding effect. Perhaps increased activity in the dopamine neurons enhances transmission of the reward signal, whereas decreased activity reduces or even blocks its transmission.

The strongest support for the "permissive role" hypothesis derives from a microdialysis study designed to measure the levels of dopamine released in the nucleus accumbens during self-stimulation for equi-rewarding pulses that consisted of different combinations of stimulus parameters of the electrical stimulation (Miliaressis, Emond, & Merali, 1991). It was argued that if the reward signal travels along dopamine neurons, the release of dopamine

should not depend on the stimulus parameters because equi-rewarding stimuli should produce a constant output in all neural stages carrying the reward signal, regardless of the spatio-temporal nature of the signal. However, the results showed that the magnitude of dopamine release differed between sets of self-stimulation parameters that, nevertheless, produced the same rewarding effect. The finding that the rewarding effect of the stimulation is not mirrored in the magnitude of dopamine release as measured by microdialysis argues against the hypothesis that the reward signal elicited by MFB stimulation is relayed by the mesolimbic dopamine neurons.

Using pharmacological methods, Yeomans and his collaborators have demonstrated another key element in the BSR circuit, specifically, the cholinergic neurons of the pedunculopontine nucleus (PPTg) (Kofman, McGlynn, Olmstead, & Yeomans, 1990; Yeomans, Kofman, & McFarlane, 1985; Yeomans, Mathur, & Tampakeras, 1993). These cells have inhibitory muscarinic autoreceptors on their cell bodies. Moreover, these cholinergic cells synapse monosynaptically to VTA dopamine neurons that have excitatory muscarinic receptors on their cell bodies. Inhibition of cholinergic neurons by a muscarinic agonist injected in the PPTg produces large and consistent decreases in the rewarding effect of LH self-stimulation. A similar effect is seen when a muscarinic antagonist is injected into the VTA. On the other hand, excitation of the cholinergic neurons by a muscarinic antagonist injected in the PPTg strongly reduces thresholds for BSR.

Taken together, these findings led to the proposal that the rewarding effect of MFB stimulation arises from directly stimulated activity in descending MFB fibers that is relayed to midbrain dopaminergic cells by brainstem cholinergic neurons (Yeomans et al., 1993). This may or may not be the case. The data also allow for the alternative possibility whereby cholinergic neurons in concert with dopamine neurons play a permissive role in BSR. The nature of the interaction between first stage and cholinergic/dopaminergic neurons remains to be established. Importantly, it is not yet known whether (or how) myelinated MFB axons mediating self-stimulation activate cholinergic and dopaminergic neurons.

1.2. THE NATURE OF THE BSR SIGNAL

1.2.1. The Relationship Between BSR and Natural Rewards

A widely held tenet in BSR research is that the neuroanatomical systems important to intracranial self-stimulation may be the same systems that guide an animal in organizing its behavior relative to goal objects important to survival, such as food, water, shelter, and mates (Hoebel, 1965; Hoebel, 1969; Routtenberg & Lindy, 1965). Perhaps, electrical stimulation produces its rewarding effect by activating the fibers that are normally activated by conventional rewards. In the past, this assumption was taken to imply that an animal's responsiveness to BSR should be influenced by factors which normally influence its responsiveness to conventional reinforcers. This line of reasoning underlies several studies that examined the effects of food- or

water-related factors on self-stimulation. Thus, food or water deprivation were shown to increase responsiveness for BSR (Hoebel & Teitelbaum, 1962; Margules & Olds, 1962), whereas gastric distention decreased rates of self-stimulation (Hoebel, 1968; Hoebel, 1969; Hoebel & Thompson, 1969). However, it is not clear to what extent changes in rate reflect changes in reward value and to what extent they reflect changes in response variables. Later work by Carr and his collaborators showed that, for certain electrode placements, the threshold for BSR can be reduced by decreasing body weight (Carr, 1996; Carr & Papadouka, 1994; Carr & Wolinsky, 1993). Still, one can question whether these curve shifts really reflect the selective alteration of the rewarding impact of the stimulation rather than the contribution of more general behavioral activation mechanisms.

The relationship between BSR and gustatory rewards was scrutinized in an extensive series of experiments by Conover and Shizgal (Conover & Shizgal, 1994a; Conover & Shizgal, 1994b; Conover, Woodside, & Shizgal, 1994). In these studies, under various physiological states, rats had to choose between LH stimulation varying in strength and either gustatory reward alone or a compound reward consisting of a tastant plus fixed BSR. Preference was estimated by varying the frequency of the stimulation triggered by one spout while holding constant the reward triggered by a second spout. The frequency required to produce isopreference was measured. The experimental protocol was designed to render the gustatory reward as similar as possible to BSR. Thus, the gustatory reward was intraorally infused in small volumes

via a catheter, while an intragastric cannula minimized the accumulation of gustatory reward in the gut, to simulate the instantaneous and insatiating nature of BSR respectively.

Initially, Conover & Shizgal (1994a) showed that when a choice between a gustatory stimulus (an intraoral infusion of sucrose) and LH stimulation is presented, rats choose the sucrose infusion if brain stimulation is weak, but shift their preference as the LH stimulation becomes stronger. What is noteworthy is that with sucrose availability, rats eschew suprathreshold levels of brain stimulation in favor of the sucrose reward. Clearly, the availability of sucrose alters the choice for BSR. That is, sucrose is evaluated together and competes with BSR to determine exclusive choice. For this to occur the two rewards must be evaluated in a common system of measurement whereupon the larger reward is selected. In a subsequent experiment, LH stimulation was pitted against a compound reward consisting of sucrose and an equipreferred train of brain stimulation to determine whether the results of the common evaluation can summate (Conover & Shizgal, 1994a). Indeed, the rats assigned a higher value to the compound reward than to its sucrose component alone. The strength of LH stimulation required to balance the compound reward exceeded the stimulation strength required to balance the sucrose reward alone. The finding that BSR and sucrose reward can be combined lends further support to the idea of evaluation in a common system of measurement.

The competition and summation experiments confirmed the popular conception that BSR and natural rewards have something important in common. Moreover, these experiments shed light on what the two kinds of reward have in common: BSR and gustatory rewards are evaluated on a common currency scale. But are the gustatory and electrical rewards affected similarly by internal variables such as deprivation or satiety?

The answer is "no". The rewarding effect of LH stimulation remains highly stable after manipulations of the physiological state of the animal, although these manipulations extensively alter the value of gustatory rewards. By closing the gastric cannula and allowing the sucrose to accumulate in the gut, the value of sucrose is degraded until sucrose becomes aversive. Then, a compound reward consisting of sucrose and BSR is worth less than the BSR component alone, but the value of the electrical reward is not substantially altered (Conover & Shizgal, 1994b). When subjects are depleted of sodium and given a choice between saline and BSR, the value of the saline solution is dramatically increased without producing any change in the value of BSR (Conover et al., 1994). These results suggest that physiological signals modulate gustatory reward prior to the point where the rewarding effects of gustatory stimuli and electrical stimulation are combined.

1.2.2. Unidimensional Coding in the BSR Substrate

The above mentioned studies of BSR and gustatory reward provide the basis for a new view about the nature of the neural signal mimicked by the

rewarding stimulation. In this section, I develop this view in its broad outlines.

Natural selection has produced within animals an array of complex abilities to switch from one activity to another, to modulate the intensity and patterning of their responses, and to direct their activity toward specific goals. To select the goal most pertinent to current needs, animals have to evaluate competing alternatives that differ widely in sensory qualities and relevance to everchanging physiological states. Action toward a relevant goal requires that the multidimensional quality of goal objects along with internal variables are represented in the brain. A salt deprived rat with low body weight when faced with a choice between various food sources must be able to discriminate between edibles that are high or low in sodium and fat. However, as McFarland & Sibley (1975) first suggested, selecting the course of action likely to yield the most desirable outcome requires that currently available options be evaluated along a common dimension. Going back to my example, in order for the different foodstuffs to be compared, their multiple attributes, weighed by the physiological state, must be conjointly mapped into a single, common currency representation that contains no information per se about saltiness, texture, or odor. The food with the highest common currency value, presumably the one that has the highest concentration of salt and fat, will be selected provided that factors such as procurement cost are constant among alternatives. Following Shizgal's (1997) suggestion, I call the attribute that reflects the contribution of concentration to gustatory reward the "intensity of

reinforcement." The unidimensional representation of intensity is derived from a weighing of sensory input by signals reflecting physiological state.

How could the one-dimensional coding demanded for the common currency implementation be realized in the brain? One-dimensional coding could occur in neuronal populations whose average firing rate suffices to determine the magnitude of the coded variable. In such neuronal populations artificial and intrinsic stimulation should both produce identical and equally meaningful effects. This argument has been substantiated in the case of neurons that code for motion (Newsome & Salzman, 1993; Salzman, Britten, & Newsome, 1990; Salzman, Murasugi, Britten, & Newsome, 1992).

Focusing back on BSR, it is evident that the stimulation electrode injects a meaningful signal that exerts a powerful grip over behavior. The strength of this grip is determined solely by the number of firings generated by the stimulation (within a fixed time window), regardless of their spatio-temporal distribution (Gallistel, 1978; Gallistel & Leon, 1991; Gallistel et al., 1981; Simmons & Gallistel, 1994). The experiments examining the relationship between BSR and natural rewards showed that the signal injected by the electrode is evaluated in the same unidimensional scale used to assess the value of natural rewards (Conover & Shizgal, 1994a). Furthermore, the BSR signal intervenes at a late stage of the evaluative circuitry downstream from where physiological feedback signals exert their influence on the value of goal objects (Conover & Shizgal, 1994b; Conover et al., 1994). Taken together, the

above points suggest that the electrode-induced signal is meaningful because it is transduced in a neural population where the multiple dimensions of a natural stimulus have been collapsed into one (Shizgal, 1997; Shizgal & Conover, 1996). Shizgal (1997) proposed that the electrode-induced signal mimics a unidimensional natural code corresponding to reward intensity.

1.3. OVERVIEW

I started this chapter by outlining some of the central discoveries of the last decades concerning the substrate for BSR. I supplied a brief account of the methods that have been used to identify the neuronal basis of BSR and the key findings that have emerged as a result of applying these methods. Major unresolved controversies were also highlighted. Psychophysical (Bielajew & Shizgal, 1982; Bielajew & Shizgal, 1986; Boye & Rompre, 1996; Murray & Shizgal, 1996b; Yeomans, 1979), electrophysiological (Murray & Shizgal, 1996c; Rompré & Shizgal, 1986; Shizgal et al., 1989), and lesion (Arvanitogiannis et al., 1996b; Janas & Stellar, 1987; Murray & Shizgal, 1996a) studies of the MFB have led to the proposal that at least some of the first stage neurons have myelinated axons, somata in the basal forebrain and synaptic terminals in, or caudal to, the VTA. Although there is general agreement about the electrophysiological properties of the first stage neurons (Shizgal & Murray, 1989), because of inconsistencies in the findings of lesion studies, the location of their somata is still a matter of controversy (Gallistel et al., 1996; Malette & Miliaressis, 1995). Pharmacological interventions indicate that MFB self-

stimulation is dependent on the mesolimbic dopamine system (Stellar & Corbett, 1989; Wise, 1996; Wise & Rompré, 1989) as well as the cholinergic projection from the PPTg to the VTA (Yeomans et al., 1993). However, there is no consensus yet as to what place these systems occupy in the neural substrate giving rise to the rewarding effect.

The methods employed to date to uncover the first stage substrate for BSR cannot provide information about neural morphology, chemistry and projections. Such information would seem essential if the rewarding effect is to be linked to a particular set of neurons. The experiments in chapter 2 were undertaken as a step toward filling this gap by assessing expression of the immediate-early gene, *c-fos*, following self-stimulation. Expression of *c-fos* is not restricted to the neurons responsible for the rewarding effect. The results of studies in which BSR is challenged with lesions provide an indication of which regions provide reward-related neurons. In chapter 3 I assess the contribution of the medial basal forebrain to self-stimulation of the LH and the VTA.

Finding the identity of the first stage neurons is ultimately dependent on knowing the function of these neurons. Assume for a moment that one isolates a set of neurons that seem likely to give rise to a portion of the substrate for self-stimulation. To show that the neurons in question belong to the first stage, it will be crucial to study electrophysiologically the activity of these cells in behaving animals and predict their responses in a variety of

tasks. But how is one to know which tasks to test and what the responses of the first stage neurons to a particular task should be without having at least some idea concerning the natural function of the first stage neurons? Thus, in the second part of this chapter I reviewed exciting new findings about the relationship between BSR and natural rewards (Conover & Shizgal, 1994a; Conover & Shizgal, 1994b; Conover et al., 1994) that have led to the idea that brain stimulation may be meaningful because it activates a neural system at a unidimensional stage of processing (Shizgal, 1997; Shizgal & Conover, 1996). This idea will be elaborated in chapter 4 to build a framework for developing a new method with the potential to address the above mentioned unresolved issues concerning the BSR substrate.

CHAPTER 2

STIMULATION-INDUCED EXPRESSION OF FOS

In view of the complexity of the MFB, it would be impracticable to search, by applying psychophysical, electrophysiological and lesion methods, to all the brain regions that contain substantial numbers of neurons activated by stimulating the MFB, let alone, to determine which pathway(s) is(are) critical for self-stimulation. The task would be made easier if a functional imaging method were available that could register antidromic activation of somata with cellular resolution. Applying such a method would make it possible to begin a truly cellular analysis of the BSR substrate. Recent reports have described a technique for studying neuronal activation in the brain using immunohistochemical procedures to detect the protein product of the immediate-early gene *c-fos* (referred to as Fos) (Dragunow & Faull, 1989; Krukoff, 1993; Morgan & Curran, 1991; Sagar, Sharp, & Curran, 1988). It has been suggested that Fos expression is triggered by neuronal activation, at least in some neurons. If so, mapping the distribution of the Fos protein is a means of visualizing the neurons that respond to natural and artificial stimuli (Dragunow & Faull, 1989; Sagar et al., 1988). In this chapter, I will describe the use of this approach to visualize neurons activated by rewarding stimulation.

2.1. NEURONAL ACTIVITY AND FOS EXPRESSION

Stimulation of neurons causes changes in gene expression that are critical for neuronal survival, differentiation and plasticity (Black et al., 1987). Research on the signaling pathway connecting the plasma membrane to gene activation has revealed a class of genes designated "immediate-early genes" (Morgan & Curran, 1991; Sheng & Greenberg, 1990). These genes are expressed at low levels in quiescent cells but upon stimulation are induced rapidly, transiently, and independently of protein synthesis. Many immediate-early genes are thought to encode nuclear proteins that govern genomic responses to extracellular stimuli by coordinating expression of downstream genes. In the nervous system several immediate-early genes have been identified, including *c-fos* (Hughes & Dragunow, 1995; Morgan & Curran, 1991; Sheng & Greenberg, 1990). Transcription of *c-fos* is mediated through calcium entry into the neuron or by receptor-coupled second messengers such as cyclic-adenosine monophosphate (Gallin & Greenberg, 1995; Hill & Treisman, 1995). The Fos protein, forms heterodimers with members of the Jun protein family which upon binding to an activating protein (AP)-1 site, activate target genes (Kerppola & Curran, 1991a; Kerppola & Curran, 1991b; Kouzarides & Ziff, 1988). The transient nature of Fos activation may be related to the ability of Fos to inhibit its own expression (Morgan & Curran, 1991).

Neuronal activation has been shown to be accompanied by the induction of Fos. In vitro, depolarizing agents such as KCl and the sodium

channel activator veratridine cause Fos expression, while the sodium channel blocker tetrodotoxin antagonizes this effect (Morgan & Curran, 1986). In vivo, numerous studies have demonstrated that various treatments to the nervous system that cause neuronal excitation result in increased Fos expression. These treatments include direct electrical stimulation (Dragunow & Robertson, 1987; Wisden et al., 1990), electrical activity due to seizures (Morgan, Cohen, Hempstead, & Curran, 1987), kindling (Dragunow & Robertson, 1987), and sensory stimulation (Hunt, Pini, & Evans, 1987).

Early on it was discovered that in spite of the broad range of stimuli that are able to induce Fos, the expression of this protein is stimulus specific. Moreover, Fos is localized in the cell nucleus. This is neuroanatomically advantageous because neurons that express Fos can potentially be characterized neurochemically and/or morphologically by co-labeling their cytoplasm with transmitter enzymes and tracers. Based on the unique characteristics of Fos expression, Sagar et al. (1988) and Dragunow & Faull (1989) suggested that Fos immunostaining may be used to map neuronal activation with high resolution and sensitivity.

2.2. FOS-LIKE IMMUNOREACTIVITY IN FOREBRAIN REGIONS FOLLOWING SELF-STIMULATION OF THE LATERAL HYPOTHALAMUS

2.2.1. Introduction

Converging evidence from psychophysical, electrophysiological and lesion experiments suggests that the somata of at least some of the first-stage neurons are located in the basal forebrain, perhaps in the vicinity of the anterior LH, the LPO , and/or the SI (Arvanitogiannis et al., 1996b; Bielajew & Shizgal, 1982; Bielajew & Shizgal, 1986; Murray & Shizgal, 1996a; Murray & Shizgal, 1996b; Murray & Shizgal, 1996c; Shizgal et al., 1989). However, the rewarding effect has not yet been tied to morphologically- or neurochemically-characterized populations of cells in these nuclei. A first step toward obtaining such information would be to visualize neurons activated by rewarding stimulation of the MFB. Barring systematic bias in the visualization technique, the first stage neurons should compose part of the visualized population.

In this experiment, immunohistochemical labeling of Fos was employed to visualize neurons activated by rewarding stimulation of the lateral hypothalamic level of the MFB. In the histological analysis emphasis was placed on Fos-like immunoreactivity (FLIR) in the basal forebrain regions implicated in BSR by psychophysical, electrophysiological, and lesion studies. Background labeling was assessed through comparisons with control rats that

did not have access to rewarding stimulation prior to perfusion but otherwise received training and testing similar to the experimental subjects.

The results of this work have been published (Arvanitogiannis, Flores, Pfaus, & Shizgal, 1996a).

2.2.2. Materials and Methods

2.2.2.1. Subjects and Surgery

Subjects were nine male Long-Evans rats weighing 350-550 g. They were housed individually, with free access to food and water, in a room with a reversed 12 h dark, 12 h light cycle.

Shortly after the administration of atropine sulphate (0.25 mg/kg), the rats were anesthetized with pentobarbital (Somnotol, 65 mg/kg) and placed in a stereotaxic frame. Monopolar electrodes fashioned from 00 insect pins and insulated with Formvar to within 0.5 mm of the tip were aimed bilaterally at the LH. In two subjects, the following level-skull coordinates were used: AP, 2.8 posterior to Bregma; ML, 1.7 lateral to the mid-sagittal sinus; DV, 7.7 ventral to the dura surface. In the remaining seven subjects, the incisor bar of the stereotaxic was set at +5.0 mm and the coordinates were: AP, 0.6 posterior to Bregma; ML, 1.7 lateral to the mid-sagittal sinus; DV, 8.0 ventral to the dura surface. The current return consisted of an uninsulated wire wrapped around three stainless-steel screws. The entire assembly was secured to the skull with dental acrylic. After surgery, Buprenorphine (Buprenex, 0.05 mg/kg) was

administered to reduce pain, and the rats were placed on top of a heat source until recovery from anesthesia was complete.

2.2.2.2. Testing Apparatus

Before actual testing, subjects were screened for self-stimulation in wooden boxes (25 cm x 25 cm x 70 cm) with Plexiglas front panels and wire-mesh floors. A Lehigh Valley lever protruded from the center of one wall, 5 cm above the floor. A yellow key light signaling stimulus availability was located 5 cm above the lever. A 7-channel, slip-ring commutator provided a connection to the stimulator, while allowing the subject to circle without twisting the leads. Electrical stimulation was provided by dual constant-current amplifiers and controlled by hand-set integrated circuit pulse generators. Stimulation parameters were monitored on an oscilloscope. To prevent tissue damage from electrode polarization, the stimulator outputs were connected electronically, between stimulation pulses, via a low impedance path.

The experiment proper was conducted in a computer-controlled setup housed in a dedicated testing room. Test chambers were similar to those used for training but constructed entirely from Plexiglas. They were equipped with removable floors, two levers located on opposite walls 5 cm from the floor and 5 cm from the nearest corner, a white houselight (40 watt), and two key lights situated 3 cm above each lever, a yellow one on one side and a red one (not used in this study) on the other. The test chambers were enclosed in

50 cm x 50 cm x 90 cm sound-attenuating boxes. The Styrofoam insulation along with the background noise from ventilation fans at the back of the boxes prevented external sources of noise from disrupting the rats during testing. Rats were monitored by means of a remote-controlled video camera from an adjoining control room. Temporal stimulation parameters for each test cage were controlled by a microprocessor and were monitored on an oscilloscope.

2.2.2.3. *Behavioral Testing*

Following at least one week of postsurgical recovery, the rats were trained, using conventional shaping procedures, to press a lever for 0.5 s trains of cathodal, rectangular, constant-current pulses, 0.1 ms in duration delivered to one of the LH stimulating electrodes. At the beginning of training the current was set at 800 μA and frequency was adjusted individually for each rat so as to maintain reliable rates of responding with minimal motor effects. For certain subjects the current had to be lowered to 600 μA in order to avoid motor effects and/or stimulation-induced seizures. Self-stimulation was assessed for both stimulating electrodes but only the electrode yielding the best combination of vigorous self-stimulation and minimal stimulation-induced movements was selected for further testing.

Testing consisted of two phases. In the first phase, with the current held constant, five curves relating the response rate to the number of pulses per train (rate-number curves) were collected as follows: the number of lever

presses per 30 s trial was recorded for a range of stimulation frequencies. The frequency was decreased after every trial in 0.05 $\log_{10}$ unit steps from a value that produced maximum responding to one that yielded fewer than 10 responses. Each trial was preceded by five priming trains with parameters identical to those of the trains available during the trial. The purpose of collecting the rate-number curves was to estimate the lowest stimulation frequency for which each subject would respond near its maximal rate, that is, the frequency falling on the "shoulder" of the rate-number curve.

Following this determination subjects underwent the second phase of testing. In this phase, the rats were allowed to lever-press continuously for 1 h with the stimulation parameters fixed throughout the session. The number of pulses per train for a given subject was equal to the number of pulses falling on the shoulder of the rate-number curve, as described above. After the completion of at least one such session, the rats were left in their home cages for at least 48 h. Seven were then retested for 1 h with the stimulation parameters fixed. The remaining two rats were trained and tested in an identical manner except that the stimulator was disconnected during the final 1-h test.

2.2.2.4. *Immunohistochemistry*

Fifteen minutes after the completion of the final 1-h self-stimulation session, the rats were given an overdose of sodium pentobarbital (120 mg/kg) and perfused transcardially with cold phosphate buffered saline (300 ml)

followed by cold freshly prepared 4% paraformaldehyde in 0.1 M phosphate buffer (300 ml). For each brain, the side contralateral to the stimulating electrode was marked with two razor-blade cuts, one running vertically through the brainstem, parallel to the neuraxis, and the second running through the cortex along the lateral aspect of the hemisphere. Brains were then postfixed in 4% paraformaldehyde for 4 h, cryoprotected overnight in 30% sucrose in 0.1 M phosphate buffer, frozen with dry ice, and cut on a sliding microtome into 30 μm frontal sections. Sections were collected in Tris-buffered saline (TBS, pH=7.2) and then processed for Fos immunohistochemistry according to the ABC method (Hsu, Raine, & Fanger, 1981). The primary Fos antibody, a mouse monoclonal directed against residues 4-17 of the N-terminal sequence of Fos protein (NCI-BCB Repository, Quality Biotech, Camden, NJ), was diluted to 1:8000 with 0.05% Triton X-100 and 1% normal horse serum (Vector) in TBS. Sections were incubated with the primary antibody at 4°C for 48 h, then rinsed in TBS, and incubated for 1 h at 4°C with a 1:33 dilution of a rat-adsorbed biotinylated horse anti-mouse secondary antibody (Vector) with 0.05% Triton X-100 and 1% normal horse serum. After another rinse in TBS, sections were incubated at 4°C for 2 h in an avidin-horseradish peroxidase complex (Vectastain Elite ABC Kit, Vector) and rinsed sequentially in TBS, in 50 mM Tris buffer (pH 7.6), and in 0.05% 3,3'-diaminobenzidine (DAB) in 50 mM Tris. Sections were then incubated for 10 min with constant agitation in DAB/Tris buffer with 0.01% H_2O_2 added to catalyze the DAB and 8% $NiCl_2$ to color the DAB chromogen product black.

The reaction was stopped by transferring the sections to TBS. The sections were then placed onto electrostatically-treated slides (SuperFrost Plus, Fisher Scientific) that were allowed to air-dry for at least 1 day before the sections were dehydrated in ethanol and the slides cleared in xylene and coverslipped. Background staining was sufficient to allow for the localization of the tip of the stimulating electrodes using the stereotaxic atlas of Swanson (1992).

2.2.2.5. Data Analysis

The tissue stained for FLIR was examined using a Leitz Laborlux S microscope, and quantitative analysis of the Fos distribution was undertaken using images digitized with a computerized image-analysis system (M1, Imaging Research Inc., St. Catherines, Ont.). Cell counts were restricted to structures in the basal forebrain and diencephalon. The different brain regions were defined using the borders in the Paxinos & Watson (1986) atlas. Staining of cell nuclei ipsilateral to the stimulating electrode was compared to staining in homologous contralateral structures. Cell counts were made using a 5 x objective from three sections per structure, non-consecutive when possible, for each animal. The average number of labeled nuclei per structure in each animal for both the stimulated and non-stimulated hemispheres was computed. Differences between the average cell counts of Fos-positive nuclei between the stimulated and the unstimulated side for a particular structure were evaluated with two-tailed, paired Student t-tests conducted at the level of $P \leq 0.05$ (GB-STAT™, Dynamic Microsystems, Inc.). Ratios were calculated

to describe the asymmetry of activation by dividing the sum of the available average counts per structure on the stimulated side across all animals by the sum of the average counts for the unstimulated side.

2.2.3. Results

Sparse labeling (≤ 4 labeled cells/structure) was seen in the brains from the two unstimulated subjects. In contrast, brains from animals that self-stimulated prior to perfusion exhibited robust and qualitatively reproducible patterns of FLIR. Most of the labeling was substantially heavier ipsilateral to the stimulation sites. Fig. 2.1 presents the mean number of labeled cells found in the stimulated and unstimulated hemispheres in brain regions where asymmetric activation was observed in at least some of the tested subjects. It should be noted that several sections from one animal were damaged during processing for immunohistochemistry, making it impossible to quantify activation in certain structures for that animal. The tips of the LH stimulation electrodes are shown in Fig. 2.2.

Asymmetric FLIR was detected in numerous subcortical telencephalic, diencephalic, and midbrain structures. Table 2.1 shows the ratio of FLIR between the stimulated and unstimulated hemispheres. The most consistently pronounced asymmetry was observed in the LH where a large number of labeled cells surrounded the tip of the stimulation electrode, but not the contralateral, inactive electrode (Fig. 2.3e, 2.3f); asymmetrical activation was also seen consistently in the medial preoptic area, the LPO (Fig.

2.3a, 2.3b), the ventral pallidum, the SI (Fig. 2.3c, 2.3d), the amygdaloid complex, the septum, the basal nucleus of the stria terminalis, and the claustrum. Although less pronounced, FLIR in the nucleus accumbens and the caudate putamen was heavier ipsilateral to the stimulating electrode. In each of these areas neurons exhibited reliable FLIR across every stimulated animal for which tissue was available for analysis. Differences in FLIR between the stimulated and unstimulated hemisphere for the above mentioned structures were all significant at the $p \leq 0.05$ level.

Strikingly asymmetrical staining was seen in both the nucleus of the lateral olfactory tract and lateral habenula of most animals, but was absent in some subjects. In cases where these regions were heavily stained ipsilateral to the stimulating electrode, the contralateral side displayed negligible or no FLIR.

Fig. 2.1. Mean number of neurons exhibiting FLIR (mean ±S.E.M.) ipsilaterally and contralaterally to the stimulation electrode in forebrain regions where asymmetric activation was observed and analyzed. (^{ns} = $P > 0.05$).

Abbreviations: Acb, nucleus accumbens; Amg, amygdala; BST, bed nucleus of the stria terminalis; Cl, claustrum; CPu, caudate putamen; LHb, lateral habenular nucleus; LH, lateral hypothalamus; LOT, nucleus of the lateral olfactory tract; LPO, lateral preoptic area; MPO, medial preoptic area; Spt, septum; SI, substantial innominata; VP, ventral pallidum; VTA, ventral tegmental area.

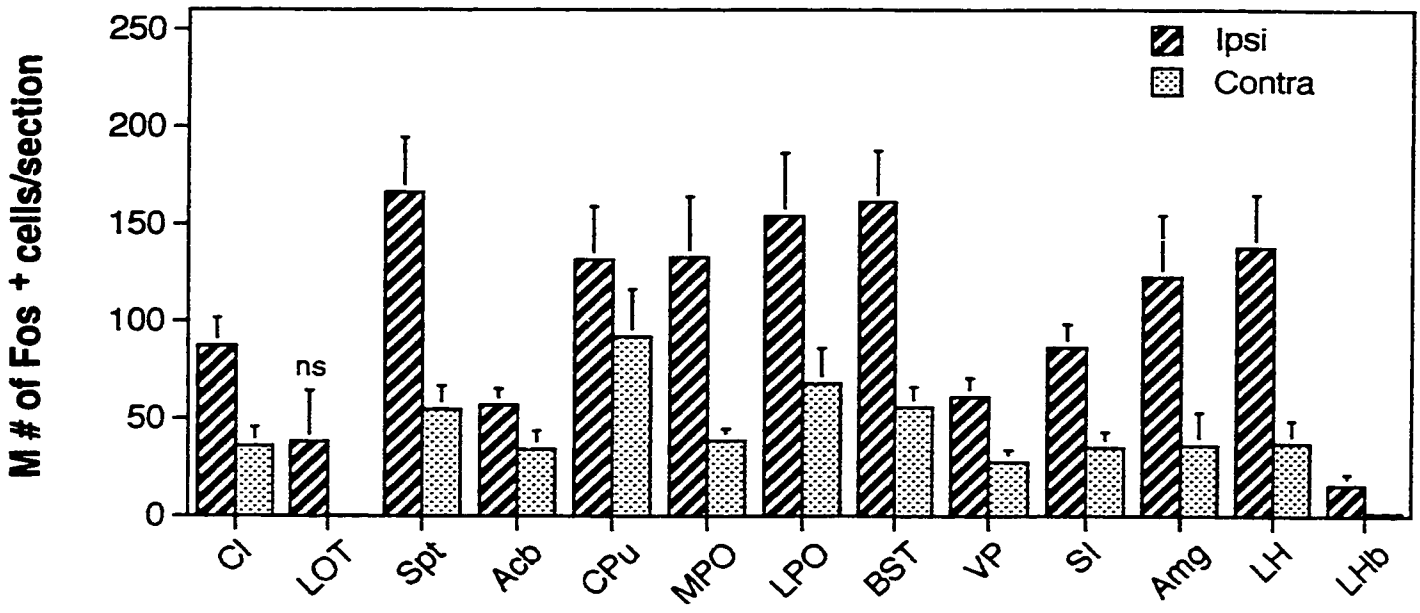
M # of Fos + cells/section
250
200
150
100
50
0
Ipsi
Contra
ns
Cl
LOT
Spt
Acb
CPu
MPO
LPO
BST
VP
SI
Amg
LH
LHb

Fig. 2.2. Stimulation sites for the seven experimental subjects. Electrode tips, represented as stars, are reconstructed onto tracings of coronal plates from the Swanson atlas (1992).


- 2.45
- 2.85
- 3.25
- 2.00
- 2.85

Table 2.1

FLIR ratio in the stimulated versus the unstimulated hemisphere across brain regions

Structure	Ratio	n
Cl	2.4:1	6
LOT	unilateral	6
Spt	3:1	7
Acb	1.7:1	6
CPu	1.4:1	6
MPO	3.4:1	7
LPO	2.3:1	7
BST	2.9:1	7
VP	2.2:1	6
SI	2.5:1	6
Amg	3.4:1	6
LH	3.7:1	6
LHb	unilateral	6

Fig. 2.3. Representative digitized images (5 ×objective) showing FLIR at two different levels (A, B; C, D) of the basal forebrain and at the LH stimulation site (E, F). Substantial FLIR can be seen in the stimulated hemisphere (A, C, E) as opposed to the unstimulated one (B, D, F). Scale bar = 250 μm (for A-F).

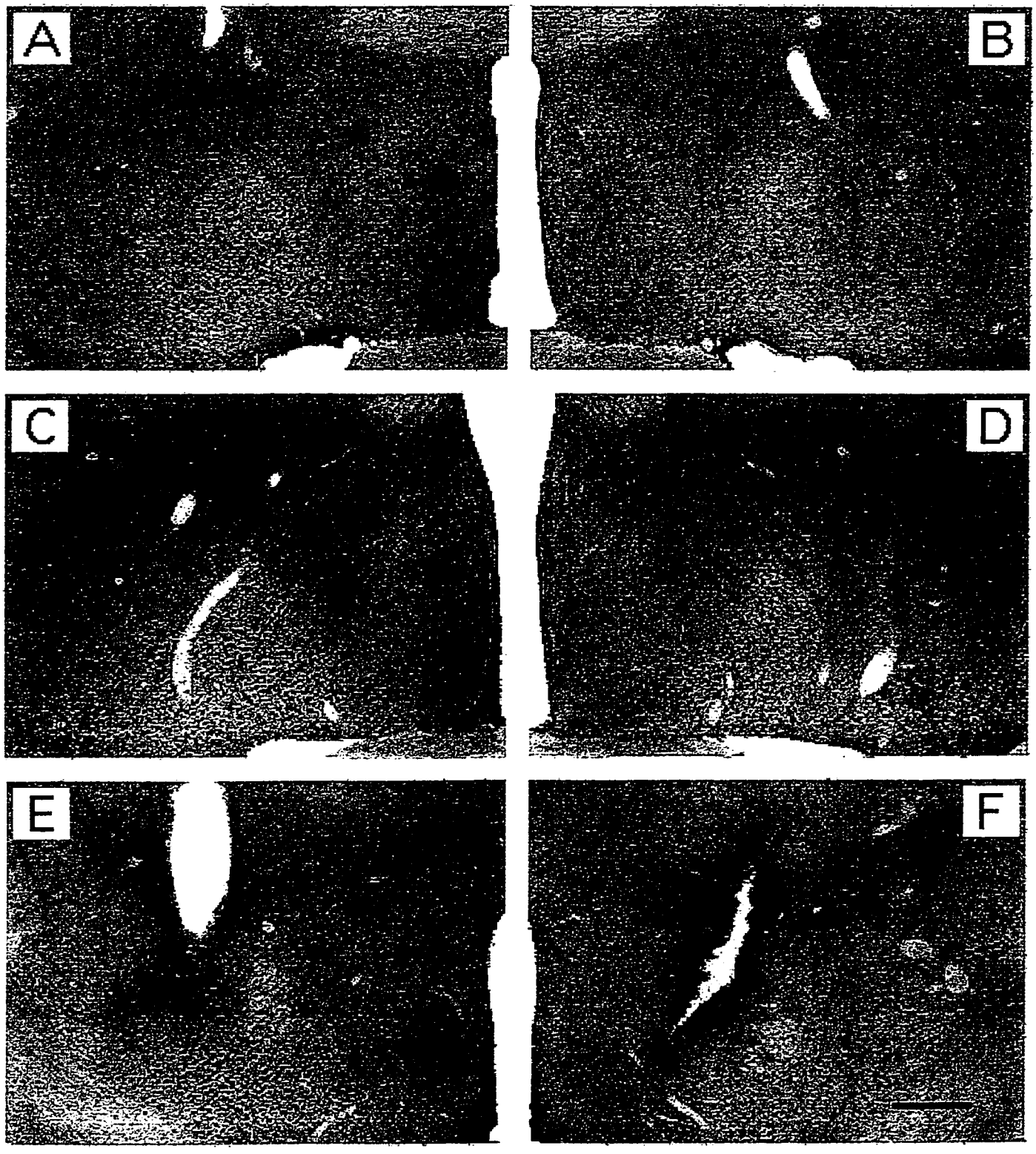
A
B
C
D
E
F

2.2.4. Discussion

The purpose of this study was to visualize neurons activated by rewarding stimulation of the LH. Although the origins of the directly-stimulated fibers subserving MFB self-stimulation have not been established definitively, psychophysical, electrophysiological, and lesion data point to basal forebrain structures such as the rostral LH, the SI, and the LPO. If so, rewarding stimulation of the MFB should activate cells in these structures. This prediction was borne out by the results. Fos expression was seen in the rostral LH, the SI, and the LPO following LH self-stimulation and was more pronounced in the stimulated than in the non-stimulated hemisphere.

In analyzing these results, I concentrated on structures that showed a greater increase in FLIR ipsilateral than contralateral to the stimulation electrode. This decision is based on the predominance of ipsilateral projections in anatomical descriptions of the MFB (Nieuwenhuys et al., 1982; Veening, Swanson, Cowan, Nieuwenhuys, & Geeraedts, 1982) and on the paucity of reports that lesions contralateral to MFB stimulating electrodes decrease reward effectiveness. Nonetheless, a role for bilaterally-activated structures cannot be ruled out, particularly in stages of the circuitry beyond the directly-stimulated stage.

Not all of the regions that exhibited FLIR after lateral hypothalamic stimulation are equally implicated in MFB self-stimulation. For instance, knife-cuts that transected the descending outflow of the septal complex and

the MPO were either ineffective in changing self-stimulation or increased the reward effectiveness of MFB stimulation (Waraczynski, 1988). Similarly, reward effectiveness was not diminished by electrolytic lesions of the amygdala (Waraczynski et al., 1990) or by excitotoxic lesions of the nucleus accumbens or ventral pallidum (Johnson & Stellar, 1994). Fos induction in structures where lesions fail to affect BSR may result from the activation of neurons that play no role in the rewarding effect. Induction in structures where lesions increase reward effectiveness may stem from the activation of neural systems that counteract the rewarding effect of MFB self-stimulation.

Interpretation of the results reported here is constrained by several factors. First, the immunohistochemical method employed cannot distinguish reward-related neurons from other stimulated cells. Second, induction of Fos may occur in transsynaptically-activated as well as antidromically-activated neurons (Sagar et al., 1988). Thus, the population of stained cells may include directly-stimulated ("first-stage") neurons subserving the rewarding effect, neurons composing later stages of the reward-related circuitry, and neurons subserving other functions. Finally, the possibility that some first-stage neurons might not express Fos in response to rewarding stimulation of the LH must also be considered. FLIR may not be a universal marker of neuronal activation. For example, some brainstem regions known to be activated electrophysiologically by painful stimulation do not show FLIR (Bullitt, 1990). Thus, failure to observe staining in a

particular structure does not necessarily rule out the possibility that the constituent neurons contribute to the first-stage.

The constraints on interpretation notwithstanding, Fos immunohistochemistry offers significant advantages over imaging methods used in prior experiments on MFB self-stimulation. The first such method to be used in BSR research was autoradiography for the metabolic marker ^{14}C-2-deoxyglucose (2DG) (Esposito et al., 1984; Gallistel, Gomita, Yadin, & Campbell, 1985; Porrino et al., 1984; Porrino, Huston-Lyons, Bain, Sokoloff, & Kornetsky, 1990). The 2DG method relies on the assumption that active neurons take up more glucose than inactive neurons. 2DG is a glucose analogue that can be transported into neurons, but once there, cannot be metabolized and therefore keeps accumulating. The accumulated 2DG because it is radioactive can be visualized by autoradiography. Using 2DG autoradiography, Gallistel et al. (1985) found evidence of activation in several forebrain regions after MFB self-stimulation. The region of the diagonal band and medial septum showed high uptake of the metabolic marker as did regions of the anterior MFB, including the preoptic area. The high metabolic activity continued caudally along the MFB to the level of the VTA. Increases in glucose utilization during LH self-stimulation have also been reported in regions such as the nucleus accumbens and the olfactory tubercle.

Another technique to visualize long-term increases in metabolic activity is cytochrome oxidase (CO) histochemistry. CO is an endogenous

mitochondrial enzyme that is linked to metabolic processes and its distribution can be quantified by assessing the degree of enzymatic reactivity, in relative optical densities between structures, following chronic exposure to rewarding brain stimulation. Using CO histochemistry, Bielajew (1991) found evidence of increased metabolic activity resulting from LH stimulation mainly in the septum and the nucleus accumbens.

One problem with the 2DG and CO techniques is that both have poor spatial resolution (in addition, the CO technique has poor temporal resolution since it reflects long-term changes). The partitioning of increased metabolic activity between cell bodies and synaptic terminals is unclear in 2DG autoradiography, and some observers contend that the synaptic compartment dominates the images obtained with this method (Sharp, Sagar, & Swanson, 1993); if so, one would expect CO staining to also emphasize activation of synaptic terminals rather than cell bodies. A striking example showing that the activity-dependent uptake of 2DG occurs in synaptic terminals was provided by Kadekaro, Crane, & Sokoloff (1985), who showed that when the sciatic nerve of anesthetized rats is stimulated, a frequency dependent increase in 2DG uptake occurs in the dorsal horn of the spinal cord (where afferent sensory axon terminals make synaptic contacts with second-order interneurons), but not in the dorsal root ganglion, where the cell bodies of the sensory neurons are localized. What's more, there is evidence that 2DG uptake occurs in astrocytes, which have recently been shown to be the

primary site of glucose uptake during neuronal activity (Tsacopoulos & Magistretti, 1996).

In contrast to the previously used imaging methods, Fos immunohistochemistry brings the visualization of activity induced by rewarding MFB stimulation to the cellular level. Fos immunohistochemistry labels a known cellular compartment: the nucleus. Given that the labeled compartment is near the membrane regions that give rise to cell body spikes and bear the receptors where excitotoxins act to induce cell death, the observed staining can be readily linked to results from single-unit recording and excitotoxic lesion experiments. Finally, Fos immunohistochemistry can be combined with additional staining methods to provide information about the morphology, projections, and neurochemistry of the activated cells. The anatomical and neurochemical information provided by such double-labeling experiments could serve as the basis for application of specific lesioning methods, which, in turn, could serve to assess the role of well-characterized neural populations in the rewarding effect.

On the basis of the considerations discussed above, one would expect to see partial overlap between the results obtained with Fos immunohistochemistry and those obtained by means of the other metabolic mapping methods. Both methods would be expected to reveal activity in regions of excitatory synaptic contacts, but Fos immunohistochemistry would be expected to better reflect antidromic activation of somata. It is interesting to

note that structures such as the bed nucleus of the stria terminalis, the medial preoptic area, and the LH were activated ipsilateral to the stimulation electrode in a 2DG study of MFB self-stimulation (Gallistel et al., 1985) as well as in our study. However, Gallistel et al. (1985) did not report activation anterior to the genu of the corpus callosum nor the lateral habenula and found no hemispheric differences for activation of the nucleus accumbens, septum, and SI. It should be mentioned, however, that the currents used in the 2DG study were much lower than the ones used in the present experiment.

In summary, the work reported here is complementary to psychophysical, electrophysiological, and lesion studies suggesting that basal forebrain nuclei are a source of at least some of the directly-stimulated neurons subserving self-stimulation of the MFB. As expected the rostral LH, the SI, and the LPO were among the regions where rewarding LH stimulation induced Fos expression, preferentially in the stimulated hemisphere. The visualization of neurons activated by rewarding MFB stimulation sets the stage for experiments that can link the rewarding effect to the direct activation of morphologically- and neurochemically-characterized neurons.

2.3. FOS-LIKE IMMUNOREACTIVITY IN THE CAUDAL DIENCEPHALON AND BRAINSTEM FOLLOWING LATERAL HYPOTHALAMIC SELF-STIMULATION

2.3.1. Introduction

In the previous experiment I showed that rewarding electrical stimulation of the LH increased ipsilateral Fos expression in discrete regions of the forebrain and diencephalon. The choice to focus on the forebrain was guided by the results of a long series of psychophysical, electrophysiological, and lesion experiments that address the descending-path hypothesis of MFB self-stimulation. Despite the accumulated evidence in favor of the descending-path hypothesis, recent proposals argue against it and implicate neurons placed to the posterior of the VTA in the directly stimulated substrate for MFB self-stimulation (Gallistel et al., 1996; Malette & Miliaressis, 1995). Moreover, proposals stemming from pharmacological studies implicate caudal diencephalic or brainstem neurons as postsynaptic elements of the circuitry subserving the rewarding effect (Wise, 1980; Yeomans et al., 1993). Of course, if the descending-path hypothesis is correct, postsynaptic elements must lie caudal to the electrode. Nevertheless, previous imaging studies using 2DG autoradiography or CO histochemistry failed to detect activation posterior to the VTA after LH self-stimulation (Bielajew, 1991; Gallistel et al., 1985; Porrino et al., 1990). In this experiment we decided to revisit the question of activation in diencephalic, midbrain and hindbrain sites, by

taking advantage of the high resolution of the Fos immunostaining technique. As in the previous experiment, staining of cell nuclei ipsilateral to the stimulation electrode was compared to staining in homologous contralateral structures.

A report describing the results of this experiment has been published (Arvanitogiannis, Flores, & Shizgal, 1997).

2.3.2. Materials and Methods

The procedures and equipment used for this experiment were similar to those described in section 2.2.2. Only those aspects that differ will be described below.

Under pentobarbital anesthesia (65 mg/kg), monopolar electrodes were aimed stereotaxically at the LH (AP, 2.8 mm behind bregma; ML, 1.7 mm lateral to the mid-sagittal sinus; DV, 7.8 mm below dura) in nine male, Long-Evans rats (350-400 g). Subjects learned to lever press for 0.5 s stimulation trains composed of 0.1 ms, 1000 μA rectangular cathodal pulses. Rate-frequency curves were collected, and the minimum stimulation frequency that supported asymptotic responding (the "shoulder" frequency) was determined for each subject. During the final 1 h-long test session, conducted 3 days after the previous session, the rats self-stimulated at the "shoulder" frequency. For two control subjects, the stimulator was disconnected during the final 1-h test.

Fifteen min after the end of that session, the rats were deeply anesthetized with sodium pentobarbital (120 mg/kg) and intracardially perfused with 200 ml of cold physiological saline followed by 400 ml of cold 4% paraformaldehyde in 0.1 M phosphate buffer. Brains were removed and stored overnight in 4% paraformaldehyde at 4°C. Coronal, vibratome (50 µm) sections were cut and then processed for FLIR, using a mouse monoclonal antibody raised against N-terminal residues 4-17 of the human Fos protein (NCI/BCB Repository, Quality Biotech, Camden, NJ). Because of the tissue thickness 0.3% instead of 0.05% Triton X-100 was used for the antibody incubations. FLIR was detected with a Vectastain *Elite* ABC Kit (Vector) using diaminobenzidine as chromogen.

The distribution of FLIR was examined under a Leica microscope (Leitz DMRB). An image-analysis program (NIH Image) was used to count the cells within a circumscribed region and to convert the cell counts to densities; the borders of the region to be analyzed were defined manually to correspond to structure boundaries in the Paxinos & Watson (1986) atlas. The density of Fos-positive cells was taken as the mean for a given structure in the three sections exhibiting maximum FLIR for the structure in question.

2.3.3. Results

Substantial staining, heaviest ipsilateral to the stimulating electrode, was seen in the seven stimulated brains. In the caudal diencephalon, midbrain, and hindbrain of the unstimulated subjects, labeling was absent or very sparse

(≤13 Fos-positive cells/mm^2); what little labeling was seen was bilaterally symmetrical. Estimates of the density of Fos-positive cells in the Fos-positive subjects are shown in Fig. 2.4. FLIR tended to be the highest in the caudal diencephalon and to fall off in the brainstem. Nonetheless, intense staining was seen in the locus coeruleus. Although a predominance of labeled cells ipsilateral to the stimulation electrode was found in the substantia nigra pars compacta, the difference between FLIR in the ipsilateral and contralateral sides was not significant. In the VTA FLIR was confined to the most anterior part of the nucleus. Bilateral staining was seen in the lateral geniculate nucleus, rostral linear nucleus of the raphé, median raphé nucleus, and superficial gray layer of the superior colliculus (not shown in Fig.2.4). In one subject, the anterior part of the nucleus of the solitary tract was examined and moderate FLIR was observed, predominantly ipsilateral to the stimulating electrode. Bilateral comparisons of the relative density in homologous structures are shown in Table 2.2, along with ordinally scaled values indicating absolute density. Fig. 2.5 and Fig. 2.6 illustrate the asymmetrical distribution of FLIR in some of the structures analyzed.

Fig. 2.4. Mean (±S.E.M.) FLIR density ipsilaterally and contralaterally to the stimulating electrode in caudal diencephalic, midbrain, and hindbrain regions where asymmetric activation was observed and analyzed. Densities were calculated from mean numbers obtained using the three sections per region exhibiting maximum FLIR for each animal (ns = $P > 0.05$, t-test).

Structure Abbreviations: Arc, arcuate hypothalamic nucleus; CG, central grey; DM, dorsomedial hypothalamic nucleus; DR, dorsal raphé nucleus; LC, locus coeruleus; LDTg, laterodorsal tegmental nucleus; LH, lateral hypothalamic area; LHb, lateral habenular nucleus; MTu, medial tuberal nucleus; PBN, parabrachial nucleus; PH, posterior hypothalamic nucleus; Pn, pontine nuclei; PPTg, pedunculopontine tegmental nucleus; PrC, precommissural nucleus; PVP, paraventricular thalamic nucleus, posterior; pv, periventricular fiber system; RRF, retrorubral field; SNC, substantia nigra, compact; SuM, supramammillary nucleus; VMH, ventromedial hypothalamic nucleus; VTA, ventral tegmental area.

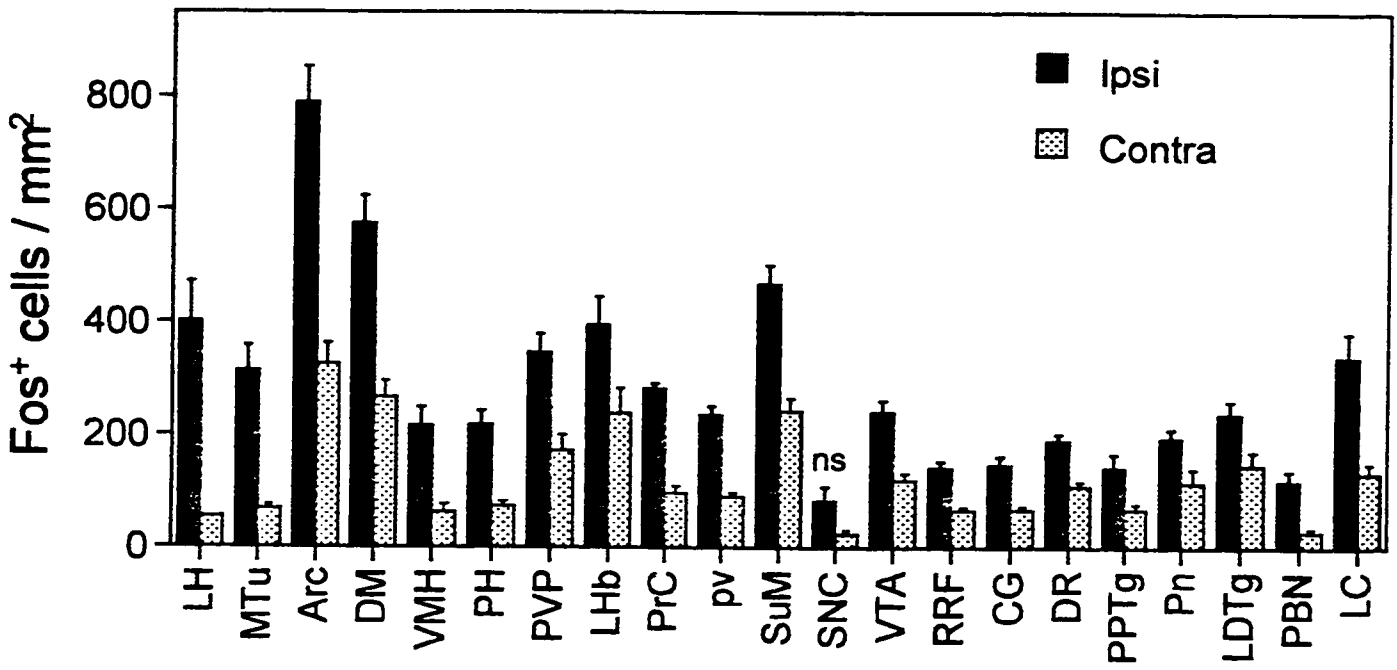
Fos+ cells / mm2
800
600
400
200
0
Ipsi
Contra
ns
LH
MTu
Arc
DM
VMH
PH
PVP
LHb
PrC
pv
SuM
SNC
VTA
RRF
CG
DR
PPTg
Pn
LDTg
PBN
LC

Table 2.2

Relative and absolute FLIR density in the stimulated versus the unstimulated hemisphere across brain regions

Structure	Ratio	Density	n
LH	7.4 : 1	++++	7
MTu	4.6 : 1	+++	7
Arc	2.4 : 1	++++	7
DM	2.2 : 1	++++	7
VMH	3.5 : 1	++	7
PH	3.0 : 1	++	7
PVP	2.0 : 1	+++	7
LHb	1.7 : 1	+++	7
PrC	3.0 : 1	+++	7
pv	2.6 : 1	++	7
SuM	1.9 : 1	++++	7
SNC	3.4 : 1	+	7
VTA	2.0 : 1	++	7
RRF	2.2 : 1	++	7
CG	2.2 : 1	++	7
DR	1.7 : 1	++	7
PPTg	2.1 : 1	++	7
Pn	1.7 : 1	++	6
LDTg	1.6 : 1	++	5
PBN	4.2 : 1	++	5
LC	2.6 : 1	+++	5

Column 2 contains the ratios of FLIR densities in homologous structures in the two hemispheres (stimulated/unstimulated). Column 3: 0-100 cells/mm^2='+'; 101-250 cells/ mm^2='++'; 251-400 cells/ mm^2='+++'; and >400 cells/ mm^2='++++'.

Fig. 2.5. Representative digitized images showing substantially more FLIR in the stimulated (left) as opposed to the unstimulated (right) hemisphere. Structures pictured: LH, MTu, Arc, DM (A: bregma, -3.6 mm); SuM, SNC, VTA (B: bregma, -4.8 mm); CG (C: bregma, -5.8 mm). Scale bars: A-C, 250 μm. (3V, third ventricle; Aq, cerebral aqueduct; cp, cerebral peduncle; f, fornix; ic, internal capsule; ml, medial lemniscus)

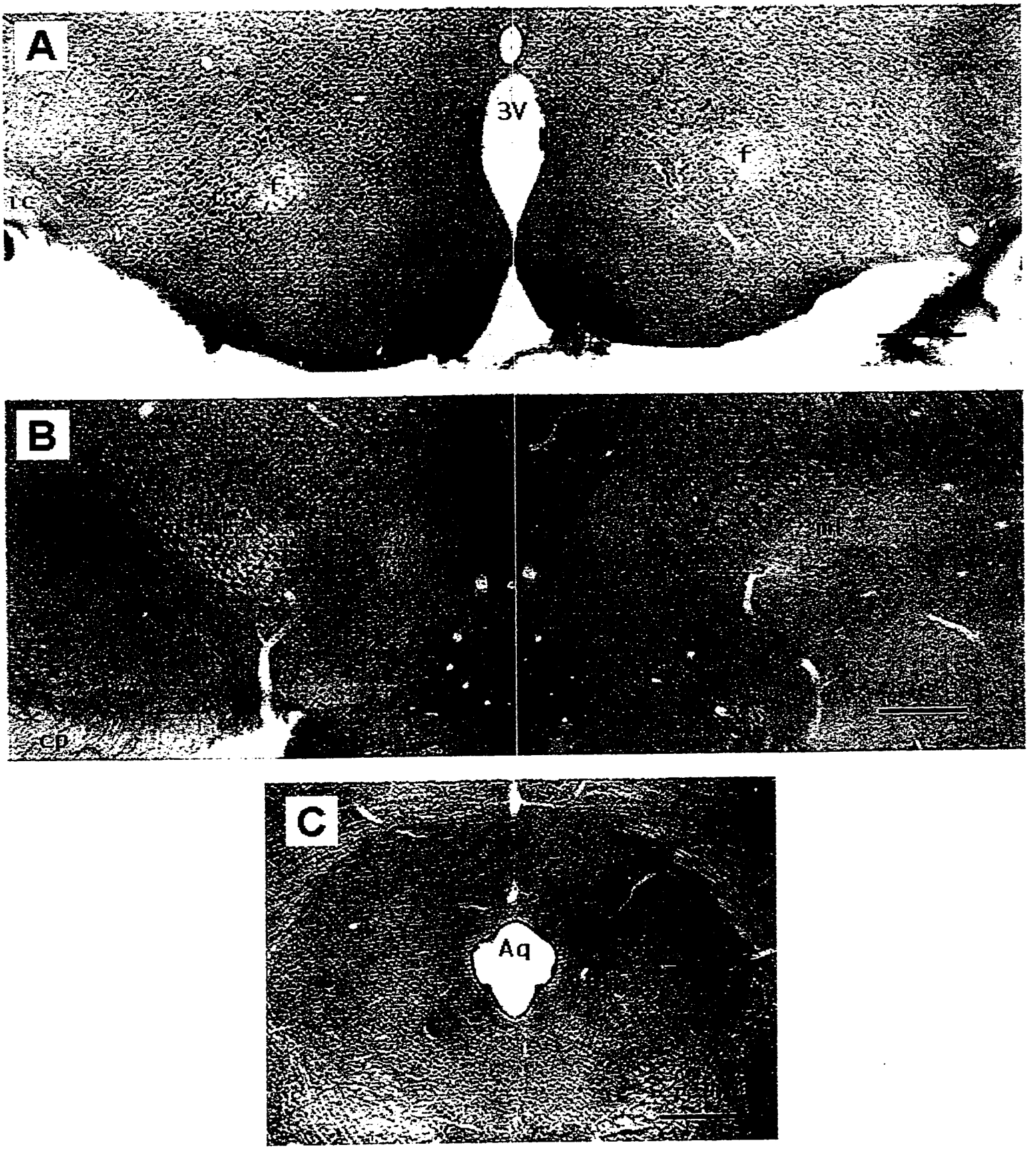
A
3V
f
f
B
cp
C
Aq

Fig. 2.6. Representative digitized images showing substantially more FLIR in the stimulated (left) as opposed to the unstimulated (right) hemisphere. Structures pictured: PPTg (A: bregma, -7.8 mm); DR, LDTg, PBN (B: bregma, -8.7 mm); LC (C: bregma, -9.8 mm). Scale bars: A, B, 250 μm; C, 100 μm. (me5, mesencephalic trigeminal tract; mlf, medial longitudinal fasciculus; scp, superior cerebellar peduncle; xscp, decussation of the superior cerebellar peduncle)

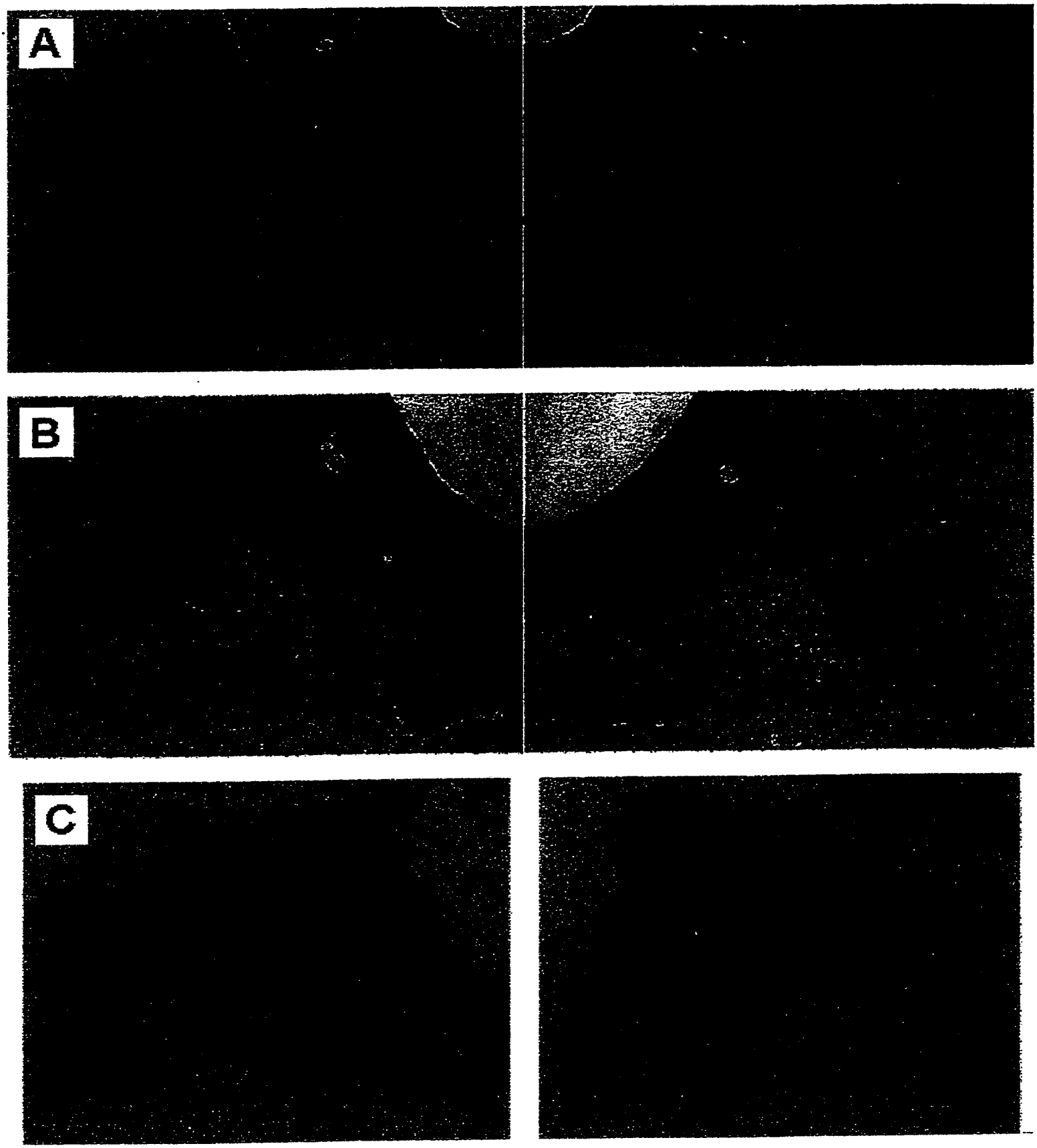
A
B
C

2.3.4. Discussion

The present study provides new information concerning the discrete distribution of the FLIR induced by LH stimulation in regions caudal to the stimulation electrode. This is the first study to provide a detailed description of the midbrain and hindbrain structures that are activated by rewarding stimulation of the LH. Gallistel et al. (1985) and Porrino et al. (1990) using 2DG autoradiography as well as Bielajew (1991), using CO histochemistry, failed to detect activation posterior to the VTA after LH self-stimulation. Esposito et al. (1984) reported increases in glucose utilization caudal to the VTA after rewarding stimulation of the VTA, but only in a subset of the structures that showed activation in the present study. Thus, apart from offering cellular resolution, Fos immunostaining appears to be a highly sensitive method for visualizing neurons activated by rewarding stimulation. I should note, that the LH stimulation current used in this study falls toward the upper range of currents typically self-administered in BSR experiments. Thus, it is not surprising that a substantial density of Fos-positive cells was found in many nuclei that give rise to or receive synaptic input from fibers passing through the LH (Barone, Wayner, Scharoun, Guevara-Aguilar, & Aguilar-Baturoni, 1981; Hallanger & Wainer, 1988; Nieuwenhuys et al., 1982; Saper, Swanson, & Cowan, 1979; Steininger, Rye, & Wainer, 1992; Veening et al., 1982; Villalobos & Ferssiwi, 1987). It would be interesting to determine whether substantially lower currents produce a similar patterns of Fos staining.

Cells in two of the regions showing increased Fos expression, the VTA and PPTg, have been implicated as postsynaptic elements in the circuitry subserving the rewarding effect of LH stimulation (Wise, 1996; Wise & Rompré, 1989; Yeomans et al., 1993). In future studies, Fos immunostaining can be combined with anterograde and retrograde tracers and with specific stains for dopaminergic and cholinergic neurons to determine the neurochemistry of Fos-positive neurons as well as their afferent and efferent connections. McGregor & Hunt (1996) have already taken a first step in that direction by combining Fos and tyrosine hydroxylase labeling (I describe the results of this experiment in section 2.4.2.).

Combining methods could also serve to test specific hypotheses about the identity of the first stage neurons. For example, Gallistel et al. (1996) recently proposed that these neurons are bipolar, extensively collateralized, cells with both their somata and the majority of their terminals located caudal to the diencephalic MFB. Do any of the Fos-positive neurons in the midbrain or hindbrain have these morphological characteristics? To find out, Fos immunostaining could, for example, be combined with the anti-200 KiloDalton neurofilament immunostaining method that permits the visualization of myelinated axons (Yao, Komoly, Zhang, & Webster deF, 1994). Thus, if neurons responsible for BSR do indeed express Fos, the combination of morphological, neurochemical and tracing methods with Fos immunohistochemistry should make possible a detailed cellular analysis of the reward-related circuitry.

2.4. EXTENDING THE APPLICATION OF THE FOS IMMUNOSTAINING TECHNIQUE TO HIGHLIGHT REWARD-RELATED NEURONS

To date, knowledge concerning the substrate for MFB self-stimulation was based primarily on psychophysical, electrophysiological, lesion, and pharmacological studies. These approaches have yielded only oblique inferences about which neurons may play a role in BSR. To complement these approaches I used Fos immunohistochemistry to visualize neurons activated by LH self-stimulation. Judging from the results, Fos immunostaining surpasses in resolution and sensitivity imaging methods used in prior studies.

A major advantage of Fos immunostaining, one that arises from the nuclear location of the Fos protein, is that this technique is readily combined with labeling methods for visualizing retrograde/anterograde tracers and antibodies to cytoplasmic proteins associated with particular neurotransmitter systems. By combining Fos immunohistochemistry with such methods, the trajectories, neurochemical coding, and location of candidate cells can be described. Such information can serve as the foundation for additional lesion and pharmacological studies aimed at determining which of the candidates actually contribute to the rewarding effect of MFB stimulation. Thus, the Fos experiments I presented set the stage for a series of follow-up experiments with the potential to bring us closer to the characterization of the substrate for

MFB self-stimulation. To demonstrate this, I will briefly describe two, already completed, follow-up experiments.

2.4.1. Fos-Like Immunoreactivity in Forebrain Regions Following Self-Stimulation of the Lateral Hypothalamus and the Ventral Tegmental Area.

A relative drawback of Fos immunolabeling is the inability to discriminate between reward-related neurons and other activated neurons that do not contribute to MFB self-stimulation. Stimulation of the LH activates a large number of pathways. Some means is needed of narrowing down the search for the neurons that subserve the rewarding effect of the stimulation. One means of doing so is to take advantage of the psychophysical finding that at least some of the first stage fibers responsible for MFB self-stimulation are continuous between the LH and VTA (Bielajew & Shizgal, 1982; Shizgal et al., 1980). Regions where Fos expression is increased following rewarding stimulation of both the LH and the VTA should be considered particularly promising as potential origins of first stage fibers.

Using this logic, Flores, Arvanitogiannis, & Shizgal (1997) examined FLIR in a preselected number of forebrain regions following self-stimulation of the LH and the VTA. Asymmetrical FLIR following stimulation of both the LH and the VTA was observed in twelve of the fifteen structures that were examined: the nucleus accumbens, olfactory tubercle, septum, amygdala, bed nucleus of the stria terminalis, medial preoptic area, SI, LH, dorsomedial

hypothalamus, paraventricular nucleus of the hypothalamus, and VTA. A notable absence from this list is the LPO. Fos labeling in the LPO was weighted in favor of the stimulated hemisphere only in the case of LH stimulation. Excitotoxic lesions targeted at the LPO, despite producing large decreases in the reward effectiveness of LH stimulation, did not appreciably decrease the reward effectiveness of VTA stimulation (Arvanitogiannis et al., 1996b). Taken together these findings suggest that LPO neurons make a more important contribution to the rewarding effect of LH than VTA stimulation and thus, that these neurons may not make a substantial contribution to the collision effects obtained with concurrent LH and VTA stimulation. Indeed, not all the projections from the LPO to the LH extend as far as the VTA, only those arising in the posterolateral aspects of the nucleus (Nieuwenhuys et al., 1982).

It is already evident in this discussion that the results of studies in which BSR has been challenged with lesions provide an indication of which of the listed regions may contain reward-related neurons. Only in the case of the SI, LH, and VTA have relatively large and long-lasting decreases in the reward effectiveness of MFB stimulation been observed following lesions (Arvanitogiannis et al., 1996b; Gallistel et al., 1996). Although the SI was damaged in the excitotoxic study aimed at the LPO, it has not served as the principal focus of any lesion experiment. Thus, a pressing issue is to directly assess the role played by SI neurons in the rewarding effect of MFB stimulation.

Lesion studies have also been used to address the role that some of the other structures play in BSR. Unfortunately, the methodology used in most of these studies restrict their interpretation. Only two studies, focused on the amygdala (Waraczynski et al., 1990) and the dorsomedial hypothalamus (Waraczynski et al., 1992), were conducted using a multiple-current design and a small sampling grain. Electrolytic lesioning of these structures failed to attenuate the reward effectiveness of MFB stimulation. Excitotoxic lesions of the nucleus accumbens (Johnson & Stellar, 1994) and transsections of the medial septum, diagonal band, and medial preoptic area (Waraczynski, 1988) were also interpreted as being ineffective in degrading MFB reward. However, in both of these studies the rate-frequency curves were sampled at low resolution. Moreover, in the excitotoxin study data collection was suspended for 3 weeks following the lesions and thus, possible transient changes could not be measured, while in the knife-cut study each subject was tested only at a single current. In the latter study, two subjects with lesions just posterior to the LH stimulation electrode showed uncharacteristically modest, for this kind of damage, rightward curve shifts. Further lesion work will be required to assess the contribution to MFB self-stimulation of neurons residing in these structures. Finally, on the basis of the FLIR results, lesion studies of the role played by the olfactory tubercle, bed nucleus of the stria terminalis, and paraventricular nucleus neurons are warranted.

To extend these findings, I re-examined the immunostained tissue from this experiment and searched for areas other than the ones analyzed that may

have been activated by stimulation of both the LH and the VTA. One area clearly stands out from this re-examination: the lateral habenular nucleus. The lateral habenular nucleus projects to dopamine neurons in the VTA, extends posteriorly to the dorsal and median raphé, central grey, pontine nuclei, and anteriorly through the MFB to the LH, LPO, and SI (Araki, McGeer, & Kimura, 1988; Herkenham & Nauta, 1977; Herkenham & Nauta, 1979; Li, Takada, & Mizuno, 1993a; Parent, Gravel, & Boucher, 1981). It receives reciprocal connections from the VTA and several basal forebrain nuclei as well as from the nucleus accumbens and the prefrontal cortex (Greatrex & Phillipson, 1982; Li et al., 1993a; Li, Takada, Shinonaga, & Mizuno, 1993b). I refer to these anatomical considerations not only to explain the Fos labeling but also to point out that the anatomy of the lateral habenula suggests a potential role for this structure in self-stimulation. Gomita & Gallistel (1982) have suggested that dopaminergic drugs exert their effect on the rewarding efficacy of stimulation by way of the lateral habenula. Sutherland & Nakajima (1981) showed that rats can learn to bar press for electrical stimulation of the medial or lateral habenular nucleus but not the surrounding thalamic nuclei. However, they also showed that MFB self-stimulation was enhanced by ipsilateral habenular lesions that damaged both the lateral and medial habenular nuclei and concluded that habenular stimulation can produce a rewarding effect without requiring the participation of the well-known MFB reward system. Still, it seems worthwhile to revisit the role of this structure in MFB self-stimulation by

producing lesions (perhaps bilateral) that specifically destroy the lateral habenula and examining the effects of these lesions with modern lesion methods.

In contrast to the results obtained with Fos immunostaining, Gallistel et al. (1985) using 2DG autoradiography found that there was bilateral suppression of activity in the lateral habenula in response to rewarding stimulation of the posterior LH. The diametrically opposite results obtained with Fos immunostaining and 2DG autoradiography are consistent with the idea that the two techniques highlight different neuronal compartments. The complementary nature of the two techniques provide a rationale for their combined use to label sections taken from the same brain.

It is noteworthy, that the results of the experiment by Flores et al. (1997) with respect to LH self-stimulation are consistent with the results in Experiment 1. This comparison indicates that Fos immunolabeling is a reliable method for visualizing self-stimulation-induced neuronal activation. However, I should note that in Experiment 1 two subjects had no Fos expression in the olfactory tubercle and the lateral habenular nucleus in contrast to the subjects in the Flores et al. (1997) study that all showed robust Fos expression. This discrepancy may be due to modifications in the immunohistochemistry procedure (described in the Methods section of Experiment 2) that result in better staining.

2.4.2. Fos-Like Immunoreactivity Following Self-Stimulation of the Lateral Hypothalamus: A Double Labeling Study with Tyrosine Hydroxylase

I mentioned previously that FLIR can result from transsynaptic as well as from antidromic activation. According to Sagar et al. (1988) Fos expression occurs at least two synapses from the cells that are directly stimulated. In the discussion of my results I considered transsynaptic Fos expression a limitation of the Fos immunostaining technique inasmuch as one cannot differentiate between first stage neurons and their efferents. Nevertheless, this shortcoming can turn into an advantage. Remember, for example, that according to one hypothesis dopamine neurons in the VTA are in series with and thus, become activated by the directly-stimulated neurons. If so, dopamine neurons in the VTA should express Fos after rewarding stimulation of the LH.

Recently, McGregor & Hunt (1996) confirmed and extended the findings reported in this thesis. Once again, the goal was to identify by means of Fos immunohistochemistry brain areas activated by LH self-stimulation. However, the stimulation current used in their experiment was much lower (200 μA) than the currents used in Experiments 1 and 2. This manipulation did not change appreciably the overall pattern of Fos expression (with the exception of the olfactory tubercle where no FLIR was detected and the lateral habenula where FLIR was bilaterally symmetrical). In addition to assessing FLIR, an antibody against tyrosine hydroxylase, a key enzyme for dopamine

and noradrenaline biosynthesis, was used to co-stain neurons in order to find out whether dopamine neurons in the VTA are activated consequent to LH self-stimulation. This was not the case. That is, very few dopamine cells in the VTA were double labeled with Fos and tyrosine hydroxylase. The straightforward interpretation of this result is that dopamine neurons do not become transsynaptically activated by LH rewarding stimulation and thus, dopamine neurons do not relay the reward signal. Gallistel et al. (1985) using the 2DG method arrived at the same conclusion by noting that none of the ascending dopamine projection systems were activated by the stimulation.

The negative result of the Fos-tyrosine hydroxylase double-immunohistochemistry experiment does not lend support to the hypothesis that dopamine neurons are in series with the first stage ones. But one could raise the question of whether dopamine neurons in the VTA express Fos when stimulated. Does the absence of FLIR indicate that dopamine neurons were not stimulated, or that, despite them being stimulated, they somehow lack the machinery necessary to express Fos? Numerous studies have shown that the latter possibility is unlikely. For example, many tyrosine hydroxylase labeled neurons in the VTA express Fos after various manipulations (Deutch et al., 1991; Ma, Zhou, & Han, 1993a; Ma, Zhou, & Han, 1993b).

Another possible explanation for these data is that dopamine neurons have a higher activation threshold for Fos induction than first stage neurons. If so, the stimulation may not have been adequate to engage the Fos-

synthesis machinery of the dopamine neurons. It is known, for example, that dentate granule cells in the hippocampus can express Fos after high-frequency electrical stimulation, and this is N-methyl-D-aspartic acid (NMDA) receptor-mediated. However, a certain level of stimulation is required for Fos expression to occur. Thus, 10 bursts of high-frequency electrical stimulation do not induce Fos in the granule cells, whereas 50 bursts do (Demmer et al., 1993).

A technical aspect of this study warrants further comment. The same chromogen (DAB) was used to detect the two labels. Fos immunolabeling was performed with DAB intensified with cobalt chloride, whereas DAB only was used as chromogen for tyrosine hydroxylase immunohistochemistry. The two labels are supposed to be distinguished on the basis of their different colors and intacellular distribution--the black Fos labeling that is restricted in the nucleus versus the brown immunostaining in the cytoplasm of tyrosine hydroxylase containing cells. The main pitfall of this combined protocol is represented by the possibility of the cytoplasmic label interfering with the unambiguous visualization of the nuclear label. The denser the cytoplasmic staining the more difficult is the detection of nuclear staining. As a consequence, great caution should be adopted in interpreting the results stemming from the use of the metal-intensified DAB - DAB method. To reduce interference between the two stainings one could use two different chromogens whose color can be easily distinguished. Better yet, the

combination of two fluorescent markers that can be studied under different filters should completely eliminate interference.

Irrespective of whether or not dopamine cells are in series with the first stage neurons, the results of the experiment conducted by McGregor & Hunt, (1996) show that neurons in the VTA whose phenotype is other than that of dopamine neurons are activated by the rewarding stimulation. Further studies are needed to determine the identity and the role of these neurons in BSR as well as the BSR-relevant interactions they may have with dopamine neurons.

CHAPTER 3

IMPLICATIONS STEMMING FROM THE USE OF EXCITOTOXIC LESIONS IN SELF-STIMULATION

Once candidate brain regions containing neurons activated by rewarding stimulation have been identified with Fos immunohistochemistry, it is important to assess the strength of their candidacy. Lesion experiments provide a direct means of narrowing down the list of candidate structures. Among the various lesioning tools, excitotoxins hold a prominent position because of their specificity (Winn, 1991). That is, excitotoxins kill neurons with somata near the injection site while sparing fibers of passage (Hastings, Winn, & Dunnett, 1985; Schwarcz et al., 1979). In the first part of this chapter I describe the use of excitotoxins to find whether the medial part of the basal forebrain could be a source of first stage fibers. Then I dig further into some issues that constrain the interpretation of excitotoxin lesion experiments.

3.1. EFFECTS OF EXCITOTOXIC LESIONS OF THE MEDIAL BASAL FOREBRAIN ON MFB SELF-STIMULATION

3.1.1. Introduction

In the previous chapter, I showed that rewarding stimulation of the LH increases FLIR in an ipsilateral, basal forebrain region extending from the medial preoptic area (MPO) to the LPO and SI. It is safe to assume that

neurons with somata in but a subset of the brain structures that displayed an increase in Fos labeling make a substantial contribution to the reward efficacy of MFB self-stimulation. Lesion results are crucial to interpreting the observed distribution of FLIR. It has been already shown that excitotoxic lesions centered around the LPO and the SI produced large transient (0.3-0.55 $\log_{10}$ units) or sustained (0.2-0.5 $\log_{10}$ units) increases in the number of pulses required to sustain half-maximal lever-pressing for LH stimulation in 10 of 13 rats (Arvanitogiannis et al., 1996b). Here, I assess changes in self-stimulation of the LH and VTA following excitotoxic lesions of more medial structures, including the MPO. Changes in the reward effectiveness of the stimulation are inferred, at three different currents, from the lateral displacement of curves that relate the performance of the subject to stimulation strength. As conceived by Murray & Shizgal (1991), the three current design is geared toward maximizing the likelihood of obtaining a lesion effect in case where there is misalignment between the stimulated and the damaged tissue.

3.1.2. Materials and Methods

3.1.2.1. Subjects and Surgery

Ten male Long-Evans rats weighing approximately 400-500 g were used. The rats were housed individually, on a reversed 12 h light/dark cycle. Food and water were available continuously.

Each animal was administered atropine sulphate (0.25 mg/kg, SC) to reduce excessive salivary and bronchial secretions and was subsequently anesthetized with sodium pentobarbital (Somnotol, 65 mg/kg, IP). After a midline incision, cranium exposure, and trephining, animals were stereotaxically implanted with one monopolar stimulating electrode in the left LH (coordinates: -2.8 mm from the bregma, 1.7 mm from the midsagittal sinus, -7.7 mm from the dura mater, with skull level), and another one in the left VTA (coordinates: -4.8 mm from the bregma, 0.9 mm from the midsagittal sinus, -7.7 mm from the dura mater, with skull level). The electrodes were constructed from 00 insect pins and were insulated with Formvar except at the tip. A wire twisted around three jeweler's screws served as the current return. A 15 mm cannula constructed from 21-gauge stainless steel tubing was implanted 5 mm above the MPO (coordinates: -0.3 mm from the bregma, 0.7 mm from the midsagittal sinus, 3 mm from the dura mater, with skull level). The cannula was plugged with a removable 26-gauge obturator that extended down to the desired injection site (8 mm from the dura mater). Dental cement encased the entire assembly. Postoperative pain was reduced by administering Buprenorphine (Buprenex, 0.05 mg/kg, SC). A 5-d recovery period followed surgery.

3.1.2.2. Behavioral Procedure

The equipment used for this experiment is identical to that described in section 2.2.2.2.

During the shaping stage, rats learned to lever press for 0.5 s trains of 0.1 ms, cathodal, rectangular pulses delivered to either stimulating electrode. At the end of this stage the rats self-stimulated reliably at a wide range of stimulation parameters.

During the testing stage, the electrical stimulation parameters were the same as those used during training. On each testing day, and for each stimulation site, four curves relating the response rate to the number of pulses per train (rate-number curves) were collected at each of three currents by allowing the rats to respond for a descending series of pulse frequencies spread at intervals of 0.05 $\log_{10}$ units. Each frequency was available during a 30 s trial during which the rate of lever pressing was recorded. When the rat emitted fewer than 10 responses per 30 s trial on two consecutive trials, testing at another current was initiated and the frequency was reset at a level that supported asymptotic responding for the particular current. At the start of each trial, the rat received five priming trains of stimulation, set at the same parameters as the stimulation available at that trial. The first determination of the rate-number curve at each current served as a warm-up, and the resulting curve was not considered in the data analysis.

The number of pulses required to sustain a half-maximal response rate (the 'required number of pulses') was calculated for each rate-number curve and the three estimates of the required number of pulses for each current at a given site were averaged within sessions. The required number of pulses is

used as an index of the position of the rate-number curves along the number of pulses axis. An effective lesion is expected to laterally displace the rate-number curves toward higher frequencies, thus augmenting the required number of pulses.

3.1.2.3. Excitotoxic Lesions

After the collection of baseline data, rats were anesthetized and placed in a stereotaxic frame. A 1 µl Hamilton syringe filled with a solution of 70 nmol of NMDA (pH= 7.2) in 0.5 µl of a modified Ringer's solution (Moghaddam & Bunney, 1989) was mounted on the stereotaxic frame and slowly advanced into the MPO through the already implanted cannula. Pressure injections were made in a pulsatile fashion so as to deliver 0.05 µl every 60 s. After the injection, the syringe was left in place for an additional 5 min to allow for diffusion. Postlesion testing commenced 1 day after the lesion.

3.1.2.4. Histology

After completion of the experiment, rats were injected with a lethal dose of sodium pentobarbital (100 mg/kg, IP) and perfused with heparinized phosphate-buffered saline followed by 10% formalin. The brain was removed from the cranial vault and stored in 10% formalin. After formalin fixation, and a 24 h incubation period in 20% sucrose formalin, two parallel sets of 30 µm sagittal sections were cut on a cryostat, and mounted on SuperFrost Plus slides (Fisher Scientific). One set of sections was stained for Nissl substance

using formal thionin, and a second set of sections was stained for myelin using the hematoxylin-based Weil procedure. The location of the lesioned tissue, injection sites, and electrode tracks was identified with the aid of a stereotaxic atlas (Paxinos & Watson, 1986).

3.1.3. Results

Of the ten rats tested in this study, eight were trained to lever press for stimulation through both the LH and VTA electrodes and two self-stimulated only through the VTA electrode. Table 3.1 presents a summary of behavioral data for all ten subjects in this experiment. NMDA lesions of the medial basal forebrain were without a major long-lasting effect on MFB self-stimulation. Moderate increases in the required number of pulses (at least 0.10 $\log_{10}$ units), evident at the low and middle currents, were seen in only two of the subjects (MP5, MP6). In the case of MP5, the increase was observed for stimulation delivered to the LH, whereas for MP6 only stimulation through the VTA was affected. In six of the ten subjects (MP2, MP7, MP12, MP13, MP15, MP16), the injections failed to alter the required number of pulses. In the case of subjects MP8 and MP14, the required number of pulses, particularly for the high current, decreased substantially (at least 0.10 $\log_{10}$ units) after the lesion. For both of these subjects the effect was seen with self-stimulation of the VTA. Plots of the required number of pulses as a function of days pre- and postlesion for the subjects that showed either a substantial increase or decrease in the required number of pulses are presented in Fig. 3.1.

Analysis of maximum response rates was performed for all subjects (Table 3.1). In the case of the two subjects (MP5, MP6) that showed increases in the required number of pulses, response rates were also depressed. Among these subjects, MP5 showed the largest depression in maximum rate (0.225 $\log_{10}$ units below baseline), observed at the middle current. However, the degree to which maximum rates were affected in this study did not predict the magnitude of the observed changes in the required number of pulses. In the case of MP5 the largest effect in the required number of pulses was seen at the low current whereas response rate was maximally affected at the middle current. For subject MP6 the required number of pulses was increased at both the low and middle currents, but maximum rate substantially decreased only at the low current. Furthermore, response rates for MP5 and MP6 were decreased for stimulation delivered to both the LH and the VTA, yet the rewarding effect was attenuated after stimulation of only one of the two sites: the LH in the case of MP5 and the VTA in the case of MP6. It is striking that in the case of the rat (MP15) in which the largest and most consistent decreases in maximum rate were observed, the required number of pulses remained unchanged. Subjects MP8 and MP13 also showed some decreases in the maximum rate that were not accompanied by shifts in the required number of pulses.

Table 3.1

Postlesion changes in the required number of pulses and the maximum response rate as a function of current.

Rat	Stimulation Site	Current	Required Number of Pulses: Shift from Baseline	Maximum Rate: Shift from Baseline
MP2	LH	200	0.049	0.017
		400	0.033	-0.016
		800	0.030	0.014
	VTA	447	0.003	-0.052
		708	-0.060	-0.081
		1120	-0.053	-0.028
MP5	LH	316	0.112*	-0.152*
		562	0.103*	-0.225*
		1000	0.087	-0.090
	VTA	388	0.044	-0.120*
		631	0.063	-0.021
		1000	0.058	-0.105*
MP6	LH	200	0.003	-0.111*
		400	0.014	-0.076
		800	-0.066	-0.071
	VTA	200	0.163*	-0.143*
		400	0.114*	-0.062
		800	0.003	-0.071
MP7	LH	316	0.033	0.019
		562	0.048	-0.020
		1000	0.016	-0.021
	VTA	200	-0.007	-0.004
		400	-0.012	0.050
		800	-0.053	0.022
MP8	LH	200	0.039	-0.178*
		400	0.034	-0.054
		800	0.026	-0.064
	VTA	200	-0.056	-0.091
		400	-0.103*	0.000
		800	-0.114*	-0.045
MP12	VTA	282	-0.004	0.013
		501	-0.022	-0.047
		891	-0.036	0.046
MP13	LH	282	-0.048	-0.098
		501	-0.056	-0.077
		891	-0.072	-0.056
	VTA	282	-0.024	-0.095
		501	-0.074	-0.107*
		891	-0.057	0.042
MP14	VTA	282	-0.032	-0.062
		501	-0.037	-0.008
		891	-0.106*	-0.069
MP15	LH	282	-0.044	-0.142*
		501	0.004	-0.140*
	VTA	355	0.079	-0.245*
		562	0.076	-0.163*
		891	0.047	-0.136*
MP16	LH	282	0.027	0.083
		501	-0.020	0.017
		891	0.007	0.026
	VTA	282	0.016	0.091
		501	-0.010	0.082
		891	-0.021	0.065

Fig. 3.1. Required number of pulses as a function of days pre- and postlesion for subjects in which lesions produced either a substantial increase or decrease in the required number of pulses. The alphanumeric in the upper left side of the graphs identifies the subjects and the stimulation site from which the particular data were obtained. Prelesion and postlesion data are represented by filled and open symbols respectively. The squares, circles, and triangles represent the low, middle, and high currents, respectively. The three horizontal, dotted lines extending across each graph indicate the mean of the baseline data for each current. Error bars around some ata points represent the S.E.M. for that test day. In cases where error bars are missing, the S.E.M. for that test day was less than half the radius of the symbol.

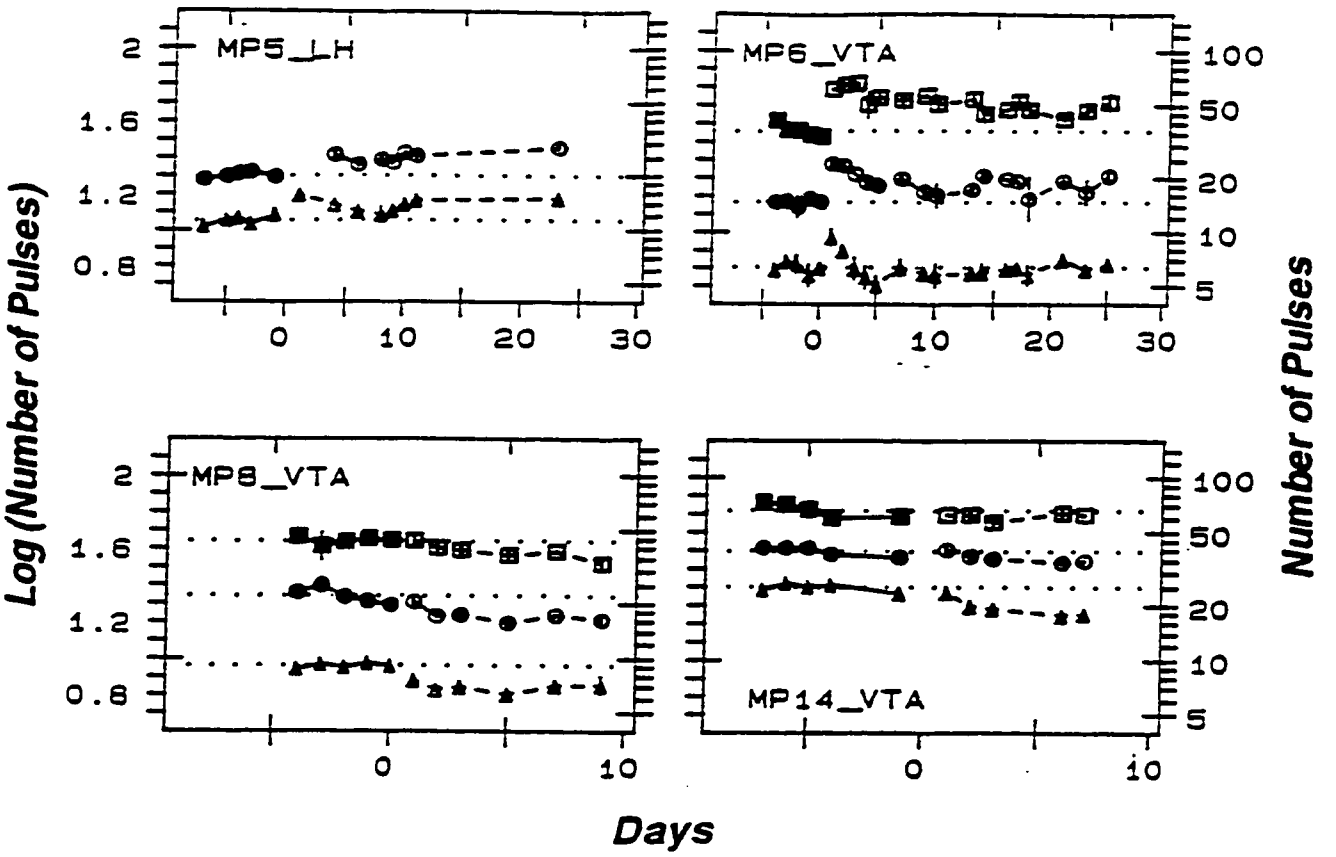
MP5_LH
MP6_VTA
MP8_VTA
MP14_VTA
Log (Number of Pulses)
Number of Pulses
Days
2
1.6
1.2
0.8
100
50
20
10
5
0
10
20
30

Histological examination confirmed that lesions in all of the subjects were medially located. Neither the LPO nor other laterally placed neighboring structures were damaged. The medial aspect of the bed nucleus of the stria terminalis and the MPO were the most consistently lesioned structures. Other areas that were more or less affected by the lesions are the septohypothalamic nucleus, medial septal nucleus, vertical limb of the diagonal band, anterior hypothalamic area, and paraventricular hypothalamic nucleus. Fig. 3.2 shows schematic reconstructions of the lesion and stimulation sites for the four subjects with a substantial increase or decrease in the required number of pulses. Histological reconstructions of the lesion damage and the stimulation sites for the rest of the subjects that did not show any postlesion changes in behavior are shown in Fig. 3.3. Varying degrees of demyelination, always less spread out than the area of cell loss, were evident in all subjects.

Fig. 3.2. Histological reconstructions of the lesion and stimulation sites for the four subjects with a substantial increase or decrease in the required number of pulses on sagittal plates from the Paxinos and Watson (1986) atlas. Filled triangles represent the electrode tips, stippled areas represent regions of cell loss, and filled areas represent regions of demyelination. The alphanumeric at the top of each column identifies the subject. The distance of the plate from bregma is given in the upper right-hand corner of each panel.

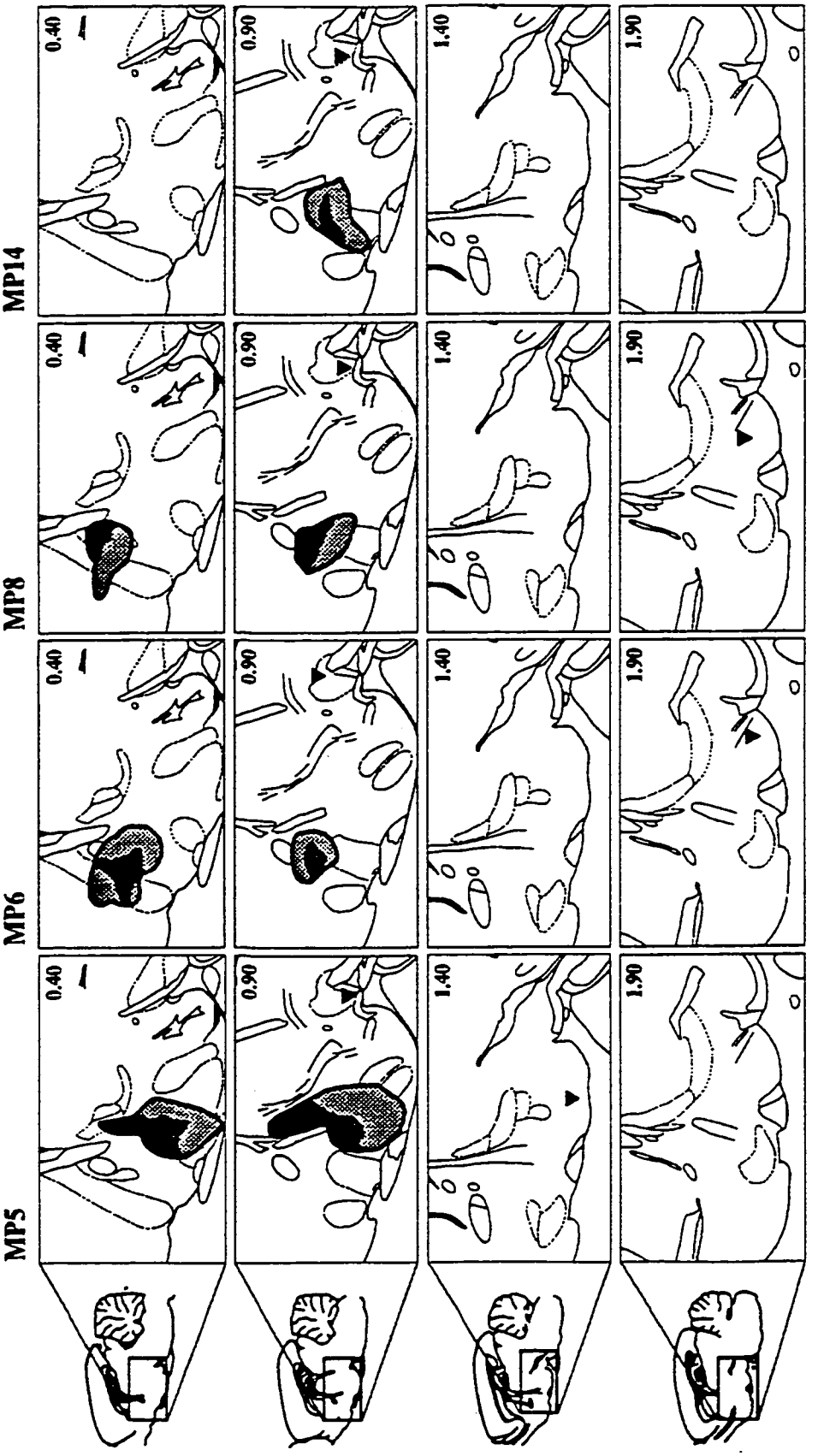
MP5
MP6
MP8
MP14
0.40
0.90
1.40
1.90

Fig. 3.3. Histological reconstructions of the lesion and stimulation sites for the subjects in which the lesions failed to alter the required number of pulses on sagittal plates from the Paxinos and Watson (1986) atlas. Filled triangles represent the electrode tips, stippled areas represent regions of cell loss, and filled areas represent regions of demyelination. The alphanumeric at the top of each column identifies the subject. The distance of the plate from bregma is given in the upper right-hand corner of each panel.

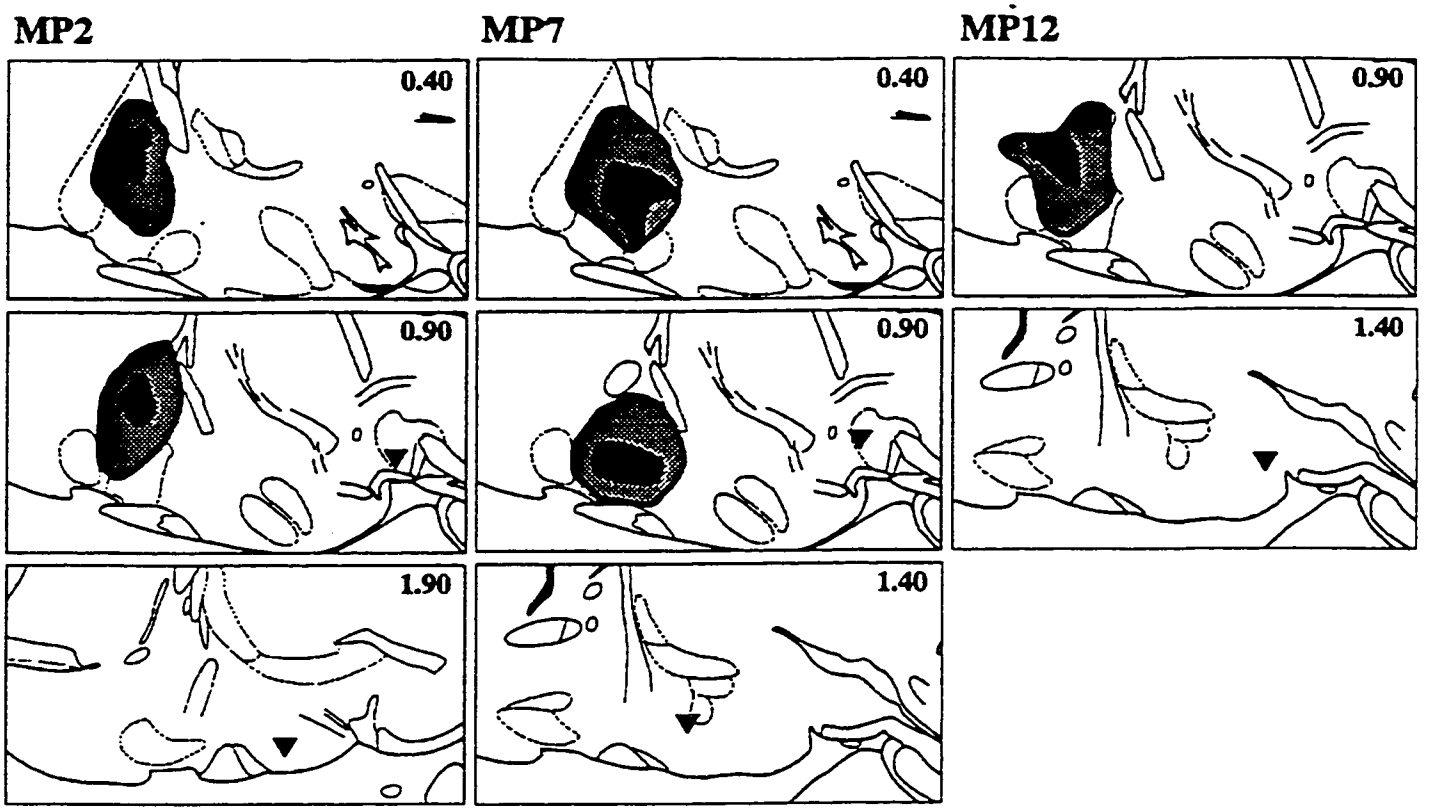
MP2
0.40
0.90
1.90
MP7
0.40
0.90
1.40
MP12
0.90
1.40

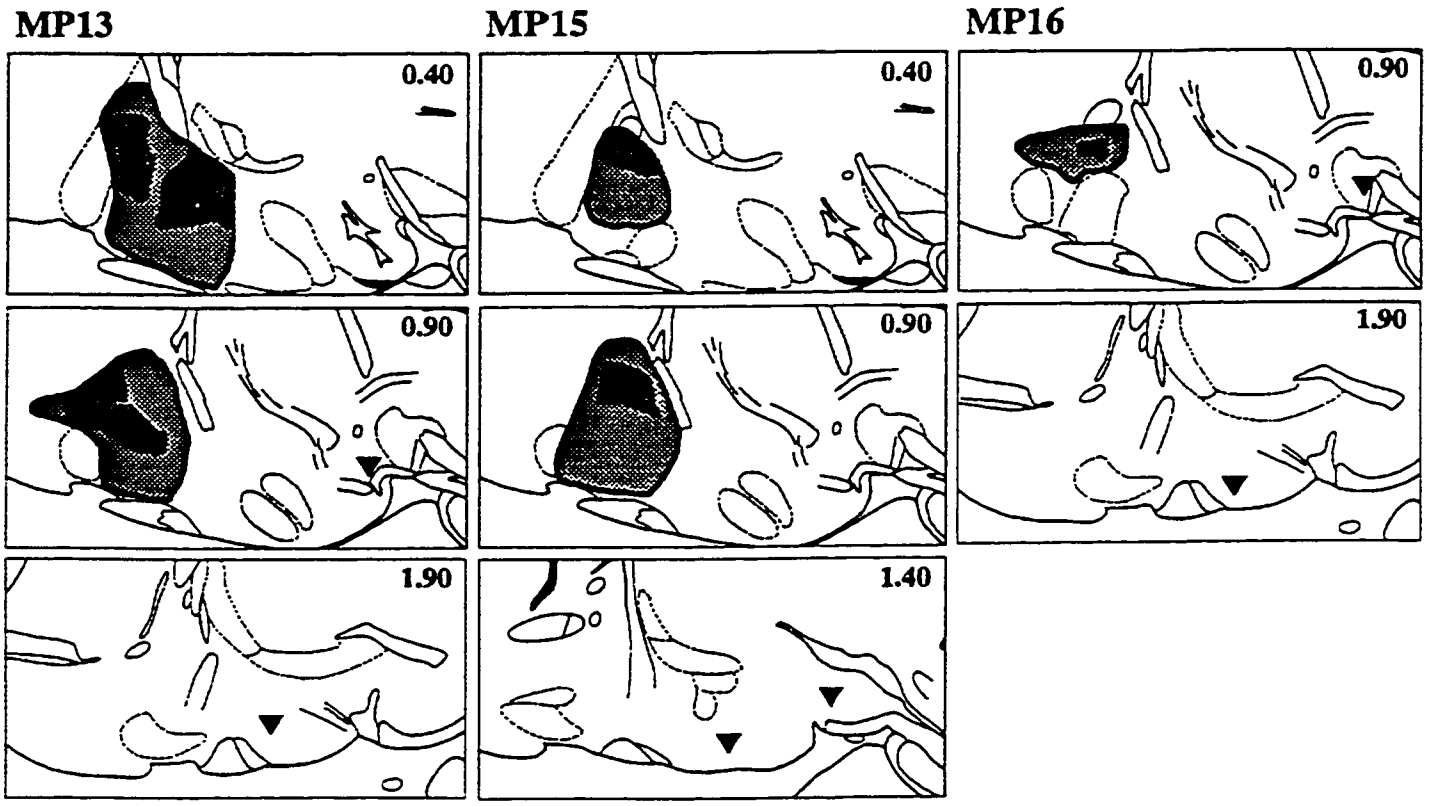
MP13
0.40
0.90
1.90
MP15
0.40
0.90
1.40
MP16
0.90
1.90

3.1.4. Discussion

Fos immunohistochemistry has revealed medially-placed basal forebrain structures such as the MPO and the bed nucleus of the stria terminalis that are activated, preferentially ipsilateral to the stimulation electrode, following rewarding stimulation of the MFB (Arvanitogiannis et al., 1996a). The damage produced by excitotoxic lesions provides a means of assessing the involvement of these structures in BSR. Taken at face value, the results of this work suggest that the MPO and bed nucleus of the stria terminalis should be excluded from the list of structures likely to contain first stage neurons.

In a study complementary to the present one, large excitotoxic lesions in the lateral portion of the basal forebrain produced among the largest effects that have been reported. Thus, it was of interest to determine whether the effectiveness of large excitotoxic lesions can be generalized to the entire basal forebrain region or whether only the more lateral region is important to BSR. Taken together, the data from the two excitotoxin lesion studies suggest that neurons residing in the lateral portion of the basal forebrain are more likely to compose at least a part of the first stage substrate for MFB self-stimulation than more medially placed neurons. Fig. 3.4 presents a comparison between the results of the present study and those obtained with excitotoxin lesions centered around the LPO. A clear dissociation in terms of lesion effectiveness is seen, that depends on the medial-lateral placement of the lesion.

Fig. 3.4. Cumulative distributions of effect sizes for subjects with MPO or LPO lesions. Each point gives the proportion of subjects showing increases in the required number of pulses equal to or less than the value along the abscissa. The curve for subjects with LPO lesions lies well to the right (towards larger increases in required number) than the curve for subjects with MPO lesions.

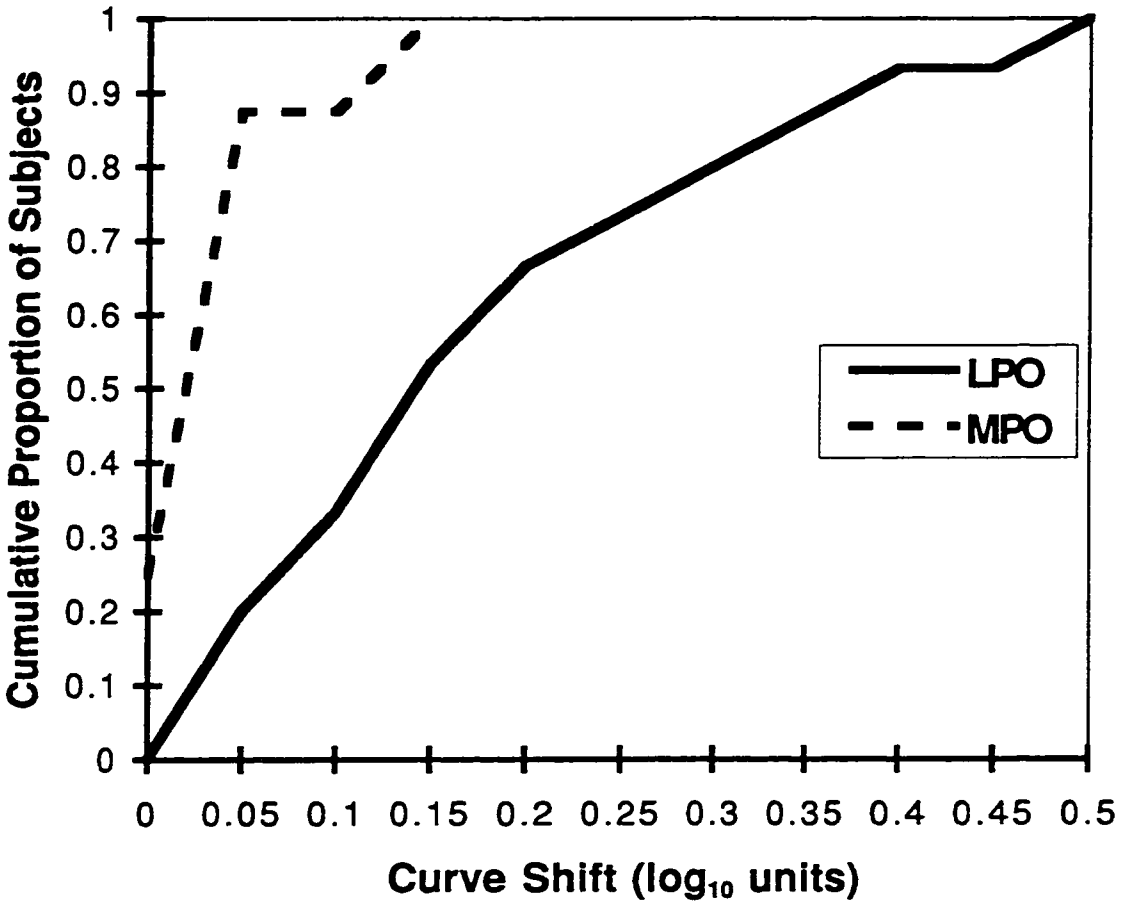
Cumulative Proportion of Subjects
1
0.9
0.8
0.7
0.6
0.5
0.4
0.3
0.2
0.1
0
0 0.05 0.1 0.15 0.2 0.25 0.3 0.35 0.4 0.45 0.5
Curve Shift (log_{10} units)
LPO
MPO

Waraczynski (1988) disrupted the descending outflow from the medial septum, diagonal band and preoptic areas without degrading the reward value of MFB stimulation. The knife-cut data were interpreted as evidence against the idea that first stage neurons might reside in forebrain nuclei. The combined data from the excitotoxic lesion studies challenge and refine this contention by revealing a placement-dependent dissociation of effective versus ineffective lesion sites. But how can the discrepant observations obtained with the knife- cut and excitotoxin lesions be reconciled?

To begin with, the two lesion methods produce different degrees of three-dimensional tissue damage. When rostro-caudal tissue damage surrounded the knife-cut, thus conferring to the lesion a three-dimensional configuration such as the one attained by excitotoxin lesions, then, knife-cuts in the LPO were somewhat effective in degrading the stimulation reward effectiveness (Waraczynski, 1988). Thus, some placement-dependent dissociation was observed in the knife cut study. There is evidence to suggest that the more the volume of the lesion, the greater is its effectiveness (Murray & Shizgal, 1991; Murray & Shizgal, 1996a). Large excitotoxic lesions or multi stage electrolytic lesions appear to be more effective than well confined electrolytic or two-dimensionally confined knife- cut lesions. This makes sense if neurons of different origins are important for self-stimulation. That is, large lesions may be effective because they destroy multiple sources of a heterogeneous reward substrate. Heterogeneity in the reward system might be as logically useful as the modern notion of multiple memory systems,

constructed to explain specific memory deficits as well as residual memory capacity after focal brain lesions in areas known to be involved in learning and memory (Tulving, 1985). If first stage neurons are spread in a relatively large area of the brain, large lesions spreading in all three planes might be required to produce long-term, substantial behavioral changes.

The lack of measurement sensitivity in the knife-cut study (Waraczynski, 1988) could be one of the reasons that a large distinction was not made between the effects of medial versus lateral lesions. In that study, the grain of stimulation frequencies tested was rather coarse (0.1 or 0.2 $\log_{10}$ units steps as opposed to 0.05 $\log_{10}$ units steps used in the excitotoxin study), thus making it hard to detect small but appreciable changes in reward efficacy. Accordingly, the criterion for a meaningful lesion effect in the knife-cut study was at least a 0.2 $\log_{10}$ units shift. But two pilot subjects that were given knife-cuts in the MFB just posterior to the electrode demonstrated curve shifts of approximately this magnitude. If disruption of the descending outflow from the stimulation site, known to produce massive decreases in reward (Gallistel et al., 1996), just reached the criterion for meaningfulness, how could slightly smaller but substantial effects of lesions placed rostrally to the stimulation electrode be detected? The problem of measurement sensitivity is compounded by the fact that the effects of knife cuts were assessed at only a single current (300-400 μA) thus, making it impossible to discern whether misalignment between the lesion and stimulation sites contributed to the lack of lesion effects.

The apparent inconsistency of the knife cut and excitotoxin results might reflect the absence of specifically-placed lateral lesions in the knife cut study. In that study, cuts in the LPO in most cases encroached, at least in part, the MPO. If, indeed, the LPO , anterior LH, and SI contain some of the first stage cells, lesioning them should decrease reward effectiveness. However, if the MPO and surrounding structures contain cells that counteract the rewarding effect of MFB stimulation, the net effect of lesioning both laterally- and medially-placed structures would leave the reward effectiveness of MFB stimulation unchanged (this argument was also made by Waraczynski, 1988). There is some evidence that medial structures may be a source of inhibition on stimulation-induced reward effects. Some of the knife cuts in the MPO actually decreased frequency thresholds for self-stimulation. Similarly, the required number of pulses was decreased in two of the subjects in the present study. Additional research is needed to determine whether a particular nucleus in the medial basal forebrain is a source of inhibition to the first stage. More specific lesions restricted to, for example, the MPO could provide us with an answer.

Provided that the lesion outcome reflects different degrees of cancellation between reward-decreasing and reward-increasing effects, the issue of lesion specificity gains in importance if the antagonistic systems are situated in close proximity. Pointing toward this possibility is the observation that in the two cases in this study that showed increases in the required number of pulses, the lesions were centered either caudally or dorsally with

respect to the MPO and thus did not produce any appreciable damage in the MPO. It is important to note, that in view of this argument one cannot conclude with certainty that all of the lesioned structures in this study do not contribute to the first stage. What if the MPO and bed nucleus of the stria terminalis are the substrates of antagonistic systems and decreases in reward effectiveness resulting from damage to the bed nucleus are compensated by lesioning the MPO? Provided that antagonistic systems do indeed exist, it is possible that large lesions may actually mask the contribution of a restricted set of neurons to the rewarding effect. Although large effects were produced with large excitotoxin lesions in the lateral basal forebrain, finding such effects in more medial structures may require lowering the dose of excitotoxin so as to produce more discrete lesions.

The issue of demyelination bears mentioning at this point. Varying degrees of demyelination were evident in all subjects. Assuming that demyelination affects the conduction properties of the fibers that course through the lesioned area, one can conclude that not only neurons residing in, but also fibers of passage running through the medial basal forebrain are not likely to be a part of the first stage. Keep in mind, however, that this conclusion cannot be drawn with certainty in case of antagonistic interactions in the reward substrate. If somata residing in and fibers coursing through the lesioned area actually carried reward signals of opposite sign, then demyelination could complicate the interpretation of the lesion results.

Excitotoxic lesions in the lateral and medial portions of the basal forebrain have offered some insight into which of the structures that are activated during MFB self-stimulation may play a role in BSR. Still, three issues limit the interpretation of the results stemming from excitotoxic lesions. The first one is the issue of demyelination. Before the classical claim concerning excitotoxin specificity is substantiated, questions about whether cell death or demyelination are responsible for the lesion effects will persist. The second issue concerns the ability of the curve shift method to measure lesion effectiveness. Curve-shifts are interpreted as changes in the rewarding efficacy of the stimulation within the model of a unitary reward substrate I presented in chapter one. However, the interpretation of such shifts becomes more complicated if the reward substrate is heterogeneous. Finally, changes in reward magnitude as assessed by the curve shift method cannot be ascribed with certainty to damage in the directly stimulated stage of the reward substrate. The remainder of this chapter explores these concerns in more detail.

3.2. EXCITOTOXIN-INDUCED DEMYELINATION

3.2.1. Introduction

One of the key advantages of excitotoxic lesions is that excitotoxins destroy cell bodies in the area of the injection, while leaving axons of passage intact. The problem of demyelination, however, muddles this scenario (Coffey, Perry, Allen, Sinden, & Rawlins, 1988; Coffey, Perry, & Rawlins, 1990; Dusart, Marty, & Peschanski, 1992). Although axons passing through an excitotoxin lesion appear intact with respect to neurotransmitter release and intra-axonal transport (Hastings et al., 1985; Schwarcz et al., 1979), their conduction properties may be compromised by loss of the myelin sheath (Waxman, 1977). Thus, a change in function after lesion may be the result of altering conduction through axons in the lesion area, and not of damaging the target nucleus. Finding a means of eliminating excitotoxin-induced demyelination would greatly increase the power of the excitotoxic lesion technique as a tool for linking function and structure.

To find such a means one has to know the mechanism underlying the demyelinating process. The dominant theory holds that demyelination results from an inflammatory response to local cell death and the subsequent infiltration through the blood-brain barrier of monocytes from the periphery (Anderson, 1991a; Coffey, 1988; Coffey, 1990). In fact, immune infiltrates appear in the area of the lesion from two to seven days after excitotoxin administration (Andersson, Perry, & Gordon, 1991a; Andersson, Perry, &

Gordon, 1991b). Demyelination should follow a similar, relatively slow, time course if blood-borne cells are responsible for the demyelination. However, direct evidence for this prediction is missing.

This study was undertaken to provide a direct test of whether excitotoxin-induced demyelination is indeed a delayed event, as predicted by the monocytic infiltration hypothesis. I looked for signs of demyelination at different times after excitotoxic insult by using both a conventional and an immunohistochemical stain. A limitation common to these stains is their lack of resolution. To remedy this, I introduce a modified immunostaining protocol to reveal the fine morphology of myelinated axons.

3.2.2. Materials and Methods

3.2.2.1. Experimental Manipulations

Six adult male Long-Evans rats weighing 300-350 g were used. They were housed two per cage in an animal colony room with a reversed 12-h light-dark cycle (light on between 20.00 and 08.00 h) and had free access to food and water.

Animals were anesthetized with pentobarbital (Somnotol, 65 mg/kg, IP), placed in a stereotaxic frame and covered with bubble-wrapper to prevent hypothermia. A midline incision was made through the scalp, the pericranium was displaced to the sides to provide a clear skull surface, and a hole was drilled over the LH. Following craniotomy, a 1.0 µl Hamilton

syringe was stereotaxically lowered to the LH (level-skull coordinates: 2.8 mm posterior to Bregma, 1.9 mm lateral to the mid-sagittal sinus, 7.5 mm ventral to the dura surface) to deliver 70 nmol of NMDA dissolved in 0.5 µl of 0.1 M phosphate-buffered saline (PBS, pH 7.4), with the pH adjusted with NaOH to 7.1-7.4. The total dose of NMDA was delivered over a 5 min period, at discrete steps of 0.05 µl/30 s, and the syringe was left in place for another 5 min. After the retraction of the syringe, a gelatin sponge was placed in the bared hole, the incised skin was sutured, and the animals were placed on top of a heat source to recover. In every rat the injection of excitotoxin induced intense seizures that started about 1 h after the end of the surgery and went on for about 2 h. To examine the development of excitotoxin-induced demyelination the lesioned rats were killed at 3 h, 12 h, and 48 h (n=2, per group).

3.2.2.2. Tissue Preparation

A lethal dose of Somnotol was administered and the circulatory system was perfused via the left ventricle with 200 ml of cold (4°C) 0.9% saline, followed by 400 ml of cold freshly prepared fixative consisting of 4% paraformaldehyde in 0.1 M phosphate buffer (PB), pH 7.4. The brains were then removed from the skull, post-fixed for 4 h in cold fixative, and cryoprotected by soaking in 30% phosphate buffered sucrose for 2 days. Three sets of adjacent sagittal sections, 20 µm thick, were cut on a cryostat and thaw-mounted onto electrostatically treated slides. The different sets of sections were stained with 1) toluidine blue, 2) hematoxylin (Weil procedure), 3)

antibodies against myelin basic protein (MBP). The slides to be immunostained were stored at -15°C.

3.2.2.3. Immunohistochemistry

Sections were processed by the ABC method (Hsu et al., 1981). The reagents were applied directly to the mounted sections. The immunostaining was performed in a home-made humid chamber composed of 2 trays. One of the trays was lined with wet paper towels. The slides rested on plastic sticks over the towels. The second tray, placed downside up, was used as a cover.

In the immunostaining procedure, when not indicated, the reported dilutions were done in 0.1 M PB. Before each incubation, the sections were washed 3 x 5 min with 0.1 M PB with the exception of the primary antibody incubation that was done right after drawing off the excess blocking solution.

Sections were treated with 0.3% H_2O_2 for 20 min to block endogenous peroxidase activity. To block nonspecific protein binding, sections were incubated overnight at 4°C in 5% normal horse serum (NHS) and 0.5% Triton X-100 in PB. Immunostaining was carried out by incubating the sections first in mouse anti-MBP (Boehringer Mannheim, Laval, QC; 1:200 with 2% Triton X-100, for 2 d at room temperature), then in biotinylated horse anti-mouse IgG (Vector Laboratories, Burlingame, CA; 1:200 with 1% Triton X-100, for 1 hr) and subsequently in ABC (Vectastain Elite, Vector Laboratories; 1:100, for 1 hr). Peroxidase activity was revealed by incubating the sections sequentially

in 0.5% $CoCl_2$ in Tris buffer for 10 min, 0.025% DAB (Sigma, Oakville, ON) for 5 min, and, finally, 0.025% DAB with 0.004% H_2O_2. The reaction was stopped 3-5 min later by rinsing in PB. Sections were air dried, dehydrated, and coverslipped.

The protocol described above is the one which yielded the best staining. In pilot studies, however, I systematically modified the following parameters: 1) time of incubation in primary antibody; 2) concentration of Triton X-100; 3) use of metal-enhanced versus plain DAB staining; 4) stage at which the $CoCl_2$ was added to intensify the DAB reaction product (before vs. after incubation in DAB).

3.2.2.4. Data Analysis

The sections were examined with a Leica microscope (Leitz DMRB) and digitized images were viewed and analyzed using a computerized image-analysis system (NIH Image 1.57). The borders of the damaged region were assessed at low magnification from the toluidine blue stained sections. Although damage was observed at many levels, detailed analysis was undertaken for the sections in which the extent of the lesion was maximal. Documentation of the maximal lesion extent was conducted from inspection of digitized images of sequential sections. Tracings were made outlining the area of the lesions. The area enclosed by each tracing was calculated by the image-analysis system. Once the sections with the largest lesion area were selected, their adjacent sections stained for myelin were thoroughly examined

under high magnification to detect signs of demyelination. Apart from the comparisons made between the different groups, paired comparisons were made between adjacent sections stained with the Weil and the immunohistochemical stain to find out whether the two staining methods yield comparable results.

3.2.3. Results

The area of the lesions at their largest extent was similar for subjects in the 12 h and 48 h groups, but was smaller for subjects in the 3 h group. It is already known that NMDA-induced cell death takes a number of hours to complete. In contrast to lesion size, the appearance of the lesion area was similar in the 3h and 12 h groups, but differed markedly in the 48 h group. In the former, the number of cell bodies appeared to be close to normal but their morphology was changed; cell bodies were shrunken and had irregular outlines. At 48 h almost no trace of the cell bodies remained at the core of the lesion area.

As expected from previous reports, both the conventional and immunohistochemical stains revealed demyelination 48 h after excitotoxin administration (Fig. 3.5 A and B). Demyelination was confined within the area of cell loss. Fig. 3.5B clearly shows the abrupt disappearance of MBP immunoreactivity in myelinated fibers coursing through the area of the lesion.

Although there was agreement between the two staining methods for myelin at 48 h there were differences between the two stains at the 3 h and 12 h groups. Extensive bleaching in the hematoxylin stained tissue was seen 12 h after the lesion (Fig. 3.5C). Some bleaching was also evident at the core of the lesion in the 3 h group (Fig. 3.5E). By contrast, MBP immunoreactivity appeared to remain unaltered in both of these groups (Fig. 3.5D and F).

Fig. 3.5. Digitized images of sagittal sections of the rat brain taken through a 10 x objective. Slices were either stained with hematoxylin (Weil procedure) (A, C, E) or were immunostained with monoclonal antibodies against myelin basic protein (MBP) (B, D, F) at different time points after the administration of NMDA (A-B, 48 h; C-D, 12 h; E-F, 3 h). Bleaching in stained tissue and accompanying disappearance of stained fibers were taken as evidence for demyelination.

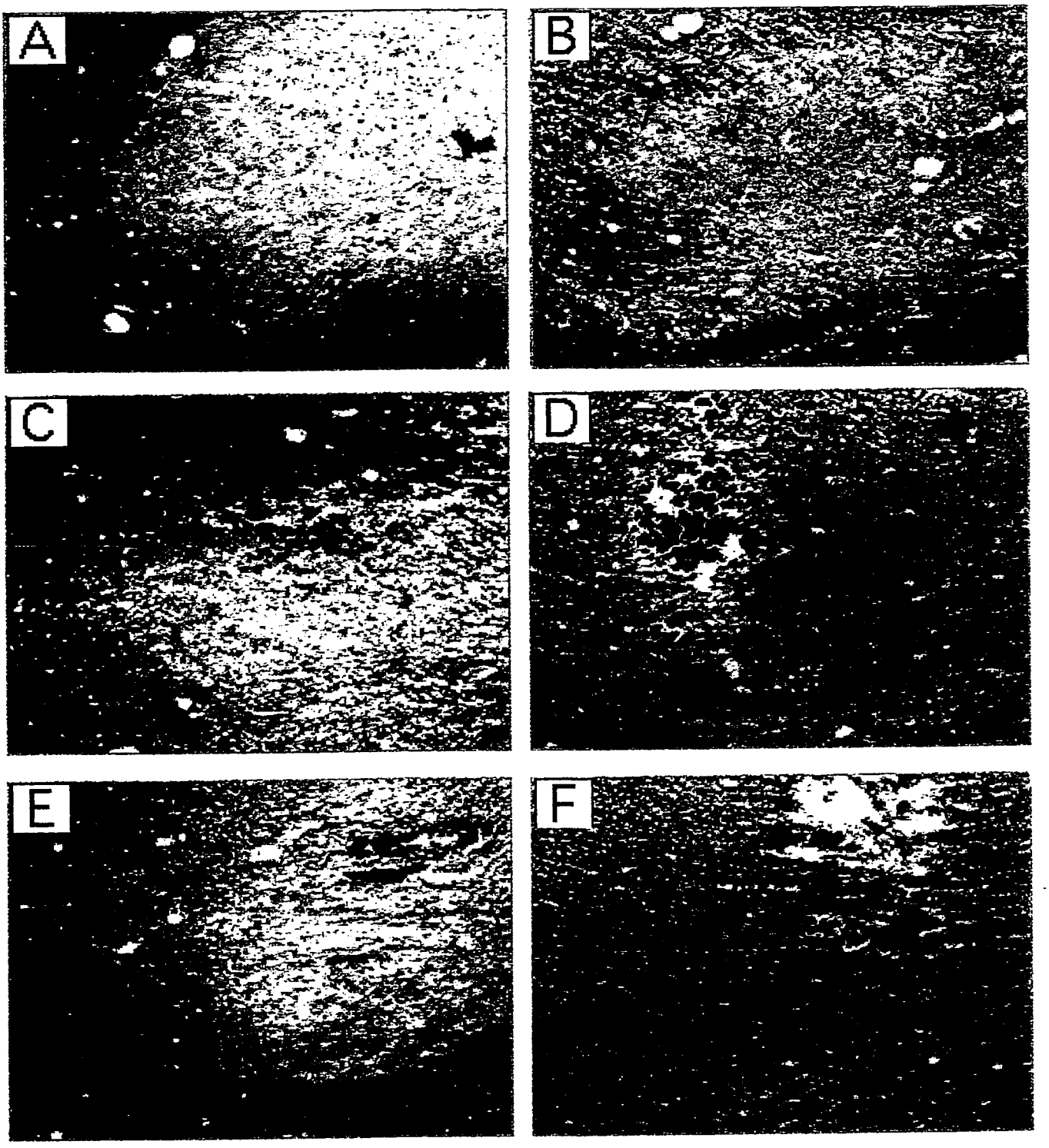
WEIL
MBP
A
B
C
D
E
F

3.2.4. Discussion

If demyelination is dependent on monocytic infiltration, it should occur later than neuronal loss. Cell death occurs within a few hours after excitotoxin administration, whereas there is approximately a two-day delay before peripheral monocytes populate the lesion area (Andersson et al., 1991a; Andersson et al., 1991b; Coffey et al., 1988; Coffey et al., 1990). There is no information concerning the status of myelin early after the lesion. In this study I employed two staining techniques to examine this issue. Surprisingly, different results, leading to conflicting conclusions, were obtained with the two techniques.

The results obtained with immunohistochemistry are consistent with the monocytic infiltration hypothesis. MBP immunoreactivity in myelinated fibers coursing through the lesion area appeared to be intact during the period of neuronal death, suggesting that demyelination occurs later on, possibly, as a result of inflammation and monocyte recruitment. On the other hand, early bleaching in tissue stained with the Weil procedure suggests that demyelination is one of the acute events following excitotoxin administration and thus, cannot be due to inflammatory recruitment of immune cells from the periphery.

Which result is one to trust? The fact is that nobody knows how conventional stains work and what exactly they stain. In contrast, immunohistochemistry is a technique with firmly established principles and

unique sensitivity. Thus, it seems logical to accept the immunostaining findings as best indicating demyelination. However, it is still premature to deliver a verdict concerning the course of demyelination and, by extension, the feasibility of the monocyte infiltration hypothesis. There are at least two ways to think about the results obtained with the Weil stain. Perhaps, bleaching is irrelevant to the status of myelin and occurs from changes in the myelin milieu after the excitotoxic insult. Alternatively, bleaching may mark an early event in oligodendrocyte degradation, occurring prior to the destruction of the protein components of myelin. To resolve these issues a transmission electron microscopy study is needed to provide a detailed and unambiguous picture of the myelin wrappings at various time points after the lesion.

Prevalently, conventional myelin stains (e.g. Weil, Klüver-Barrera) are used to assess the integrity of myelin. This is due to cost and the fact that published immunohistochemical procedures for myelin yield poor staining of diffuse projection systems. By using an improved immunostaining protocol, I showed that the picture obtained from conventional stains does not always match the picture obtained from immunohistochemistry. The message is that interpretations drawn from the use of conventional stains should at the least be confirmed by immunostaining. Moreover, the validity of previous conclusions must be put into question.

In my own work, I have attempted to prevent excitotoxin-induced demyelination by interfering with the production of nitic oxide (NO), a major cytotoxic effector of both macrophages (differentiated monocytes) and microglia (Morris & Billiar, 1994). NO can be toxic for many reasons, including the inhibition of metabolic enzymes, its direct damaging effects on cell components such as DNA, and its interaction with oxygen radicals to form highly toxic products such as peroxynitrite (Morris & Billiar, 1994). It has already been found that activated microglia or NO releasing compounds severely damage oligodendrocytes both in vitro and in vivo (Bo et al., 1994; Koprowski, Zheng, & Heber-Katz, 1993; Mitrovic, Ignarro, Montestruque, Smoll, & Merrill, 1994). NO is produced from L-arginine by the enzyme nitric oxide synthase (NOS) (Morris & Billiar, 1994). Thus, I tried to reduce the immune-mediated destruction of myelin by administering NOS inhibitors such as nitro-l-arginine, both systemically and via cannulae-fitted ALZET pumps for local administration in the brain.

None of these interventions worked as judged from examining hematoxylin stained tissue. It is conceivable that the outcome would have been different had MBP immunostaining been employed to evaluate the effectiveness of the different treatments. Given the importance of rendering the excitotoxin lesion technique as specific as initially advertised, these experiments should be replicated and their results evaluated by immunostaining. If upon replication a different outcome is obtained, one

could demonstrate that bleaching in Weil stained tissue is not indicative of demyelination.

3.3. HETEROGENEITY IN THE REWARD SUBSTRATE: A MODEL

The descending path hypothesis of MFB self-stimulation has been attacked on the grounds that lesions in forebrain areas often fail to produce decreases in BSR. Deepening the controversy is the lack of robust and/or consistent behavioral effects following electrolytic or knife cut lesions to the anterior of the stimulation electrode. In sharp contrast to these findings are the results obtained from large excitotoxic lesions. In the Arvanitogiannis et al. (1996b) study, five of the six subjects with lesions that destroyed areas traversed by the MFB, including the LPO, SI, and anterior LH, showed large postlesion threshold increases. Can the conflicting results obtained with the different lesion methodologies be reconciled?

A possible explanation for the inconsistent effects obtained between, but also within lesion studies may be found by proposing heterogeneity in the reward substrate. If the somata of reward-related neurons were segregated in different nuclei but their axons intermixed in the MFB, then a lesion restricted to any given nucleus of origin would leave intact many of the reward-related neurons stimulated by an MFB electrode. At the level of verbal description heterogeneity in the reward substrate is not a new idea (Anderson & Miliaressis, 1994; Conover & Shizgal, 1994a; Gallistel & Beagley, 1971; Phillips, 1984; Stellar, 1990). Only recently, however, has this notion

been formalized as a model specifying the possible consequences of such heterogeneity (Arvanitogiannis et al., 1996b).

The model is grounded on three premises. The first is that different subpopulations of neurons, located in different regions, are responsible for MFB self-stimulation. The second is that the outputs of the different subpopulations are separately integrated before being additively combined. The third is that, over a limited domain, reward grows steeply as a function of the firing of the first stage neurons (Gallistel & Leon, 1991). Taken together, these premises have led us to a simple model that illustrates one way that the reward substrate could be organized so as to minimize the curve shifts produced by lesions and to allow the magnitude of these shifts to vary across subjects with similar stimulation sites and lesions.

Fig. 3.6 shows two models of the way in which increases in frequency could compensate for lesion-induced damage to the reward substrate. The upper model summarizes the current thinking concerning the organization of the reward substrate. It is within the confines of this model that curve shifts are presently interpreted. The substrate is considered to be unitary and, for the sake of simplicity, homogeneous. Thus, each fiber contributes equally to the rewarding effect. The outputs of all fibers are pooled and integrated by a mechanism that acts as a spike counter. At non-saturating reward levels, the number of spikes within a given time window is then transformed into subjective reward magnitude by a power function. According to this model, a

lesion removing half of the neurons will half the output of the bundle. The magnitude of the consequent reduction in reward depends on the exponent of the growth function for a particular stimulation site in the MFB. In one experiment exponents were shown to range roughly from 2 to 10 (Gallistel & Leon, 1991) in which case, killing half the fibers would produce a four-fold (2^2) to 1024-fold (2^{10}) decrease in reward. But regardless of the magnitude of this decrease, according to the counter model, reward would be restored to its prelesion level by doubling the impulse flow in the remaining fibers. To do this, the stimulation frequency would have to be doubled, resulting in an easily detectable 0.3 $\log_{10}$ unit curve-shift.

The lower diagram in Fig. 3.6 depicts a simplified model of organization in a heterogeneous substrate. According to this hypothetical model, two subpopulations of fibers, each arising from a different region, carry the reward signal, but activity in each is integrated separately. The idea of separate integration is certainly plausible if the two subpopulations are functionally different. For example, one could be related to gustatory rewards and the other to thermal rewards. In this model, the outputs of the integrators contribute equally to the rewarding effect and converge so that the rewarding effects of stimuli germane to each function can be combined. For simplicity additive combination is assumed. If the lesion destroys one of the subpopulations, the rewarding effect of the stimulation is halved. To restore the rewarding effect to its prelesion level the output of the surviving subpopulation would have to be doubled. The frequency required to do so

would depend on the exponent of the reward growth function in the surviving subpopulation. For a large exponent, a minimal increase in stimulation frequency would allow the intact subpopulation to compensate for the twofold decrement in reward produced by lesioning the other subpopulation. For example, an exponent equal to ten would result in a non-discernible 0.03 $\log_{10}$ unit ($\log_{10}(\sqrt[10]{2})$) shift. This type of arrangement (depicted at the lower panel of Fig. 3.6) could be one of the reasons that it has proved difficult to produce substantial curve-shifts following lesions. Further, some of the variability in the magnitude of the lesion-induced changes in required number of pulses could reflect across-site differences in the exponent of reward growth.

In sum, curve shift scaling may be inadequate to reveal lesion effects in the case of a heterogeneous substrate. In such a system, it is best to measure the change in reward magnitude rather than the change in required number of pulses because the former is likely to be substantially larger than the latter. A method that can measure changes in reward magnitude in addition to curve shifts is introduced in the next chapter.

Fig. 3.6. Two models showing how increases in frequency could compensate for lesion-induced damage to the reward substrate. Intact fibers are drawn with solid lines, whereas lesioned fibers are drawn with dashed lines; the effective stimulation field is represented by a dotted circle. In the upper model (A), the output of all directly stimulated reward-related fibers impinges on a single spatio-temporal integrator. In the lower model (B), two subpopulations of fibers are stimulated, and the outputs of each are separately integrated before additive combination. Over a limited domain, reward (y) is depicted to grow as a power function of the number of stimulation pulses per train (x).

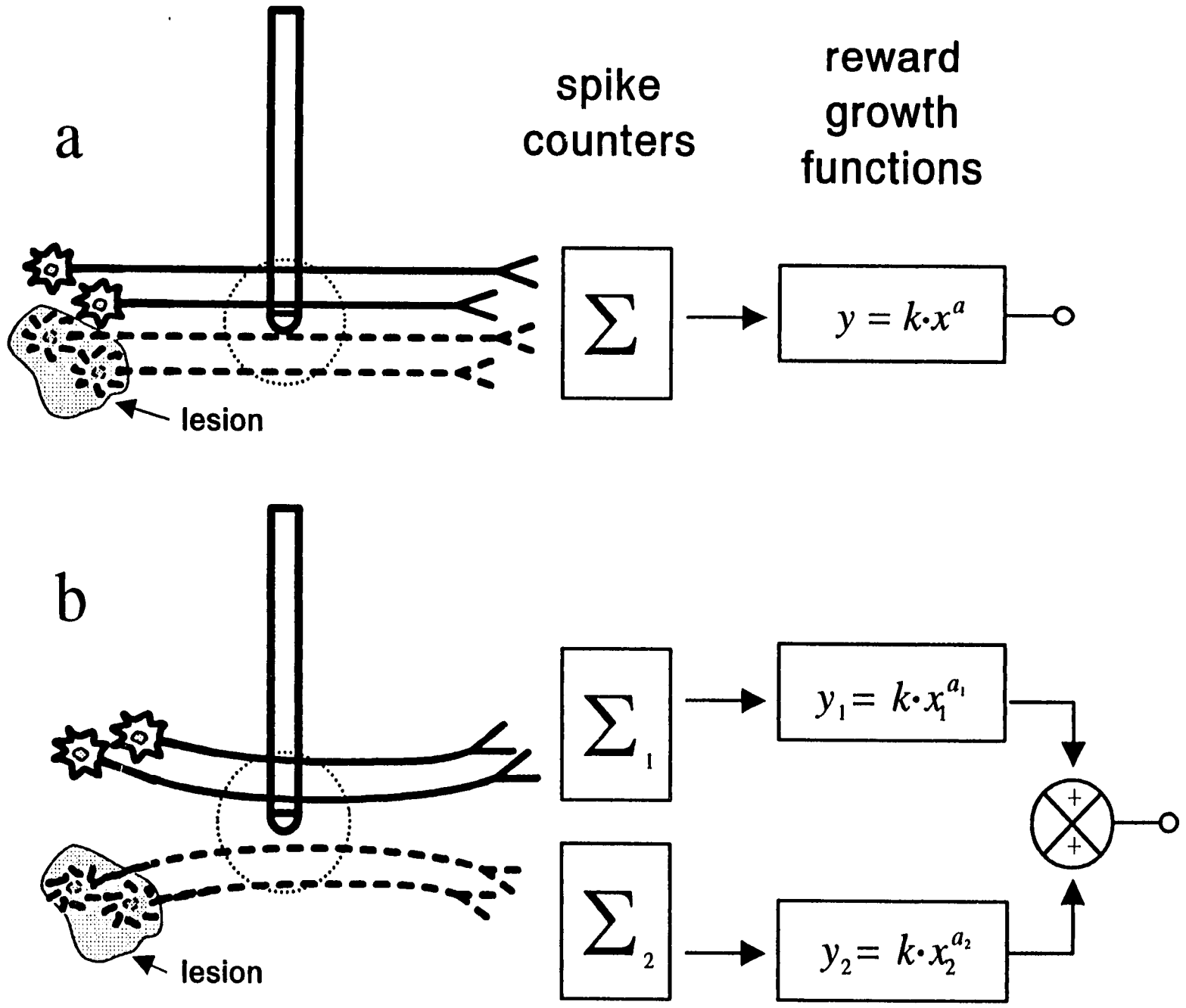
a
spike
counters
reward
growth
functions
lesion
Σ
$y = k \cdot x^a$
b
lesion
Σ_1
Σ_2
$y_1 = k \cdot x_1^{a_1}$
$y_2 = k \cdot x_2^{a_2}$
+
+

3.4. LESIONS AND THE FIRST STAGE SUBSTRATE

When discussing the relationship between curve shifts and changes in the rewarding impact of the stimulation, attention is often focused on the directly stimulated stage of the reward substrate. Commonly, it is implicitly assumed that curve shifts reflect changes in the output of the first stage neurons. Thus, the increase in the required number of pulses after a lesion is taken as an index of the percentage of first stage fibers that have been destroyed. However, changes in stimulation efficacy following lesions cannot be directly linked to damage in the first stage neurons. That is, self-stimulation can potentially be affected by damaging neurons other than the first stage ones. These could include modulatory, perhaps inhibitory, neurons gating the pathway carrying the reward signal, or even neurons efferent, several synapses away, to the ones directly activated by the electrode. It is from this angle that I considered some results of the excitotoxic lesion experiment presented in the beginning of this chapter. Thus, I interpreted the improved reward effect seen in some subjects with medial damage as resulting from the removal of some source of inhibition on stimulation-generated reward effects.

In contrast to the curve shift method, the method I describe in the next chapter has the potential to reveal whether lesions act at the input side or after the output of the integrator.

CHAPTER 4

A THREE-DIMENSIONAL ANALYSIS OF PERFORMANCE FOR BRAIN STIMULATION REWARD

In modern studies, the curve shift method has been used to quantify lesion effects (Edmonds & Gallistel, 1974; Stellar et al., 1988). In the previous chapter I argued for the need to complement this method with one that can directly measure reward reduction. In this chapter, I describe and validate such a method.

An appreciation of this advance requires stepping back to consider the relationship between behavioral output and input strength. This relationship is a composite-function relationship in which behavior (B) is a function of reward magnitude (R), and reward magnitude is a function of stimulus strength (S). Let f be a function mapping S to R, and let g be a function relating R to B. Using arrow notation we have

$$S \xrightarrow{f} R \xrightarrow{g} B.$$

The two functions, f and g, can be combined to define the composite function of g by f ($g \circ f$) that directly relates S to B. Thus, specifying f and g is what is needed to flesh-out the input-output relationship for BSR.

As mentioned previously the reward magnitude is a non-linear function of integrator input (Gallistel & Leon, 1991). Roughly speaking, the

first function, f, grows initially as a power function, but decelerates to approach saturation at high stimulation strengths. Pictorially, f is a sigmoid. The performance function, g, is, of course, dependent on reward magnitude but also a host of other variables. Among the obvious performance variables are the ability to respond for BSR and task difficulty. Equally important are variables that control goal evaluation and determine payoff for a particular goal object, for example, the rate at which the goal object becomes available. Herrnstein (1970) formulated an equation that describes the relationship between behavioral output and the variables that control it. This equation provides a basis for determining which of the performance variables have been altered by experimental manipulations.

Conventionally, the reward growth and performance functions have been studied separately. Recently, however, Shizgal (Shizgal, Conover, & Arvanitogiannis, 1996) linked the two functions and showed that, in principle, it is possible to determine whether lesions alter BSR before or after the output of the reward growth function. In what follows I will describe the model developed by Shizgal along with a series of validation experiments.

4.1. PERFORMANCE FOR BRAIN STIMULATION REWARD AS A FUNCTION OF THE RATE AND MAGNITUDE OF REINFORCEMENT

Goal directed behavior entails goal evaluation and subsequent choice among competing alternatives. Intuitively, animals choose the alternative that provides the largest payoff. Thus, payoff can be inferred by choice. In

turn, choice can be revealed by the amount of time spent on each alternative. The alternative to which the animal allocates more time is said to have higher utility than competing alternatives.

In the laboratory, choice is studied by making measurable alternatives explicitly available. Commonly, the subject in a choice experiment has two responses, such as pressing one of two levers, available simultaneously. Concurrent schedules of reinforcement are typically used, providing the subject with alternative regimes of reinforcement. When choice is made on concurrent variable-interval (VI) schedules, subjects tend to distribute their choice responses according to the relative rate at which these responses are reinforced (Herrnstein, 1961). In other words, the distribution of choices tends to match the distribution of reinforcements. In symbolic form:

$$\frac{TA_1}{TA_1 + TA_2} = \frac{R_1}{R_1 + R_2} \qquad (1)$$

where TA denotes time allocation, R denotes reinforcement rate, and the subscripts identify the two alternatives.

Herrnstein (1970) suggested that matching obtains even in the case in which there is only one specified reinforcement schedule. He reasoned that there is, strictly speaking, no such thing as a single reinforcement schedule. Rather, there are almost inevitably other reinforced behaviors (as diverse as exploring, resting, grooming, and other distractions) that may be emitted when the organism is responding on the only schedule provided by the

experimenter. Thus even in the single-schedule case the subject has a choice between responding on that schedule or making an alternative response, unspecified by the experimenter. In the single specified reinforcement schedule Equation (1) can be written as:

$$\frac{TA}{TA + TA_e} = \frac{R}{R + R_e} \qquad (2)$$

where TA stands for time allocation for the experimenter-controlled reinforcer, TA_e stands for time allocation to all other sources of reinforcement, R stands for the rate of delivery of the experimenter-controlled reinforcer, and R_e stands for the reinforcement rate provided by all other sources of reinforcement. Because the sum (TA + TA_e) reflects 100% time allocation, equation (2) becomes:

$$TA = \frac{R}{R + R_e} \qquad (3)$$

This hyperbolic function (Fig. 4.1A) links time allocation for the experimenter controlled reinforcer both to its rate and to the rate of competing reinforcers not under experimental control. R_e is actually measured in the units of the arranged reinforcer. When R equals R_e, the subject allocates half of its time responding for the arranged reinforcer. Thus, R_e is defined as the reinforcement rate required for the subject to spend half of the time responding for the experimenter-delivered reinforcer. In other words, R_e is the rate at which the experimenter-controlled reinforcer must be delivered in

order to equal the combined utility (payoff) of alternate activities. In Fig. 4.1 equation (3) is plotted in linear (Fig. 4.1A) and semi-logarithmic (Fig. 4.1B) coordinates.

In the above formulations choice was described as a function of rate. However, rate is only one of many variables that determine payoff. For example, relative preference for an alternative that is delivered twice as fast as a second alternative may be offset by increasing the intensity of the second alternative. For a hungry rat, increasing the intensity of a sucrose solution amounts to increasing the concentration of that solution. Thus, utility is evaluated along multiple dimensions that include the intensity of reinforcement and the rate of its delivery. In fact, it has been proposed that utility is determined by the multiplicative combination of these experimenter-controlled variables (Baum & Rachlin, 1969; Davison & McCarthy, 1988). If so, equation (3), can be expanded to include the intensity of reinforcement:

$$TA = \frac{I \cdot R}{I \cdot R + U_e} \qquad (4)$$

where I is the intensity and R the rate of delivery of the experimenter-controlled reinforcer. U_e is the utility of all other sources of reinforcement.

Fig. 4.1. The matching law hyperbola plotted in linear (A) and semi-logarithmic (B) coordinates. The dotted line intersecting the x-axis marks the rate of reinforcement that maintains a one-half asymptotic response rate and is equal in magnitude to R_e.

A

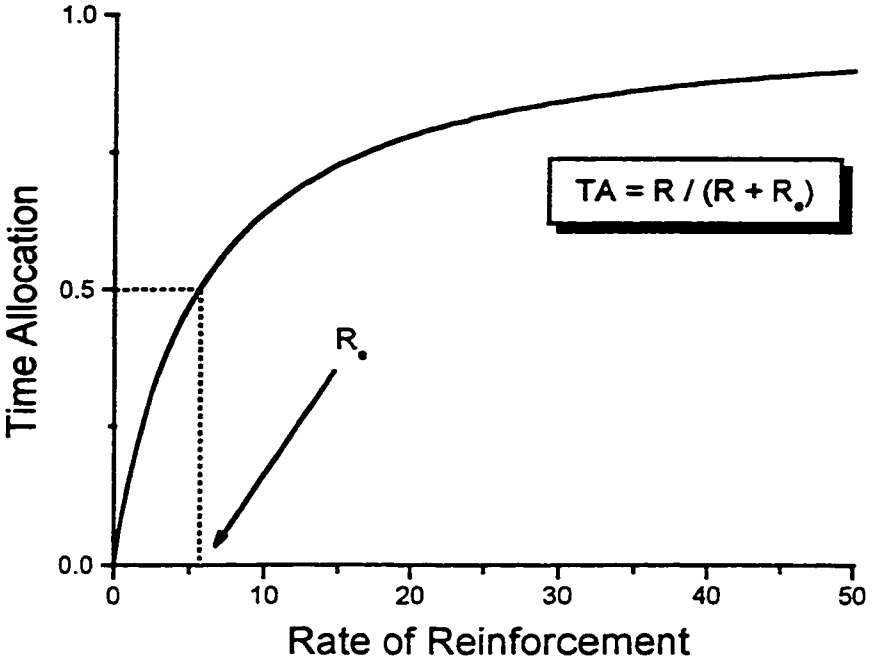
1.0
0.5
0.0
Time Allocation
TA = R / (R + R$_e$)
R$_e$
0
10
20
30
40
50
Rate of Reinforcement

B

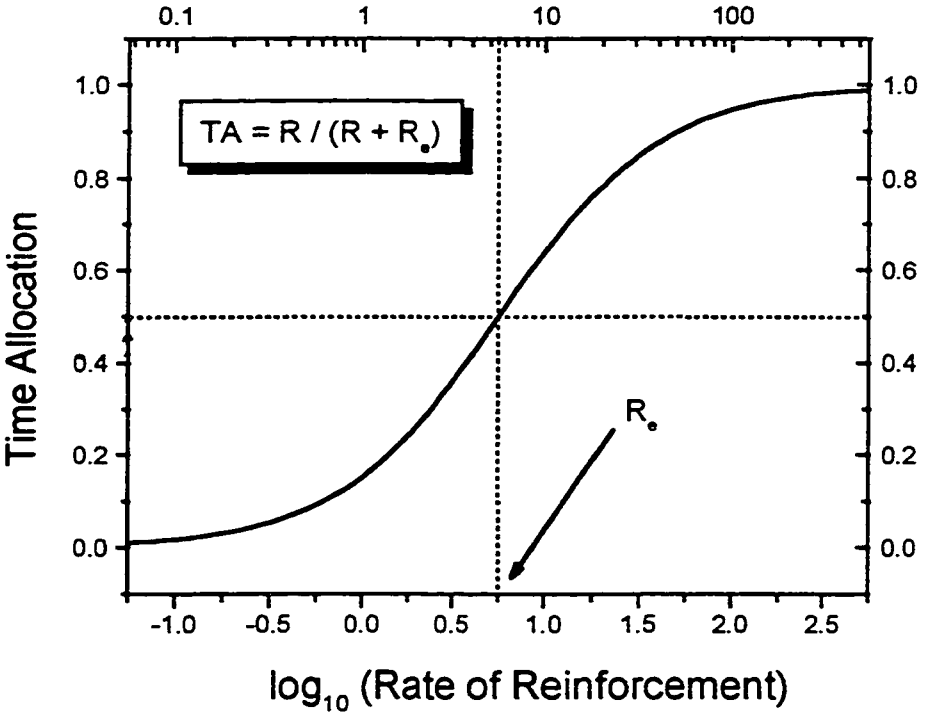
0.1
1
10
100
1.0
0.8
0.6
0.4
0.2
0.0
Time Allocation
TA = R / (R + R$_e$)
R$_e$
-1.0
-0.5
0.0
0.5
1.0
1.5
2.0
2.5
log$_{10}$ (Rate of Reinforcement)

Equation (4) can be rearranged to give:

$$TA = \frac{1}{1 + \left(\frac{U_e}{I \cdot R}\right)} \tag{5}$$

In the introduction I argued, that coding in the BSR substrate is unidimensional and that the output of the integrator may well correspond to the intensity component of utility. In the case of BSR, intensity is related to the strength of the stimulation by a steeply-rising sigmoidal function. Formally, this relationship could be expressed as a logistic function:

$$I = \frac{I_{max}}{1 + \left(\frac{N_{hm}}{N}\right)^p} \tag{6}$$

where I_{max} is the maximum reward intensity, N_{hm} is the number of pulses required to produce a reward of half-maximal magnitude, N is the number of pulses per train, and p is a parameter governing the rate of reward growth. In Fig. 4.2 the intensity of reinforcement is plotted in semi-logaritmic coordinates as a logistic function of N.

The equations (5) and (6) can be combined by substituting for I in equation (5) to obtain:

$$TA = \frac{1}{1 + \left\{\left[\frac{U_e}{I_{max}} \cdot \frac{1}{R}\right] \cdot \left[1 + \left(\frac{N_{hm}}{N}\right)^p\right]\right\}} \tag{7}$$

Fig. 4.2. Based on matching data from Gallistel's group (Gallistel & Leon, 1991; Simmons & Gallistel, 1994), the intensity of reinforcement is modeled as a steeply-rising logistic function of the number of stimulation pulses per train (p sets the steepness with which intensity grows). The dotted line intersecting the x-axis marks the number of pulses required to produce a reward of half-maximal intensity.

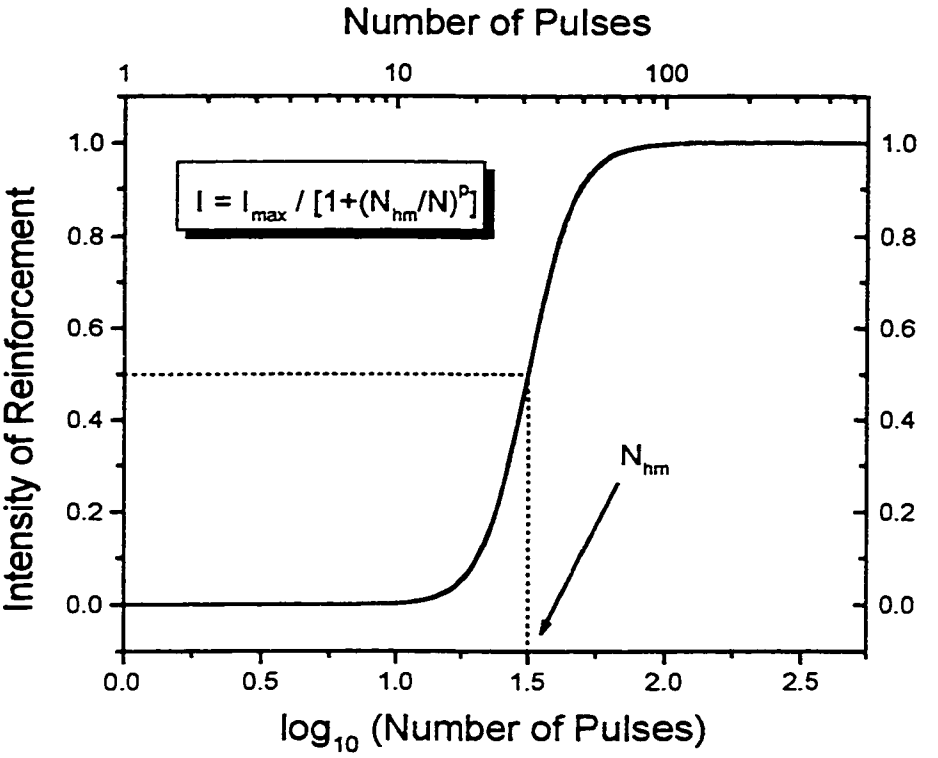
Number of Pulses
1
10
100
1.0
0.8
0.6
0.4
0.2
0.0
Intensity of Reinforcement
$I = I_{max} / [1+(N_{hm}/N)^p]$
N_{hm}
0.0
0.5
1.0
1.5
2.0
2.5
$\log_{10}$ (Number of Pulses)

Equation (7) is the composite function that relates directly the observed behavior on a single-operant VI schedule to the strength of the stimulation. The ratio U_e/I_{max} acts as a single parameter that measures the efficacy of the background reinforcers relative to a maximal BSR. Specifically, it is the rate at which a maximal BSR would have to be delivered in order to equal the combined utility of uncontrollable sources of reinforcement. Let U_e/I_{max} be equal to R_{e_min}. At R_{e_min} the subject will spend half of its time performing for a maximal BSR and the other half engaging in other activities. Equation (7) can thus be written as:

$$TA = \frac{1}{1+\left\{\left[\frac{R_{e\_min}}{R}\right]\cdot\left[1+\left(\frac{N_{hm}}{N}\right)^{P}\right]\right\}} \qquad (8)$$

In Fig. 4.3A, equation (8) is plotted in three dimensions, with R (reinforcement rate) and N (number of pulses/train) on logarithmic axes. The position of the resulting three-dimensional structure ("reinforcement mountain") is set along the N and R axes by N_{hm} and R_{e_min} respectively. Fig. 4.3B provides another view of the mountain and shows how its features can be summarized in two dimensions by slicing the structure horizontally at regular intervals and projecting the outlines of the slices onto a horizontal plane to produce a contour map. Fig. 4.4 shows that the mountain can be displaced along the N axis by manipulations that affect N_{hm}, while, changing R_{e_min}, shifts the mountain along the R axis.

Fig. 4.3. **A.** A three-dimensional plot of the reinforcement mountain. Time allocation is plotted as a function of both the strength of the stimulation and the rate of reinforcement.

B. A contour map of the reinforcement mountain obtained by projecting onto a plane the outlines of successive horizontal sections. The position of the mountain is determined by the values of N_{hm} and R_{e_min}; the slope of the diagonal segment of the contours is set by p.

A

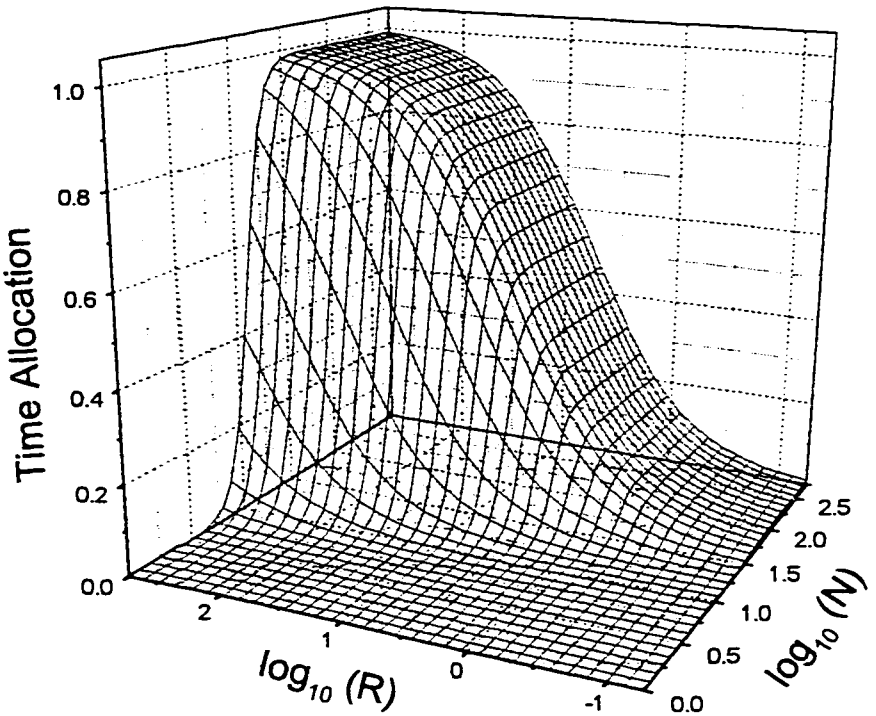
Time Allocation
1.0
0.8
0.6
0.4
0.2
0.0
2
1
0
-1
log10 (R)
2.5
2.0
1.5
1.0
0.5
0.0
log10 (N)

B

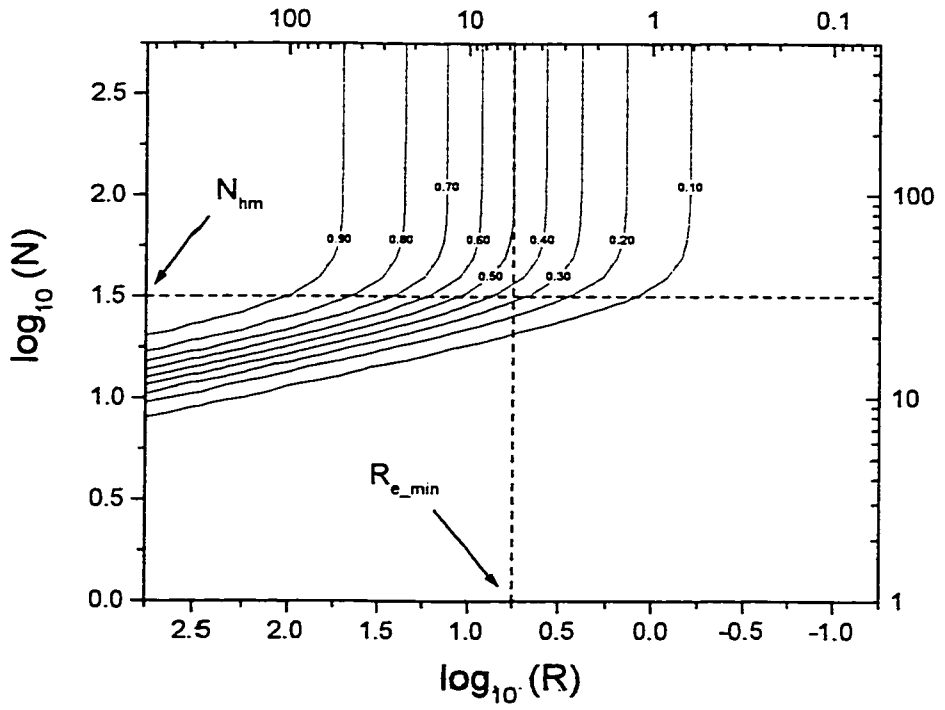
100
10
1
0.1
2.5
2.0
1.5
1.0
0.5
0.0
log10 (N)
Nhm
0.90
0.80
0.70
0.60
0.50
0.40
0.30
0.20
0.10
Re_min
100
10
1
2.5
2.0
1.5
1.0
0.5
0.0
-0.5
-1.0
log10 (R)

Fig. 4.4. Graphic representation of how changes in the value of N_{hm} or R_{e_min} shift the mountain along the axis of stimulation strength or the reinforcement rate axis, respectively.

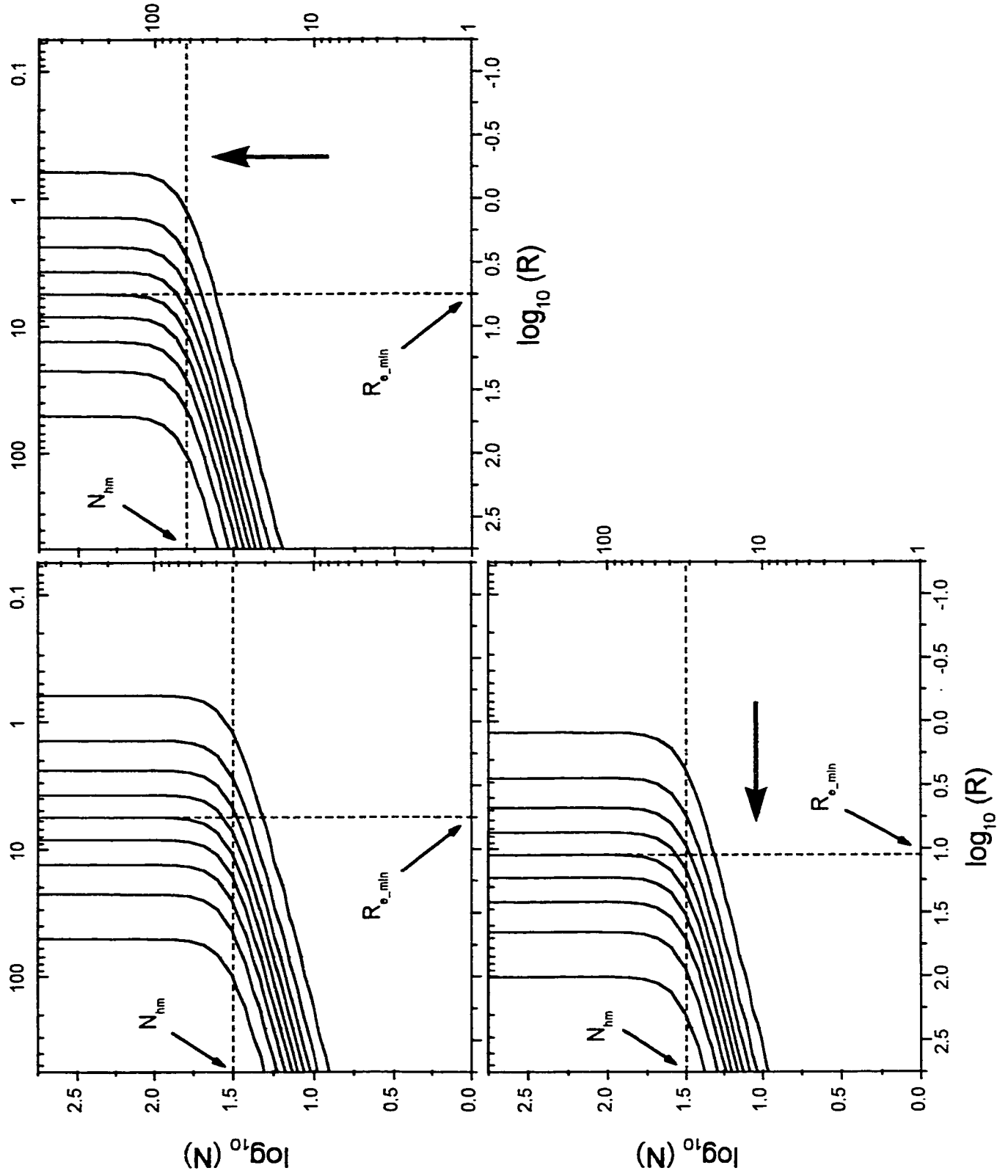
log10 (N)
log10 (R)
Nhm
Re_min

What relevance does the reinforcement mountain have for testing the effects of lesions on BSR? Before answering this question, it is useful to translate the mathematics into a schematic model. Fig. 4.5 is a "black box" representation of how utility is computed in the substrate for BSR and then translated into behavioral allocation. The stimulation-elicited volley is integrated over time and space by a device that simply counts spikes within a fixed time window. The count is translated into the intensity of reinforcement by a non-linear function that can be modelled as a logistic function. The intensity of reinforcement is then combined multiplicatively with the rate of reinforcement. The result represents the utility of the stimulation. Time is allocated to obtaining more stimulation according to the matching law, which links behavior for the experimenter-controlled reinforcer both to its utility and to the utility of competing reinforcers not under experimental control.

Lesions may alter behavior by acting either on the early or late stages of the circuitry depicted in Fig. 4.5. The three-dimensional analysis makes it possible to distinguish between actions that alter the circuitry before or after the output of the integrator. This is because the reinforcement mountain will be shifted along the N axis by manipulations that alter the input to the integrator and along the R axis by manipulations that alter its transformed output. Lesions on the directly stimulated substrate will lower the count incident on the reward-growth function. This insult can be compensated for simply by increasing the number of stimulation pulses. Thus, N_{hm} will be

Fig. 4.5. This schema summarizes the model of utility computation and behavioral allocation on which the reinforcement mountain is based. The action potentials triggered in the directly stimulated neurons are accumulated by a counter. The spike count is then transformed non-linearly into a signal representing the intensity of reinforcement. The rate of reinforcement is multiplied by the intensity of reinforcement to yield the utility of BSR. Time is allocated to obtaining additional stimulation according to the matching law, which compares the utility of BSR to the total utility of all available reinforcers. According to this model, changes in the position of the mountain following manipulations such as lesions reflect the stage of processing at which the manipulation in question acted to alter the utility of the brain stimulation.

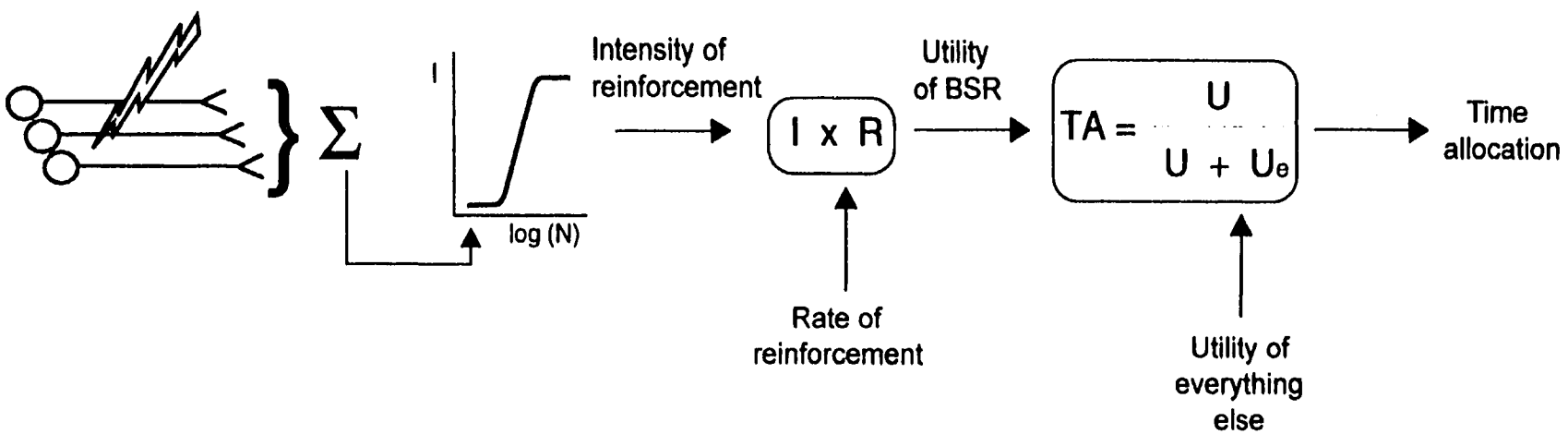
Σ
I
log (N)
Intensity of reinforcement
I x R
Rate of reinforcement
Utility of BSR
TA = U / U + Ue
Utility of everything else
Time allocation
Directly stimulated substrate
Integrator
Reward growth function
Utility computation
Response strength equation

increased and the mountain will shift along the N axis . However, once this compensation is performed, efferent stages of the system will receive exactly the same intensity signal as before the lesion. Thus, the mountain will not shift along the R axis. Conversely, lesions that act on the late stages of the system will shift the mountain along the R axis. A lesion that decreases the maximum BSR (I_{max}) would decrease the utility signal in a manner indistinguishable from a change in reinforcement rate; a compensatory increase in reinforcement rate would restore the final output to its prior level (remember that $U_e/I_{max}=R_{e\_min}$). To summarize, a lesion-induced shift along the N axis indicates a lateral displacement of the reward growth function and thus action at the input to the integrator, whereas a shift along the R axis indicates a vertical displacement of the reward growth function and thus action at the output side of the integrator.

According to equation (8) and the model of the homogeneous substrate depicted in Fig. 4.5, a lesion-induced change in I_{max} must be attributed to damage in neurons that modulate the intensity of BSR. However, a change in I_{max} following a lesion could also indicate damage to a subpopulation of first stage neurons that are part of a heterogeneous substrate. As depicted in Fig. 3.5b, a lesion that killed all of the cells providing input to one of two integrators that contribute equally to the rewarding effect would produce a twofold decrement in I_{max}. Such decrement would result in a 0.3 $\log_{10}$ unit shift in R_{e_min}. The proposed orthogonal analysis of lesion effects cannot distinguish between the two potential causes of changes in I_{max}. Still, the

ability to detect actual decreases in reward should shed some light on the oftentimes puzzling lesion results.

A gap in current knowledge that can be addressed by means of the reinforcement mountain is whether dopamine neurons contribute to BSR before or after the output of the reward-growth function. The central importance of the dopaminergic system in BSR is well recognized, however, there is currently no consensus regarding the nature of the dopaminergic contribution to BSR. Although recent microdialysis (Miliaressis et al., 1991) and Fos immunohistochemistry (McGregor & Hunt, 1996) results have tilted the balance in favor of the view that dopamine neurons play a modulatory role and do not relay the reward signal, the definite experiment has yet to be carried out. The reinforcement mountain can be used to directly assess what position dopamine neurons occupy in the BSR circuit. A shift along the N axis following 6-hydroxydopamine lesions would indicate a contribution to integrator input, whereas a shift along the R axis would place the contribution of dopaminergic cells downstream from the output of the integrator. From a functional view, the former outcome would indicate that dopamine neurons are in series with the first stage neurons and carry the reward signal, whereas the latter outcome would indicate that dopamine neurons modulate the intensity of BSR.

Before assessing the effects of lesions by means of the reinforcement mountain analysis, it is important to confirm the validity of this method. In

the rest of this chapter I will test the proposed model by manipulating current intensity, train duration, and background reinforcement.

4.2. THE EFFECT OF MANIPULATING CURRENT INTENSITY ON THE REINFORCEMENT MOUNTAIN

4.2.1. Introduction

According to equation (8) the position of the reinforcement mountain along the N axis is determined by N_{hm}. Conversely, changes in N_{hm} should shift the mountain only along the N axis. One way to test this prediction is to manipulate current intensity. The efficacy of the reward signal generated by a fixed duration train of pulses is determined solely by the number of action potentials induced by the train (counter model). The same reward intensity can be produced by a large number of first stage fibers firing slowly or a small number of fibers firing rapidly. Equivalently, a high-current, low-number of pulses train can be adjusted so that it produces the same reward intensity as a low-current, high-number of pulses train. Changing the number of stimulated first-stage axons would necessitate a reciprocal change in the number of pulses to maintain integrator output. Thus, current manipulations should shift the mountain along the N axis. In this experiment reinforcement mountains were obtained at two different current intensities. To obtain a mountain, I measured performance for BSR as a function of both the number of stimulation pulses per train (N) and the obtained rate of reinforcement (R).

4.2.2. Materials and Methods

4.2.2.1. Subjects

Subjects were four male Long-Evans rats weighing between 300 and 400 g at the time of electrode implantation. While anesthetized with sodium pentobarbitol (Somnotol, 65 mg/kg i.p.), they were implanted bilaterally in the lateral hypothalamus (level-skull coordinates: AP, 2.8 mm behind bregma; ML, 1.7 mm lateral to the mid-sagittal sinus; DV, 7.8 mm below dura) with monopolar electrodes. Electrodes were made from 00 stainless steel insect pins and were insulated to within 0.5 mm of the tip with Formvar. A stainless steel wire served as the current-return electrode. The placement of the electrodes was verified by standard histological procedures at the conclusion of the experiment. The animals were kept on a reverse 12:12-h light:dark cycle and tested during the dark phase.

4.2.2.2. Apparatus

Testing was conducted in wooden boxes measuring 28 x 28 x 69 cm, with Plexiglas front panels and wire-mesh floors. Two retractable levers (ENV-112B,MED associates, Georgia, Vermont) were centered on opposite walls of each test box, 8 cm from the floor. Only one lever was used in this experiment. A keylight, positioned 8 cm above the lever, signaled when the lever was operative. A bright, flashing light on the rear panel of each test box signaled the beginning of a trial.

Electrical stimuli were provided by a constant current amplifier that was controlled by a digital pulse generator (Mundl, 1980). Experiments were run using a PC type microcomputer, which specified all parameters of the stimulation, delivered BSR on VI schedules, and recorded the data. Stimulation consisted of fixed, 0.5-s trains of cathodal, rectangular, constant current pulses, 0.1 ms in duration. The stimulation was monitored continuously on an oscilloscope (Tektronix 2205). The VI intervals were generated by transforming the output of a computerized pseudorandom number generator to give a sample of exponentially distributed intervals with the desired mean.

4.2.2.3. Procedure

One week after electrode implantation the rats were trained to press a lever for BSR delivered at various stimulation parameters and under different VI schedules of reinforcement. To collect the reward, the lever did not need to be released. A reward was delivered immediately if the rat was holding the lever down when the VI clock timed out. If not, the lever remained enabled and the reward was delivered upon the next depression of the lever. Time allocation at the lever (the dependent measure in this experiment) was defined as the cumulative time the lever was depressed before reward delivery. After reward delivery, the lever was retracted from the test box for 5 s and the keylight was extinguished. After the "blackout" period the lever was reextended, the key light was turned on and the VI clock

restarted. The stimulating electrode that produced the best "hold-down" behavior for each subject was chosen for use in the experiment proper.

To obtain a reinforcement mountain at a particular current two kinds of experimental conditions were run. In the first, the VI was held constant throughout the session and BSR varied in strength (number of pulses per train) from trial to trial (I refer to this condition as "pulse sweep"). In the second, BSR was held constant but the rate of reinforcement varied from trial to trial (I refer to this condition as "VI sweep"). Pulse sweeps were obtained at a low (relatively rich) VI schedule of reinforcement (VI=3.8 s) and a high (relatively lean) VI schedule (VI=15 s) by exposing the subject to a descending series of pulse numbers. The session started with a maximal BSR that supported asymptotic time allocation and the strength of the stimulation decreased from trial to trial by 0.1 $\log_{10}$ unit steps until time allocation to the lever was negligible. VI sweeps consisted of exposure to an ascending series of seven VI schedules (VI 3.8 s; VI 6 s; VI 9.5 s; VI 15 s; VI 24 s; VI 38 s; VI 60 s). One VI sweep was obtained with a maximal BSR while the second was obtained with a moderate BSR for which the subject responded less vigorously. The first trial of each session was considered a warm-up and thus was always replicated. Trial length was adjusted for each VI schedule so that the subject could potentially receive up to 30 rewards per trial. Thus, trial length was determined as, $\text{Trial length} = [(VI \times 30) + (Blackout \times 30)]$, and ranged from 4.4 min to 32.5 min. A 30 s intertrial interval was signaled by the flashing light on the rear panel of the test cage. During the intertrial interval

the subject received five trains of priming stimulation identical to the stimulation that would serve as the reward.

In the first phase of the experiment the current intensity was adjusted to 316 μA (low current). To begin with, pulse sweeps were collected, first, at the lowVI and, second, at the high VI. Then, VI sweeps were collected, first, at a high number of pulses and, second, at a lower number. Multiple sessions were run at each condition until the data from four consecutive sessions per condition were judged as being stable. Only then did testing proceed to the next condition. The data from a total of 16 (4 x 4) sessions were used for the reinforcement mountain analysis. Once the first phase of the experiment (baseline) was completed, the current intensity was increased by 0.3 $\log_{10}$ units to 631 μA (high current) and the experiment was repeated as described above. For two of the four subjects (SP4, SP6) the second phase of the experiment was followed by a return to baseline so as to verify the stability of the data.

4.2.2.4. Data Analysis

The number of pulses per train and the VI were the two variables manipulated in this experiment. However, the VI is not truly an independent variable. The reason for this is that the actual rate of reinforcement the subject sees depends on the time allocated to the arranged reinforcer which in turn depends on the intensity of the delivered reinforcer. At the extreme, when responding is zero, reinforcement is also zero. Only when responding approaches its maximum, does reinforcement approach the level

programmed by the VI schedule. Thus, instead of the set rate of reinforcement, analysis was carried out by using the actual rate of reinforcement seen by the subjects in a particular trial. The obtained rate of reinforcement was computed according to the formula:

$$\text{Obtained rate of reinforcement} = \frac{\text{Number of obtained rewards}}{\text{Trial length} - (\text{Number of obtained rewards} \times \text{Blackout})}$$

For the purpose of curve fitting, all calculations used the common logarithm of the trial reinforcement rate and the number of stimulation pulses. The parameters R_{e_min} and N_{hm} were also expressed in $\log_{10}$ units. Accordingly, the following modified version of equation (8) was fit to the data obtained from the pulse and VI sweeps:

$$TA = \frac{TA_{max}}{1 + \left\{ \left[\frac{10^{R_{e\_min}}}{10^{R}} \right] \cdot \left[1 + \left(\frac{10^{N_{hm}}}{10^{N}} \right)^{p} \right] \right\}} \qquad (9)$$

Notice that this equation has an extra parameter, TA_{max}, that stands for maximum time allocation. Theoretically, the maximum possible time allocation is 1.0 (100%). However, to avoid constraining the curve fitting, maximum time allocation was determined from the experimental data. Equation (9) was fit by the least squares method to a data set containing values for $\log_{10}(N)$, $\log_{10}(R)$, and TA (MicroMath SCIENTIST 2.0). The values of TA_{max}, N_{hm}, R_{e_min}, and p were estimated along with the 95% confidence regions around them. Goodness-of-fit statistics for the data set, including the

coefficient of determination that provides a measure of the fraction of the total variance accounted for by the model, were also calculated. The obtained parameter values were used to plot the corresponding reinforcement mountains (ORIGIN 4.0).

4.2.3. Results and Discussion

Table 4.1 summarizes the parameter and goodness-of-fit estimates as a function of current for the four subjects. According to the coefficient of determination estimates, the time allocation data conformed very well to the surface of the reinforcement mountains. However, serial correlation parameters (not shown) indicated a systematic non-random trend in the residuals in five of the fitted mountains. The serial correlation was not significant in the case of SP2 (low current), SP3 (low current), and SP4 (high current). Fig. 4.6 shows an example of a fitted data set (SP4; high current), whereby time allocation is plotted as a function of both the stimulation pulses per train and the obtained rate of reinforcement. The curved trajectory of the pulse sweeps is due to the fact that at low time allocations the rate of reinforcement obtained by the subjects departs substantially from the programmed rate of reinforcement.

Table 4.2 shows the current-induced changes in the two parameters that specify the position of the reinforcement mountain: N_{hm} and R_{e_min}. Fig. 4.7 shows graphically the position of these parameters at the two currents tested.

Fig. 4.6. A three-dimensional scatterplot/wireframe view of the results of both N- (circles) and VI-sweeps (squares) obtained at the high current for subject SP4. For the N-sweeps, VI was held constant at either a high or low rate of reinforcement, and N was varied. For the VI-sweeps, N was held constant at either high or low pulses per train, and VI was varied. Filled circles, N-sweep at high VI; Hatched circles, N-sweep at low VI; Filled squares, VI-sweep at high N; Hatched squares, VI-sweep at low N.

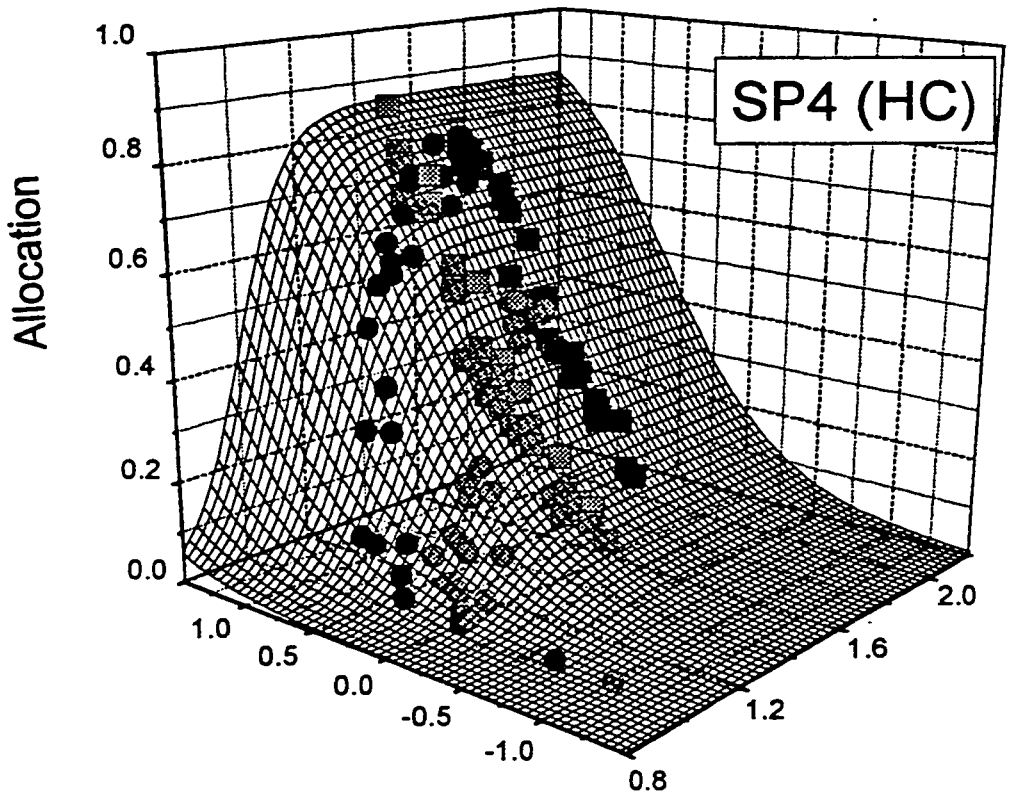
SP4 (HC)
Allocation
1.0
0.8
0.6
0.4
0.2
0.0
1.0
0.5
0.0
-0.5
-1.0
0.8
1.2
1.6
2.0

Table 4.1

Parameter and goodness-of-fit estimates as a function of current. Confidence intervals (95%) are given below the parameter values.

Rat	*Current (μA)*	N_{hm} (log_{10})	R_{e_min} (log_{10})	TA_{max}	*p*	*Coefficient of Determination*
SP2	316	1.925 1.907-1.942	0.643 0.478-0.808	1.199 1.044-1.355	17.956 8.264-27.647	0.942
	631	1.736 1.622-1.850	0.149 -0.037-0.335	1.021 0.944-1.099	4.061 2.058-6.065	0.954
SP3	316	1.729 1.700-1.762	0.283 0.119-0.447	0.930 0.846-1.015	10.172 5.646-14.698	0.946
	631	1.458 1.434-1.482	-0.083 -0.245-0.079	0.788 0.738-0.838	11.861 8.967-14.755	0.955
SP4	316	1.655 1.629-1.681	0.734 0.622-0.845	1.081 0.968-1.193	6.679 4.753-8.606	0.965
	631	1.379 1.342-1.417	0.634 0.528-0.741	0.981 0.900-1.063	5.445 3.965-6.925	0.964
SP6	316	1.771 1.690-1.851	0.001 -0.186-0.188	0.887 0.818-0.956	4.424 3.198-5.650	0.951
	631	1.392 1.351-1.432	0.166 0.021-0.311	0.914 0.844-0.985	6.445 4.421-8.478	0.942

Table 4.2

Changes in N_{hm} and R_{e_min} after current intensity manipulations. Asterisks denote that there is no overlap in the 95% confidence intervals surrounding these parameter estimates at the two different currents.

Rat	ΔN_{hm} (log_{10})	$\Delta R_{e\ min}$ (log_{10})
SP2	0.189 *	0.494 *
SP3	0.271 *	0.366 *
SP4	0.276 *	0.100
SP6	0.379 *	0.165

Fig. 4.7. Scatterplots superimposed on contour maps showing the effect of changing current intensity on N_{hm} and R_{e_min}. The alphanumeric in the bottom right side of the panels identifies the subjects from which the particular data were obtained. The graph in the upper left corner shows the data obtained at a low current intensity (LC). These data are compared with respect to both stimulation strength and reinforcement rate axes with the data obtained at a high current intensity (HC). The horizontal, solid lines extending across each graph indicate the position of N_{hm}, while the vertical solid lines indicate the position of R_{e_min}. The dotted lines indicate the 95% confidence intervals for these parameters.

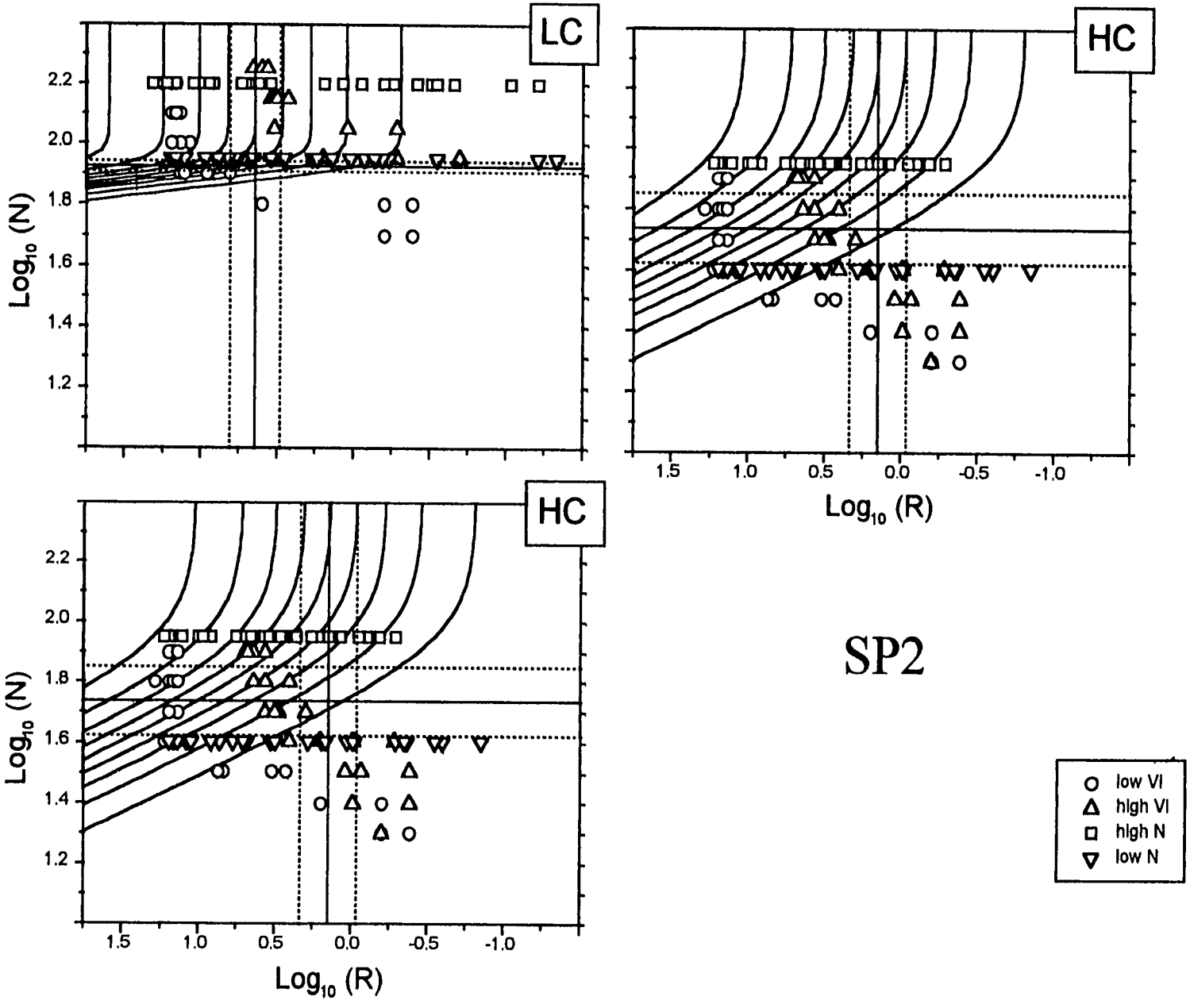
LC
HC
HC
Log10 (N)
Log10 (R)
2.2
2.0
1.8
1.6
1.4
1.2
1.5
1.0
0.5
0.0
-0.5
-1.0
low VI
high VI
high N
low N

SP2

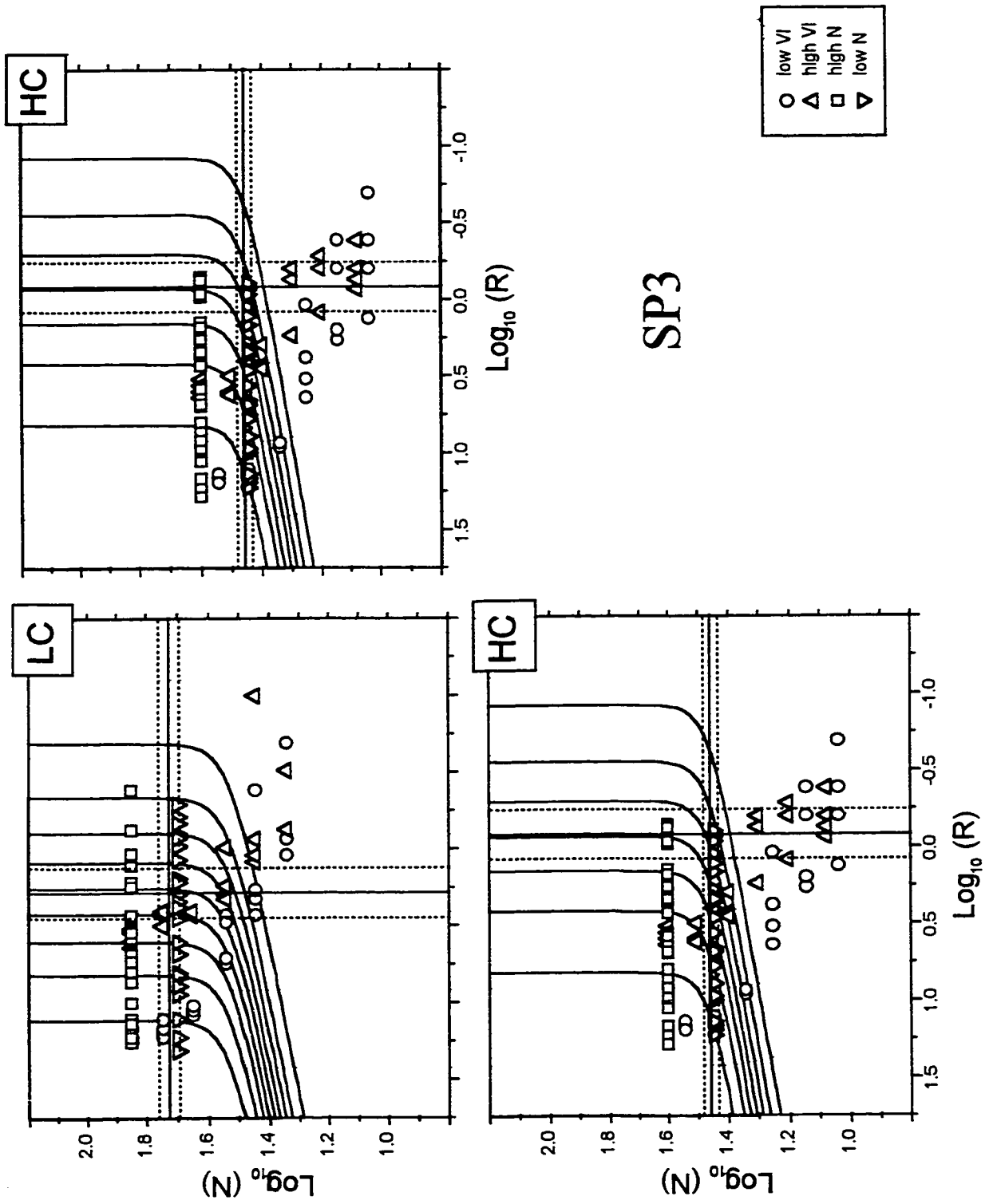
HC
LC
HC
low VI
high VI
high N
low N
SP3
Log10 (R)
Log10 (N)
Log10 (R)
Log10 (N)

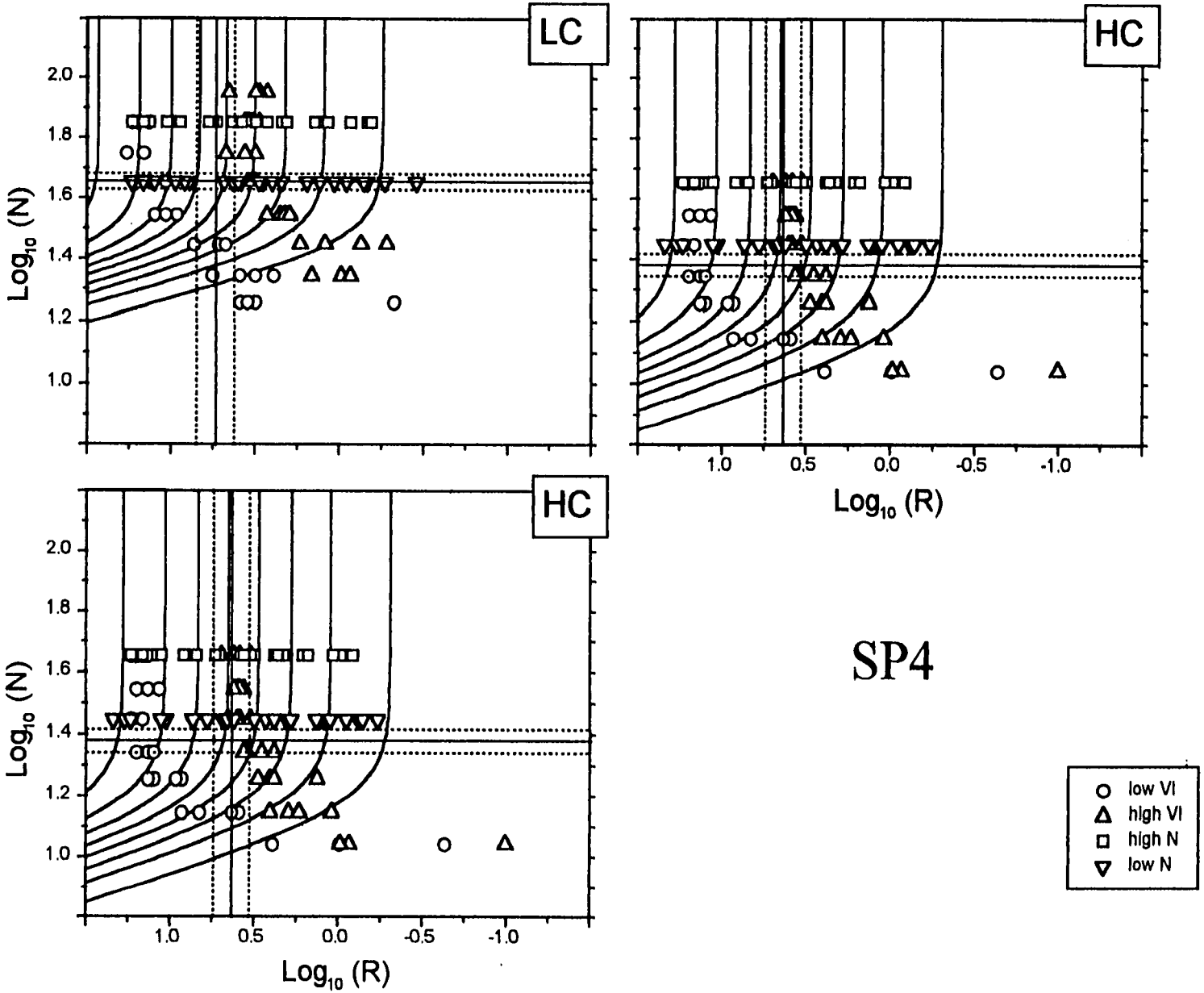
LC
HC
HC
2.0
1.8
1.6
1.4
1.2
1.0
Log10 (N)
1.0
0.5
0.0
-0.5
-1.0
Log10 (R)
SP4
low VI
high VI
high N
low N

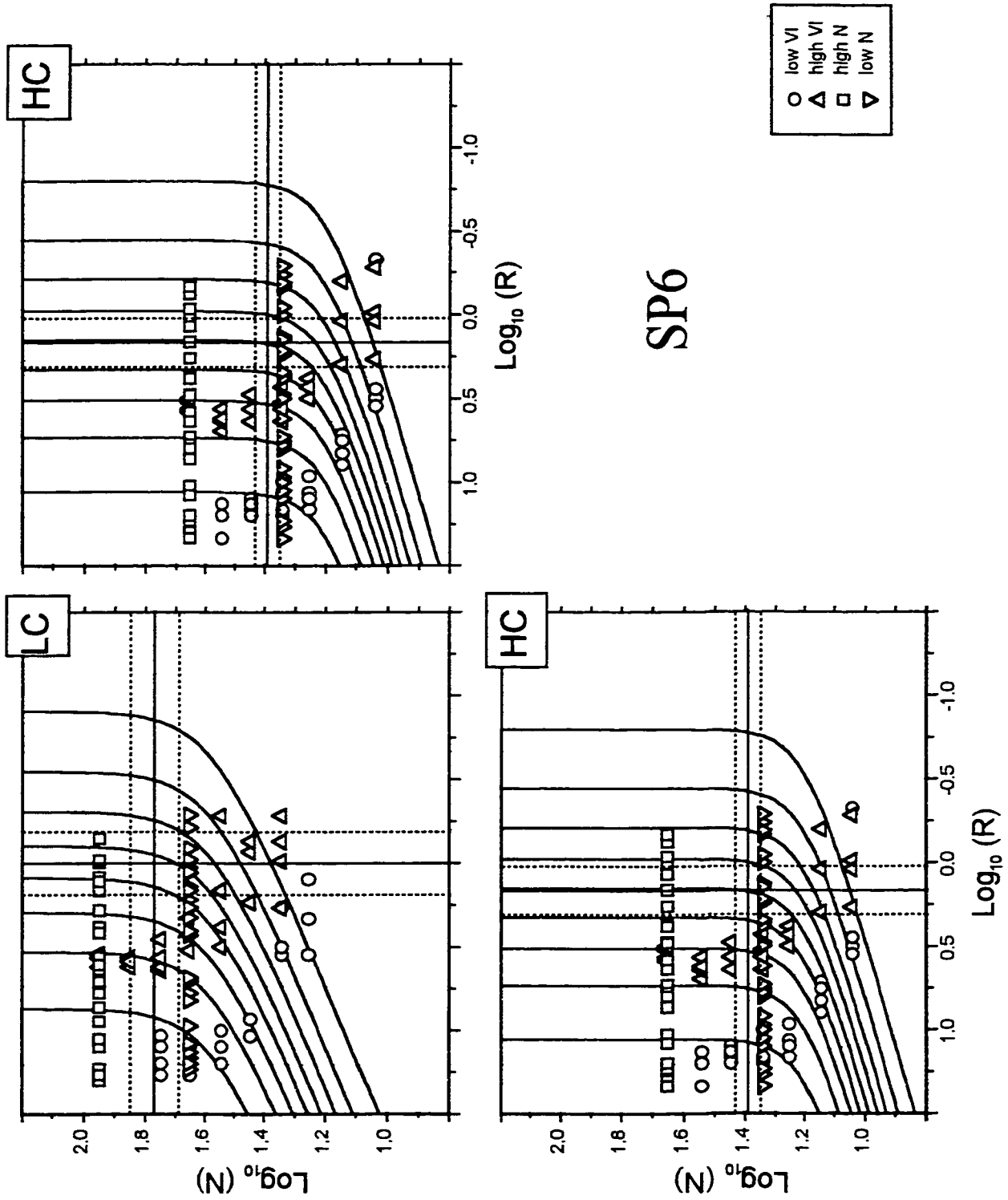
HC
LC
HC
SP6
low VI
high VI
high N
low N
Log10 (N)
Log10 (R)
2.0
1.8
1.6
1.4
1.2
1.0
-1.0
-0.5
0.0
0.5
1.0

The 95% confidence intervals show that the fits were better for N_{hm} than for R_{e_min}. This is due to the different slopes that curves have at the two sides of the reinforcement mountain. Small changes in N result in large changes in the rewarding efficacy of the stimulation, and thus in TA, whereas corresponding changes in R result in much more gradual changes in TA. It stands to reason, that the position of a steep curve can be determined more accurately than that of a slow rising curve.

According to the model of the BSR substrate presented in Fig. 4.5, current manipulations should only affect N_{hm}. Because the tested currents were spaced 0.3 $\log_{10}$ units apart, under the assumptions of the counter model, N_{hm} was expected to change by 0.3 $\log_{10}$ units. The observed absolute changes in N_{hm} ranged from about 0.2 to 0.4 $\log_{10}$ units across subjects. A 0.3 $\log_{10}$ unit change was well within the confidence range of the estimates.

As expected, R_{e_min} did not change in the case of subjects SP4 and SP6. However, in the remaining two subjects there was no overlap in the confidence intervals for R_{e_min} at the two currents. To visually assess these shifts, I plotted the time allocation data taken from the VI sweeps at the high number of pulses, for both the low and high currents, as a function of reinforcement rate (Fig. 4.8A). The curves were fit to the data by the mountain model. Although a lateral shift in the data and the fitted functions for the low and high currents is apparent for SP2, the data from the VI sweeps do not appear to be separated in the case of SP3. It can also be seen in Fig. 4.8

Fig. 4.8. Time allocation data for subjects SP2 and SP3 taken from the VI sweeps at the high number of pulses, for both the low (LC) and high currents (HC), as a function of reinforcement rate. The curves were fit to the data by the mountain model. The graphs at the top of the figure (A) show the R_{e_min} estimates (denoted by the vertical lines intersecting the x-axis) obtained with the mountain model. The graphs at the bottom of the figure (B) show the rate of reinforcement corresponding to a time allocation equal to 0.5 (also denoted by the vertical lines intersecting the x-axis).

A

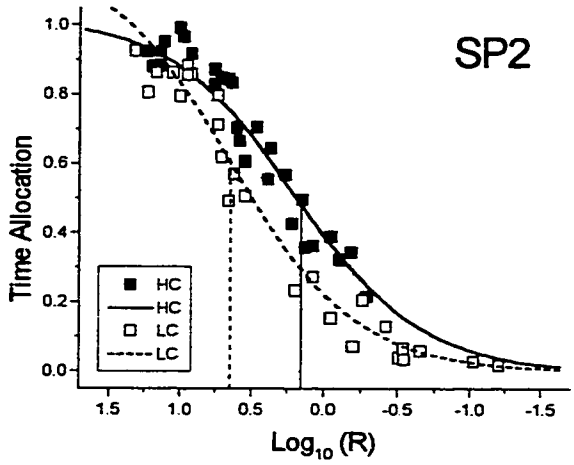
SP2
Time Allocation
Log10 (R)
HC
HC
LC
LC

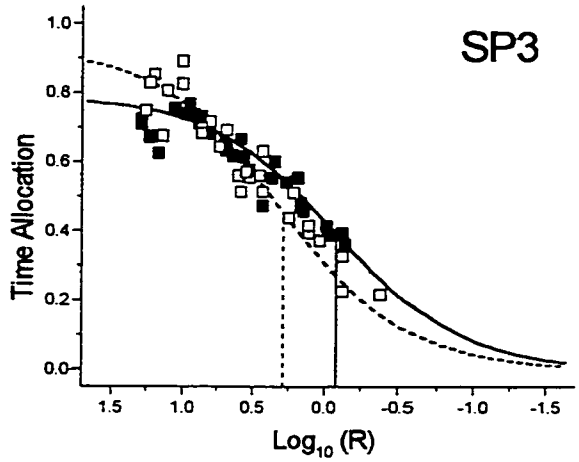
SP3
Time Allocation
Log10 (R)

B

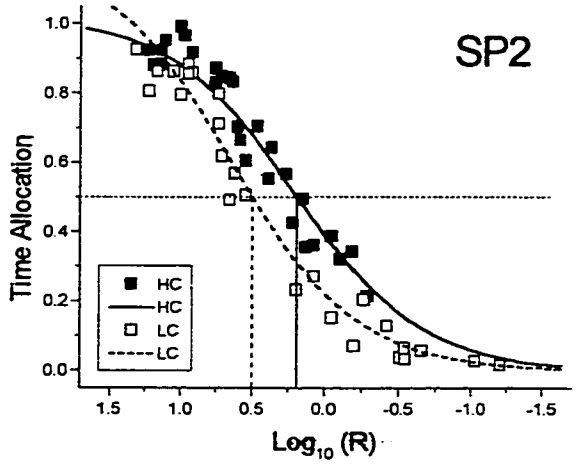
SP2
Time Allocation
Log10 (R)
HC
HC
LC
LC

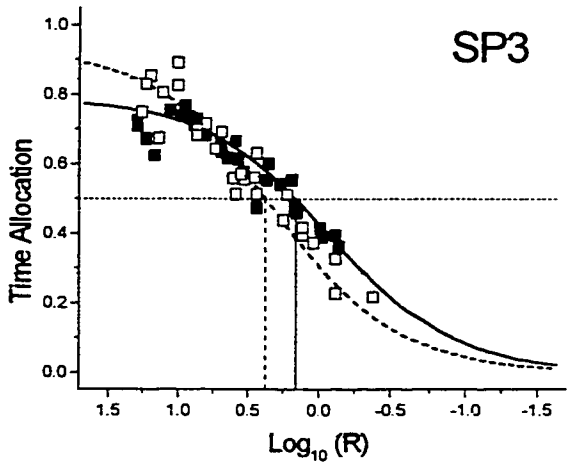
SP3
Time Allocation
Log10 (R)

that the fitted functions for SP3 have different asymptotes. It is likely that the difference in the R_{e_min} estimates for this particular subject is not real, but rather is an outcome of the differences in TA_{max}. Remember that R_{e_min} is the rate at which a maximal BSR would have to be delivered in order for the subject to spend half of its time responding for BSR. Thus, the calculation of R_{e_min} is dependent on the value of TA_{max}. Changing TA_{max} will change the half maximal time allocation for which a rate of reinforcement that corresponds to R_{e_min} is calculated. A difference in TA_{max} between conditions could result in artificial changes in R_{e_min}.

To test further this hypothesis, I calculated, for both currents, the rate of reinforcement corresponding to a time allocation equal to 0.5. This was done as follows. When N is much greater than N_{hm}, equation (9) reads:

$$TA = \frac{TA_{max}}{1 + \left(\frac{10^{R_{e\_min}}}{10^{R}} \right)} \tag{10}$$

Let TA = 0.5. Then

$$10^{R} = \frac{10^{R_{e\_min}}}{(2 \times TA_{max}) - 1} \tag{11}$$

and

$$R = \log_{10} \left[\frac{10^{R_{e\_min}}}{(2 \times TA_{max}) - 1} \right] \tag{12}$$

No difference between the two current conditions was found for SP3 when

equation (12) was used to calculate the rate of reinforcement at 50% time allocation (Fig. 4.8B). In the case of SP2, adoption of the constant criterion did not change the conclusion reached from comparing the values of R_{e_min}.

Why was R_{e_min} changed after current manipulation in the case of SP2? One possible explanation for this anomalous finding involves the notion of heterogeneity in the reward substrate. Given that the environment remained constant throughout testing and thus, U_e was invariant, the obvious conclusion is that altering the current changed I_{max}. This could happen if the increase in current recruited an additional subpopulation of reward fibers, in which case the shift in R_{e_min} could be interpreted according to the model of an heterogeneous substrate I advanced in the previous chapter. This suggestion receives support from the observation that *p*, the parameter governing the rate of reward growth, changed as a function of current. This is clearly seen as a change in the slope of the diagonal segment of the contours in Fig. 4.7.

4.3. THE EFFECT OF MANIPULATING TRAIN DURATION ON THE REINFORCEMENT MOUNTAIN

4.3.1. Introduction

Current intensity manipulations alter the stimulation field and thus the number of directly-stimulated neurons. Variations in the population of activated neurons complicate the interpretation of results stemming from manipulating the current, as, for example, was the case for SP2. In this

experiment, to eliminate the difficulties in interpretation, I manipulated train duration. Changing the train duration should only produce a shift along the N axis. At long train durations more pulses are required to drive integrator output to a given value of reward intensity due to leaky integration. Because, according to the model in Fig. 4.5, the non-linear transformation of the reward-intensity signal is produced downstream from the integrator, altering the train duration should change the number of pulses required to reach I_{max}, but not the value of I_{max}. Thus, the position of the reinforcement mountain should remain fixed along the R axis.

4.3.2. Materials and Methods

The same subjects and apparatus as described in the previous experiment (sections 4.2.2.1 and 4.2.2.2) served in the present study. Reinforcement mountains were obtained, first, with a 0.25 s long train of stimulation pulses (short train duration) and, second, with a 1.0 s train (long train duration). Stimulation consisted of fixed, 0.25-s or 1.0-s trains of cathodal, rectangular, 631 μA constant current pulses, 0.1 ms in duration. Data collection and analysis are described in detail in sections 4.2.2.3 and 4.2.2.4. Again, pulse sweeps at a low (VI 3.8 s) and high (VI 15 s) as well as VI sweeps at a high and low number of pulses were collected.

4.3.3. Results and Discussion

Table 4.3 summarizes the parameter and goodness-of-fit estimates as a function of train duration for the four subjects. The high coefficient of determination estimates indicate a strong fit of equation (9) to the data, although serial correlation parameters (not shown) reveal, for each fitted data set, a systematic non-random trend in the residuals.

Fig. 4.9 shows contour plots of the data and table 4.4 gives the absolute change in the N_{hm} and R_{e_min} parameters after changing train duration from 0.25 s to 1.0 s. In support of the proposed model, train duration manipulations moved the mountains only along the N axis. For all subjects, there was no overlap in the confidence limits of the N_{hm} estimates corresponding to the short and long train durations. In contrast, the confidence intervals for the R_{e_min} estimates in the two conditions always overlapped.

These results demonstrate that the reinforcement mountain can be moved exclusively along one axis. As predicted, changing the train duration and, thus, the activity at the input side of the integrator, shifted the mountain along the N but not along the R axis.

Table 4.3

Parameter and goodness-of-fit estimates as a function of train duration. Confidence intervals (95%) are given below the parameter values.

Rat	*Train Duration (s)*	N_{tm} (log_{10})	R_{e_min} (log_{10})	TA_{max}	p	*Coefficient of Determination*
SP2	0.25	1.581 1.553-1.610	0.127 -0.013-0.267	0.999 0.932-1.065	10.318 6.824-13.812	0.942
	1.0	1.861 1.837-1.885	0.400 0.265-0.535	1.030 0.937-1.122	12.831 5.712-19.951	0.936
SP3	0.25	1.312 1.281-1.343	0.245 0.095-0.396	0.952 0.870-1.034	10.665 6.306-15.024	0.947
	1.0	1.707 1.692-1.723	0.189 0.035-0.344	0.858 0.787-0.928	17.829 11.426-24.232	0.946
SP4	0.25	1.252 1.223-1.282	0.667 0.531-0.804	1.056 0.927-1.185	7.672 4.527-10.818	0.938
	1.0	1.589 1.561-1.616	0.520 0.413-0.627	0.963 0.887-1.039	7.039 5.095-8.983	0.957
SP6	0.25	1.351 1.280-1.422	0.102 -0.089-0.293	0.907 0.822-0.992	5.450 3.324-7.576	0.932
	1.0	1.553 1.509-1.597	0.001 -0.180-0.183	0.753 0.697-0.810	17.507 3.329-31.684	0.915

Table 4.4

Changes in N_{hm} and R_{e_min} after train duration manipulations. Asterisks denote that there is no overlap in the 95% confidence intervals surrounding these parameter estimates at the two different currents.

Rat	ΔN_{hm} (log_{10})	ΔR_{e_min} (log_{10})
SP2	0.280 *	0.273
SP3	0.395 *	0.056
SP4	0.337 *	0.147
SP6	0.202 *	0.101

Fig. 4.9. Scatterplots superimposed on contour maps showing the effect of changing train duration on N_{hm} and R_{e_min}. The alphanumeric in the bottom right side of the panels identifies the subjects from which the particular data were obtained. The graph in the upper left corner shows the data obtained at a short train duration (SD). These data are compared with respect to both stimulation strength and reinforcement rate axes with the data obtained at a long train duration (LD). The horizontal, solid lines extending across each graph indicate the position of N_{hm}, while the vertical solid lines indicate the position of R_{e_min}. The dotted lines indicate the 95% confidence intervals for these parameters.

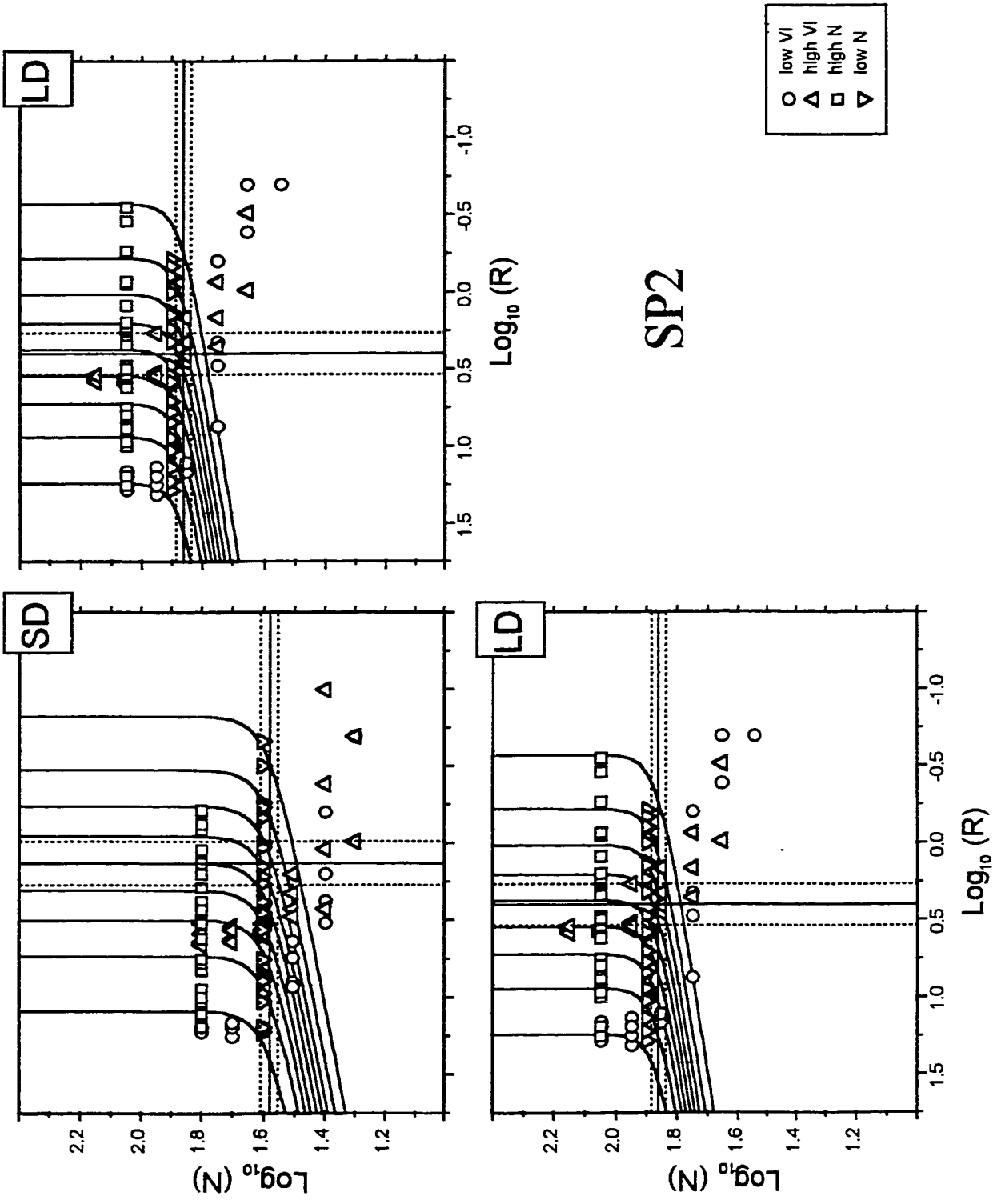
LD
SD
LD
SP2
low VI
high VI
high N
low N
Log10 (R)
Log10 (N)
2.2
2.0
1.8
1.6
1.4
1.2
1.5
1.0
0.5
0.0
-0.5
-1.0

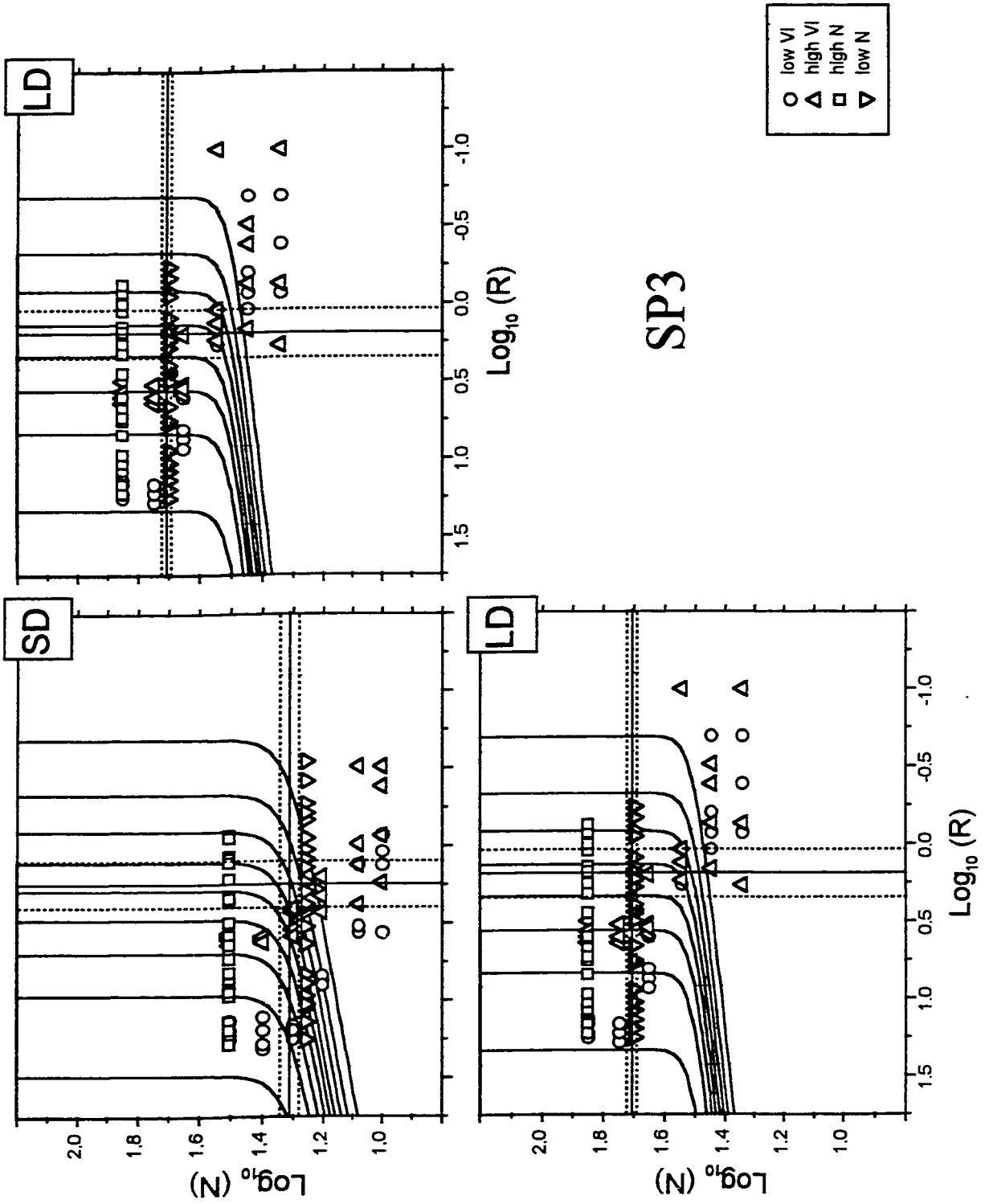
LD
SD
LD
SP3
low VI
high VI
high N
low N
Log10 (R)
Log10 (N)
Log10 (R)
Log10 (N)

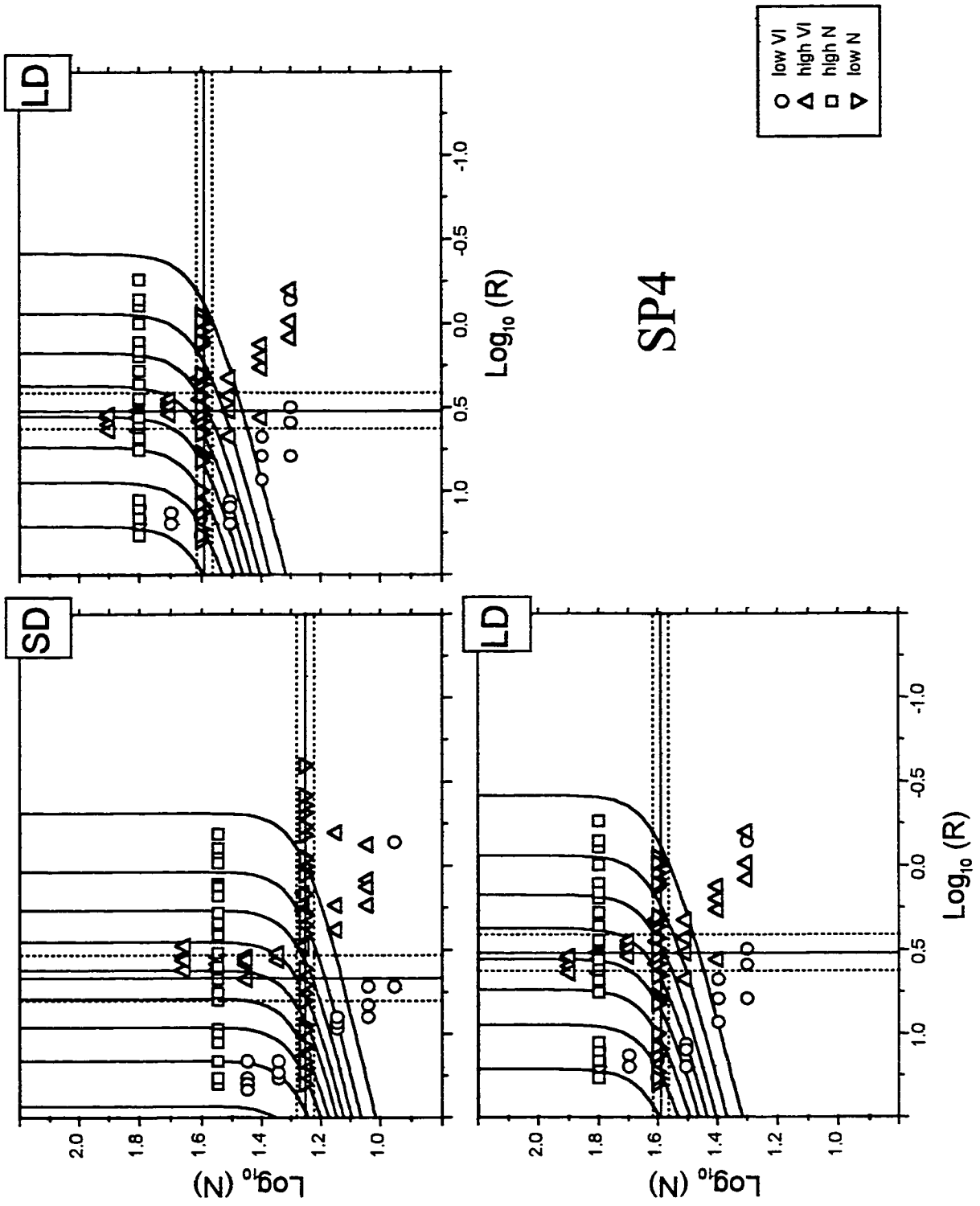
SP4
LD
SD
LD
low VI
high VI
high N
low N
Log10 (N)
Log10 (R)
Log10 (N)
Log10 (R)

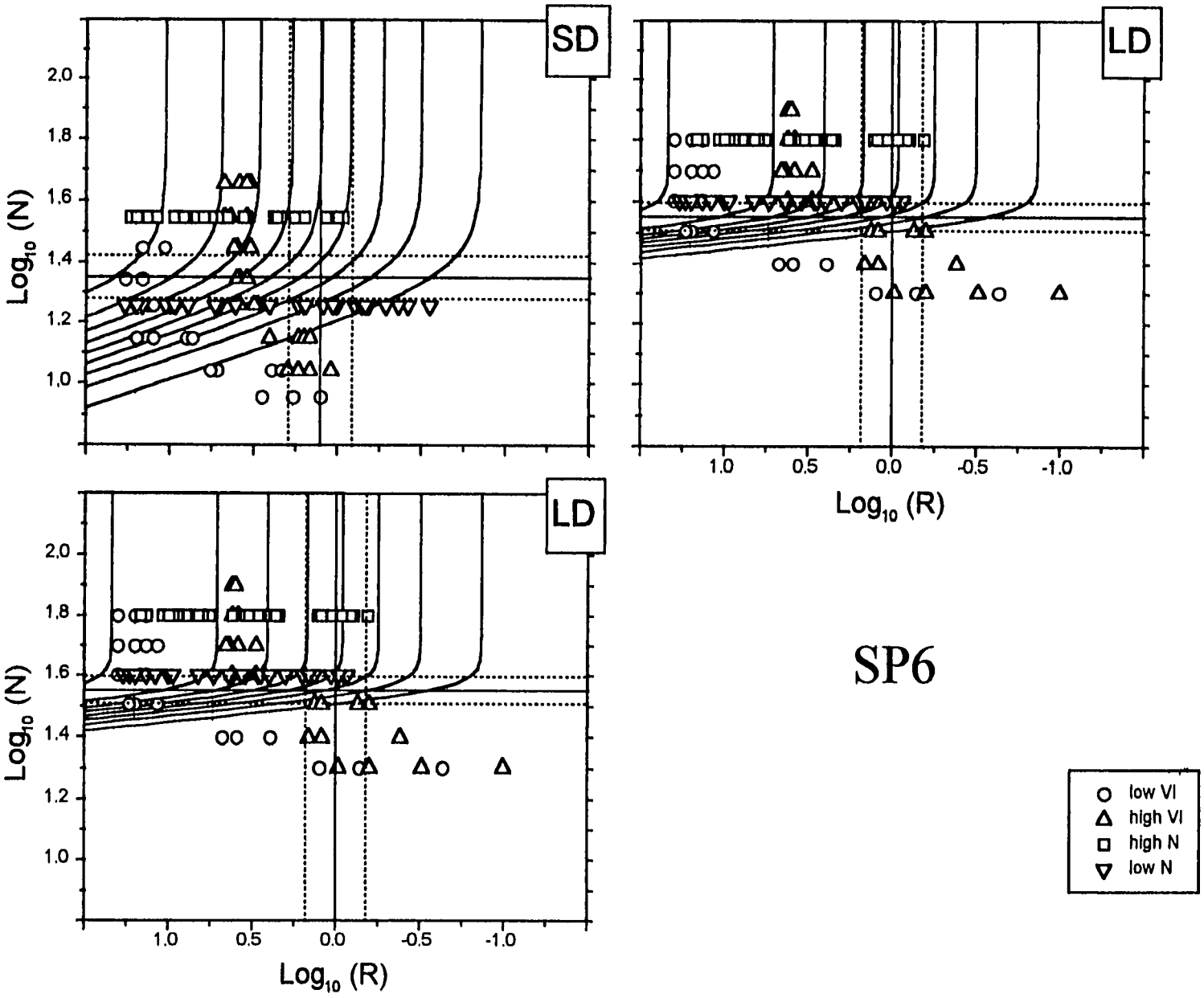
SD
LD
LD
Log10 (N)
Log10 (R)
2.0
1.8
1.6
1.4
1.2
1.0
1.0
0.5
0.0
-0.5
-1.0
low VI
high VI
high N
low N

SP6

4.4. THE EFFECT OF MANIPULATING BACKGROUND REINFORCEMENT ON THE REINFORCEMENT MOUNTAIN

4.4.1. Introduction

In the previous two experiments, manipulations were aimed at displacing the reinforcement mountain along the N axis. In this experiment, the aim was to produce a shift along the R axis. The position of the reinforcement mountain is set along the R axis by R_{e_min}. R_{e_min} is the rate at which a maximal BSR would have to be delivered in order to equal the combined utility of all the alternate reinforcers available. Thus, R_{e_min} measures background sources of reinforcement in terms of a maximal BSR and should change as a result of operations that directly affect the background reinforcement. Incorporating an additional source of reinforcement to the background would produce a shift toward higher rates of reinforcement, which would now act as lower rates had before the utility of the background was boosted. The following experiment examined the effects of delivering a maximal background BSR on the parameters of the reinforcement mountain. In contrast to the effects of manipulating current and train duration, introducing a maximal BSR to the background should shift the mountain exclusively along the R axis.

4.4.2. Materials and Methods

The details of the procedures are described in section 4.2.2. Briefly, two male Long Evans rats (300-350 g) were surgically implanted with monopolar electrodes aimed at the LH. The rats were trained to press a lever for 0.5-s trains of cathodal, rectangular, 631 μA constant current pulses, 0.1 ms in duration.

For the baseline, pulse sweeps were obtained at a low VI schedule of reinforcement (VI=2 s) as well as at a higher VI schedule (VI=8 s). VI sweeps were obtained, first, with an asymptotic and, second, with a more moderate BSR according to the following series of VI schedules: VI 2 s, VI 4 s, VI 8 s, VI 16 s, VI 32 s, VI 64 s. Equation (9) was fit to the data to estimate the parameters N_{hm}, R_{e_min}, TA_{max}, and p.

Following the collection of baseline data, the experiment was repeated as described above. However, for the second phase of the experiment, a variable time schedule delivering an asymptotic level of BSR at a rate equal to four times the baseline R_{e_min} was programmed to operate when the subjects were not pressing the lever. A 5-s blackout period followed the delivery of both contingent and non-contingent rewards. The trial times during this phase of the experiment were increased by 150 s.

4.3.3. Results and Discussion

Table 4.5 summarizes the parameter and goodness-of-fit estimates as a function of the absence or presence of background reinforcement for the two subjects. Fig. 4.10 shows contour plots of the data and table 4.6 gives the absolute change in the N_{hm} and R_{e_min} parameters after adding the background reinforcement.

Knowing that the confidence intervals around R_{e_min} are relatively large, I set the background BSR to be delivered at a rate equal to four times the baseline value of R_{e_min}. This manipulation was expected to produce an easily detectable 0.6 $\log_{10}$ units shift along the R axis. Shifts of approximately this magnitude were indeed seen. Adding background reinforcement was not expected to produce shifts along the N axis. Surprisingly, increases in R_{e_min} were accompanied by increases in N_{hm}, although the observed changes in N_{hm} were much smaller than the corresponding changes in R_{e_min}.

The shifts along the N axis cannot be explained within the context of the model proposed by Shizgal (Shizgal et al., 1996) (Fig. 4.5). According to this model, background reinforcement affects behavioral allocation by acting after the firings of the first stage neurons have been integrated to yield an intensity of reinforcement signal. In contrast, the present results, taken at face value, imply that the background reinforcement directly influences the input to the integrator. Nevertheless, it would be premature to abandon the current framework before examining the data and the method used to collect these

Table 4.5

Parameter and goodness-of-fit estimates as a function of the presence (+) or absence (-) of background reinforcement. Confidence intervals (95%) are given below the parameter values.

Rat	*Added Reinf.*	N_{hm} (log_{10})	R_{e_min} (log_{10})	TA_{max}	*p*	*Coefficient of Determination*
SP8	-	1.363 1.335-1.391	0.493 0.342-0.643	0.869 0.798-0.940	10.132 6.434-13.831	0.945
	+	1.549 1.430-1.667	0.993 0.717-1.269	0.814 0.674-0.954	4.265 2.361-6.168	0.945
SP9	-	1.459 1.431-1.487	0.508 0.345-0.671	0.946 0.859-1.032	10.453 5.563-15.342	0.942
	+	1.626 1.572-1.681	1.045 0.832-1.257	1.053 0.845-1.261	6.573 3.902-9.245	0.944

Table 4.6

Changes in N_{hm} and R_{e_min} after background reinforcement manipulations. Asterisks denote that there is no overlap in the 95% confidence intervals surrounding these parameter estimates at the two different currents.

Rat	ΔN_{hm} (log_{10})	ΔR_{e_min} (log_{10})
SP8	0.186 *	0.500 *
SP9	0.167 *	0.537 *

Fig. 4.10. Scatterplots superimposed on contour maps showing the effect of adding background reinforcement on N_{hm} and R_{e_min}. The alphanumeric in the bottom right side of the panels identifies the subjects from which the particular data were obtained. The graph in the upper left corner shows the baseline data obtained without any experimentally-arranged source of reinforcement added in the background (-BR). These data are compared with respect to both stimulation strength and reinforcement rate axes with the data obtained after adding a maximal BSR to the background sources of reinforcement (+BR). The horizontal, solid lines extending across each graph indicate the position of N_{hm}, while the vertical solid lines indicate the position of R_{e_min}. The dotted lines indicate the 95% confidence intervals for these parameters.

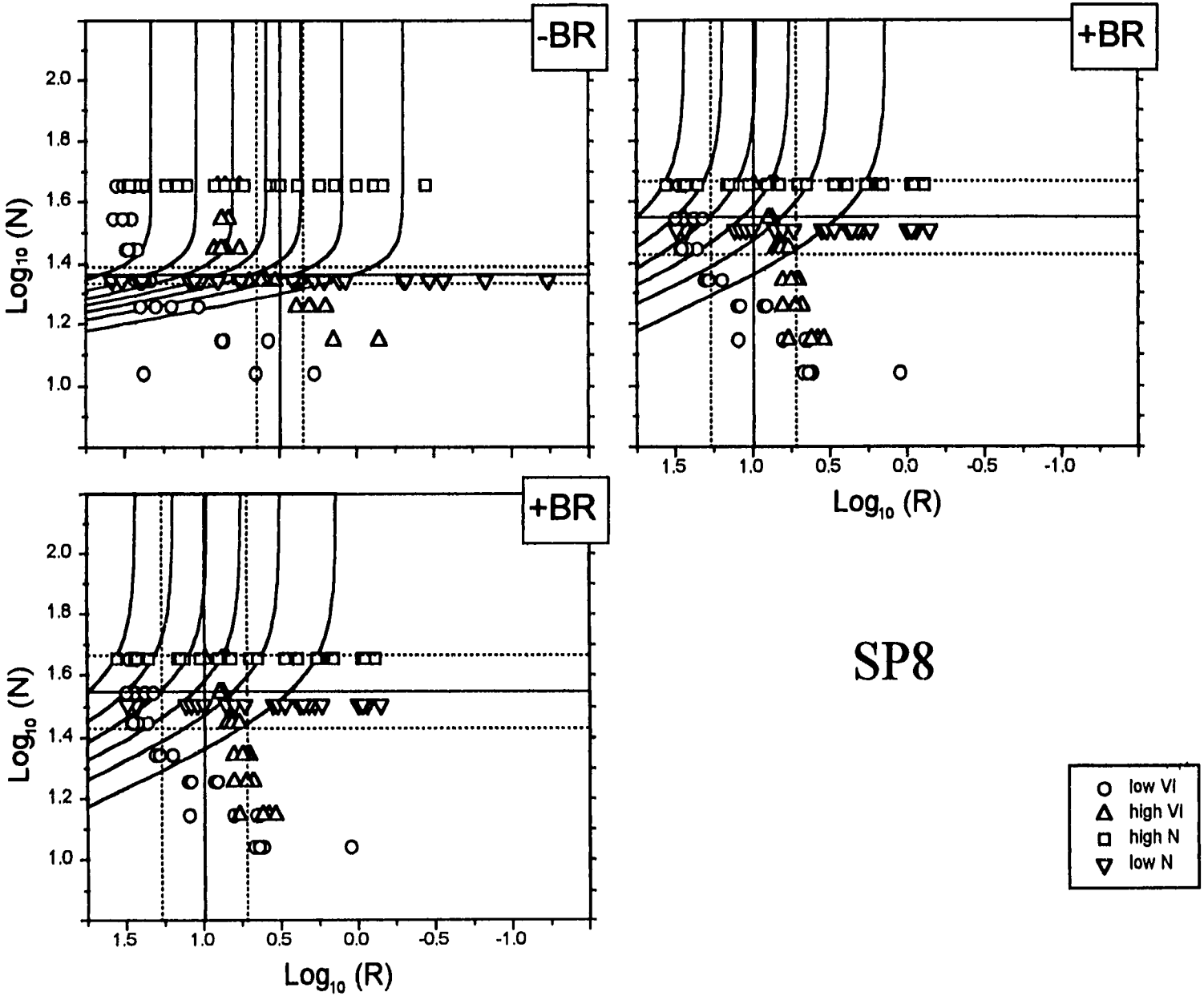
-BR
+BR
+BR
Log10 (N)
Log10 (R)
2.0
1.8
1.6
1.4
1.2
1.0
1.5
1.0
0.5
0.0
-0.5
-1.0
SP8
low VI
high VI
high N
low N

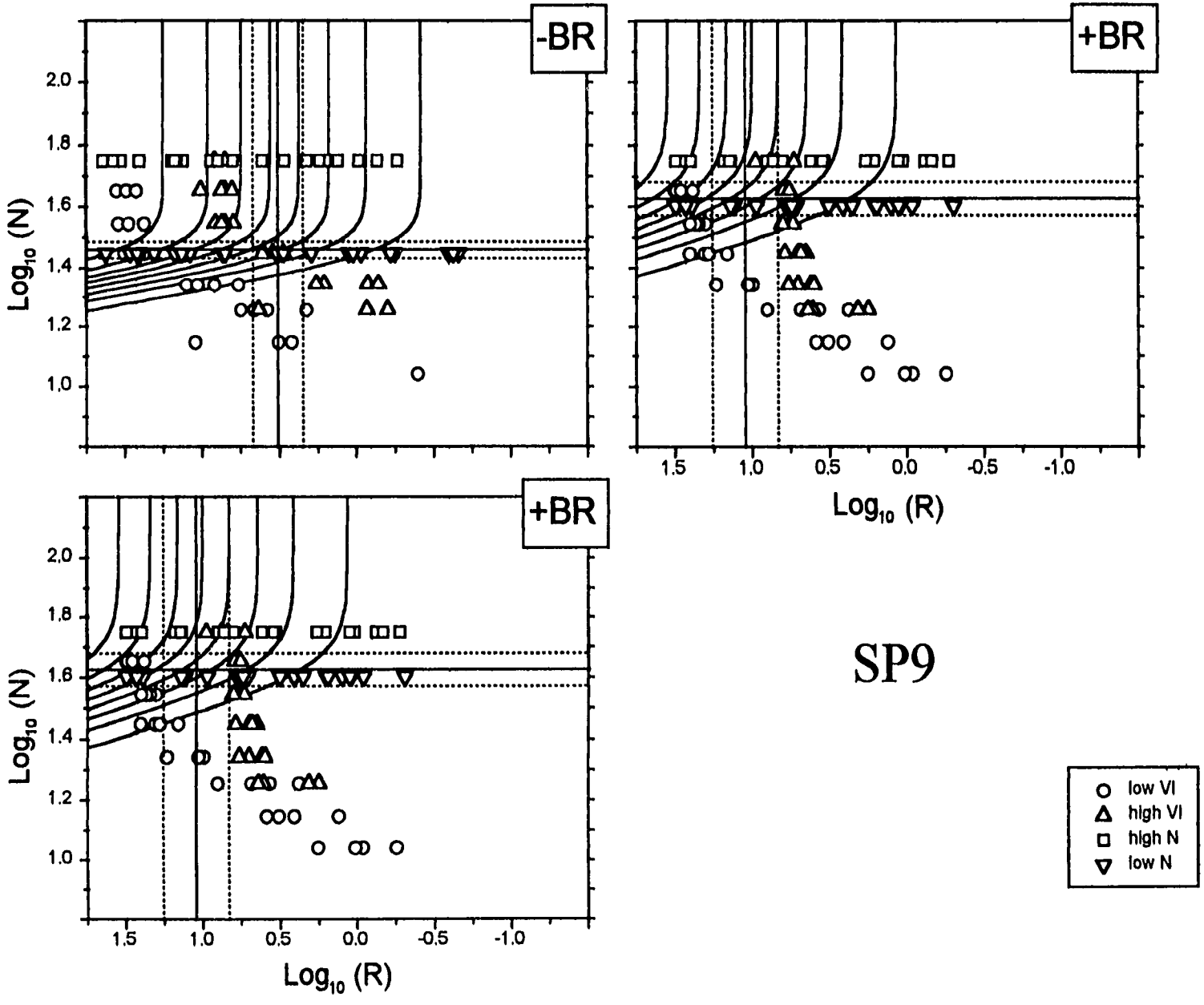
-BR
+BR
+BR
Log10 (N)
Log10 (R)
2.0
1.8
1.6
1.4
1.2
1.0
1.5
1.0
0.5
0.0
-0.5
-1.0
low VI
high VI
high N
low N

SP9

data more closely. Could the (not so large) shifts in N_{hm} be an artifact of the way the data were collected?

I have argued that choice is a matter of relative utility and that relative utility can be indexed by relative time allocation. The main benefit that ought to accrue from spending more time on a particular alternative is an increased harvest of rewards delivered by that alternative. On this account, a decrease in time allocation should produce a commensurate decrease in harvest. This premise does not hold. Fig. 4.11 shows a representative data set obtained from a baseline VI sweep at a high number of pulses: as the obtained rate of reinforcement decreased, time allocation decreased, but harvest was maintained at relatively high levels (harvest is the ratio of the rewards that were actually collected versus the rewards that could have potentially been collected).

The discordance between time allocation and harvest is due to the fact that rewards could be obtained by adopting one of two strategies. First, a subject could collect a reward by holding down the lever until the VI clock timed out. However, since rewards were stored, subjects could just make contact with the lever at any time after the VI clock had timed out and still collect the reward. Fig. 4.12 shows the proportion of the rewards obtained by "holds" or by "onsets" as a function of the rate of reinforcement for the VI sweep data shown in Fig. 4.11. At low VIs the subjects earned most of the rewards by holding the lever down, but at less rich VIs the subjects shifted

Fig. 4.11. Representative harvest and time allocation data, obtained from a VI-sweep at a high number of pulses, as a function of the rate of reinforcement. As the obtained rate of reinforcement decreases, time allocation decreases, but harvest is maintained at relatively high levels.

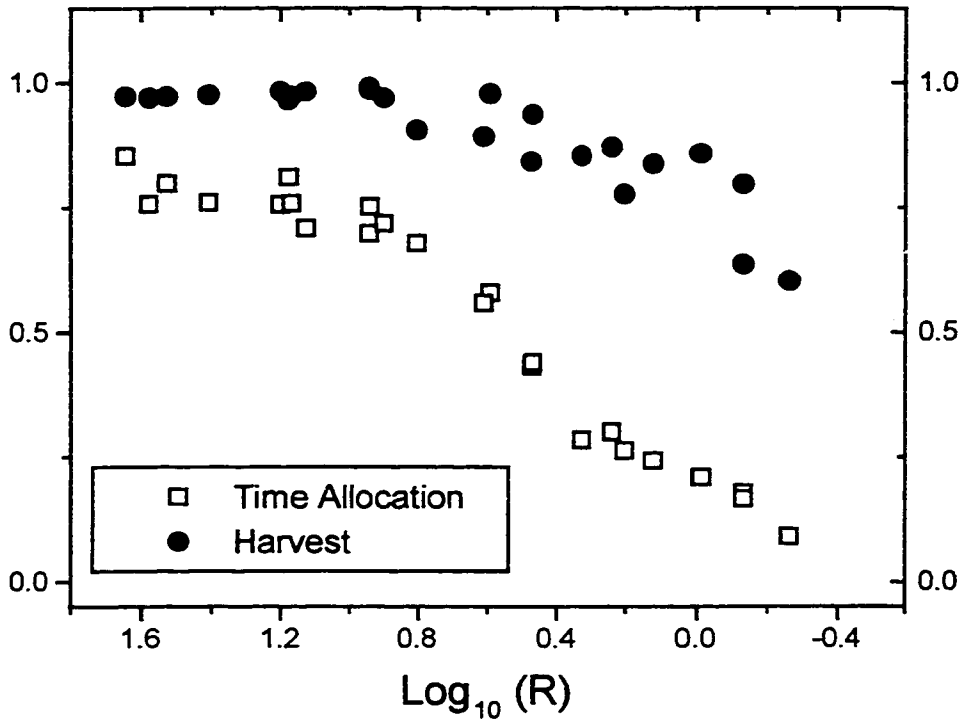
1.0
0.5
0.0
1.0
0.5
0.0
1.6
1.2
0.8
0.4
0.0
-0.4
Time Allocation
Harvest
Log10 (R)

Fig. 4.12. Proportion of rewards obtained by holding the lever down and waiting for the VI clock to time out ("holds") or by tapping the lever to obtain stored rewards after the VI clock had timed out ("onsets") as a function of the rate of reinforcement. for the VI sweep data shown in Fig. 4.11. At low VIs the subjects earned most of the rewards by holding the lever down, but at less rich VIs the subjects shifted their strategy and eventually earned only stored rewards.

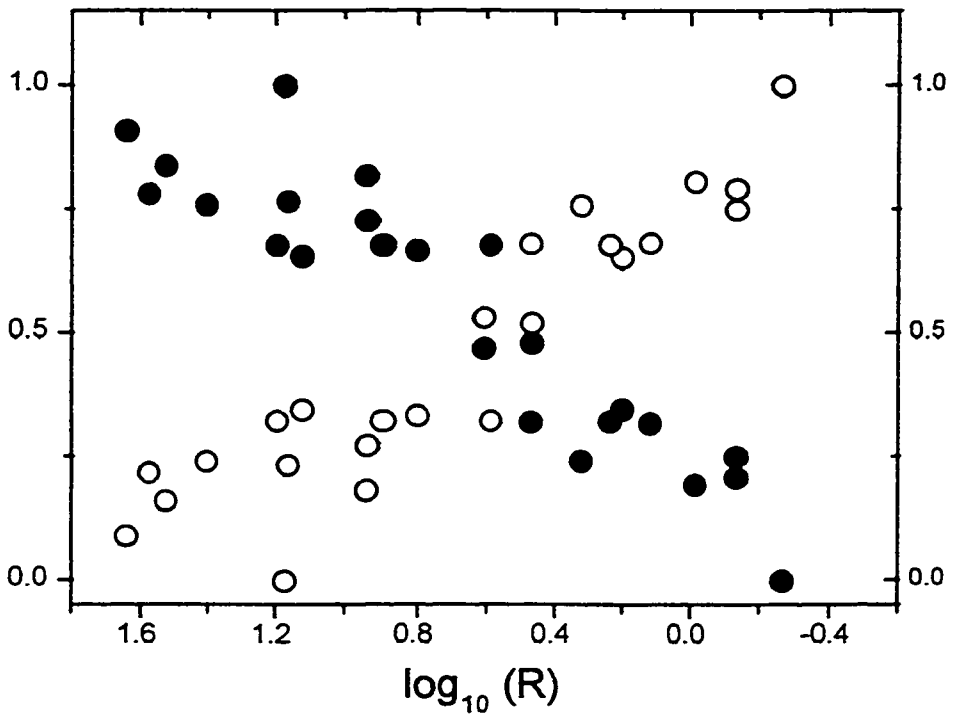
1.0
0.5
0.0
1.6
1.2
0.8
0.4
0.0
-0.4
log10 (R)
Holds
Onsets

their strategy and eventually earned only stored rewards. Switching from one strategy to the other resulted in a pronounced decrease in time allocation (a contact of negligible duration is all that is needed to obtain stored rewards), whereas the decline in harvest was much less pronounced.

By switching strategies as a function of reinforcement rate the subjects epitomized the slogan "make the most of the least." In this experiment, the trial time was set according to the VI so that the subjects could obtain the same number of rewards in each VI. Given a set trial time, at rich VIs, not holding the lever would result in lost rewards that could otherwise be obtained by making a small investment (holding the lever down for a few seconds or even milliseconds). On the other hand, when the programmed rate is low, a much larger investment (holding the lever down for tens of seconds up to more than a minute) would be needed to reap the same number of rewards. However, at long VIs, nothing would preclude the subjects from engaging in alternate activities in close proximity to the lever and to, occasionally, extend their paw to press it. By doing so, the subjects would strike a balance between obtaining a fair amount of rewards with minimal investment.

The flexibility in responding conferred by the experimental paradigm may be responsible for the observed shifts along the N axis after the addition of background reinforcement. In the present experiment, background rewards were scheduled to be delivered on the average more than four times per

minute as long as the variable time clock was not interrupted by the depression of the lever. The more the lever was held down, the less frequently background rewards were delivered. Perhaps then, the subjects were discouraged from adopting the hold down strategy, even when working for low VIs, and may have instead opted for intermittent lever pressing resulting in lower time allocation and, therefore, more background rewards. The new strategy would have allowed the subjects to earn background rewards of maximal intensity throughout a pulse sweep.

The present data are compatible with the notion that a switch in behavioral strategy may be responsible for the shifts along the N axis. To begin with, the time allocation data were indeed lower after the addition of background reinforcement. This can be seen from the decrease in the number of contour lines in Fig. 4.10 (NB, contour lines represent 10% increments in time allocation). Furthermore, the decrease in time allocation can be attributed to a shift in the strategy used to obtain the contingent rewards.

Fig. 4.13 compares the proportion of the rewards obtained by "holds" and the resulting harvest as a function of pulse number for the baseline versus the background reinforcement pulse sweep condition at the low VI (VI=2 s) for subject SP9. In the baseline condition harvest paralleled the degree to which the subject held the lever down and waited for the VI clock to time out. In contrast, the addition of background reinforcement shifted the response strategy and caused the two curves to separate. The greater the

difference in strength between the contingent and noncontingent rewards the less the subjects engaged in hold down behavior. When added background reinforcement is not available, less holds denote a drop in the rewarding efficacy of the stimulation corresponding to a drop in the number of earned rewards. However, the same is not necessarily the case when background reinforcement is added. Focus, for example, at the minimal stimulation strength that resulted in near maximal harvest in the baseline condition. To achieve that level of harvest the subject engaged for the most part in hold-down behavior. With the addition of background reinforcement, subjects still earned more than half of the available rewards of that same strength, but only a few of these rewards were collected by holding the lever down. As expected, the switch in response strategy resulted in a small decrease in harvest. However, this decrease was offset by interrupting the variable time clock less often so as to receive more background rewards than would be received if the subject engaged in hold-down behavior to the same extent as during baseline. Keep in mind, that in this case the background rewards were of higher intensity than the rewards earned from pressing the lever. It seems fair to conclude that the ability to alternate between behavioral strategies confounds the interpretation of the results and may be responsible for the observed shifts along the N axis.

Fig. 4.13. Proportion of rewards obtained by "holds" and the resulting harvest as a function of pulse number for the baseline versus the background reinforcement pulse sweep condition at the low VI for subject SP9. In the baseline condition harvest paralleled the degree to which the subject held the lever down and waited for the VI clock to time out. In contrast, the addition of background reinforcement shifted the response strategy and caused the two curves to separate.

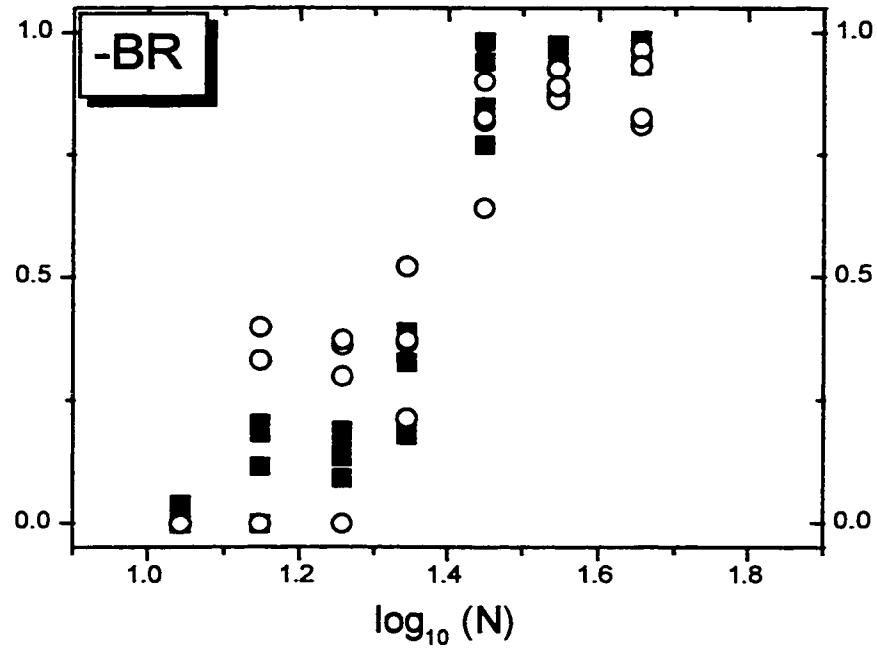
-BR
1.0
0.5
0.0
1.0
1.2
1.4
1.6
1.8
log10 (N)

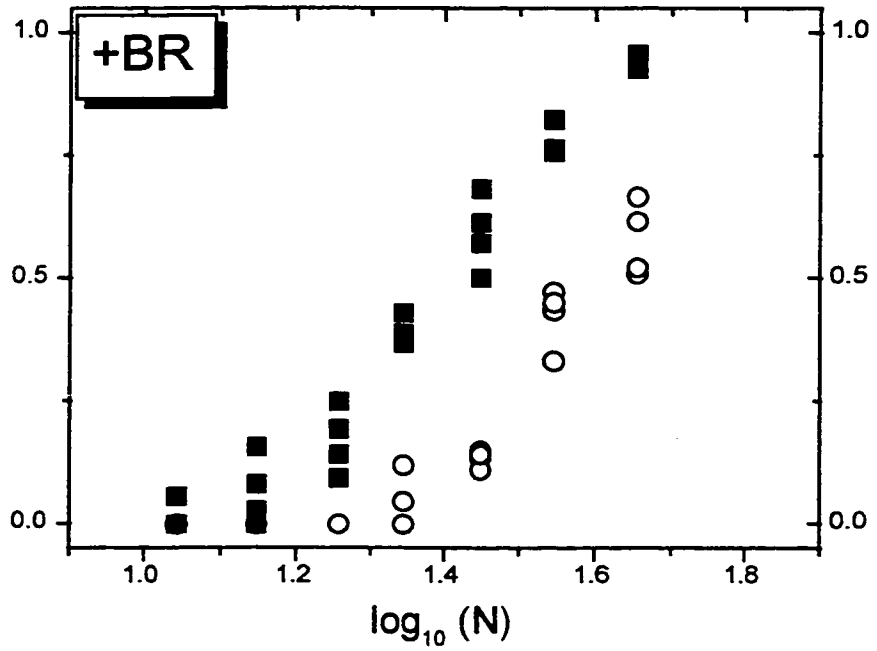
+BR
1.0
0.5
0.0
1.0
1.2
1.4
1.6
1.8
log10 (N)


Harvest
Holds

4.4. CONCLUSION

In this chapter, I employed an extension of the matching law to relate behavioral performance to the intensity and rate of reinforcement. As suggested by Shizgal (Shizgal et al., 1996), this three-dimensional analysis has the potential to distinguish changes in the mapping of stimulus strength into the intensity of reinforcement from changes in the maximum intensity of reinforcement and, therefore, to address the role played by basal forebrain, dopamine, and acetylcholine neurons in BSR. The above series of studies demonstrate the potential of this new method, but also reveal its weakness. It became clear, particularly from the last experiment, that the interpretation of the time allocation data is confounded by the ability of the subjects to choose whether to hold the lever down or to lever-press. This behavioral flexibility is directly linked to the fact that rewards are stored after they become available.

The source of the problem points to its solution. That is, if storing the rewards promotes the tendency to return to the lever after a long absence, not storing the rewards ought to counteract this tendency. Making the rewards available only at the time the VI clock runs out will force the subjects to commit to the lever in order to obtain the rewards. Then, the number of rewards earned from holding down the lever will be proportional to time allocation and thus, time allocation will serve as a true index of relative utility. Pilot experiments using this modification seem promising. However, I should note, that this modification takes the analysis away from the confines

of the matching law. Herrnstein's (1970) hyperbolic matching equation does not apply to the new hold-down contingency. Efforts are under way to describe the performance function underlying this contingency.

EPILOGUE

In their 1964 book chapter, *The Mechanisms of Voluntary Behavior,* Olds and Olds (1964) ask:

> "In the wide system of neural structures that appears to be involved in positive reinforcement by electrical stimulation of the brain, is there a field and a focus? Is there a broad set of minor entities all projecting to some constricted central area that is essential to these positive reinforcement mechanisms"?

More questions follow about the relationship between the substrates of positive and negative reinforcement and the "chemical sensitivities of these systems". "Are they controlled mainly by excitatory or inhibitory neurohumors? What are the pathways relating these mechanisms to behavior? Do these mechanisms control motor systems"?

For the most part, these same questions guide today's research. This is not to say that progress has not been made. Psychophysical studies have sketched a portrait of the first stage neurons, while pharmacological studies have established a role for dopamine and acetylcholine in BSR. Yet these lines of experimentation, probing as they are, are not sufficient to provide a clear-cut answer to the above questions. Thus, about one third of the neurons giving rise to MFB axons have the properties expected from first stage neurons while the nature of the involvement of dopamine and acetylcholine neurons in BSR is ambiguous.

It is easy to see the demand for applying new methods to the quest for definite answers. To meet this demand, I turned to tools of neuroanatomy and concepts of operant psychology. Fos immunostaining will bring the analysis of BSR at the cellular level. The multi-dimensional analysis of performance for BSR will help to answer basic questions about the organization and operating principles of the reward-related circuitry. Clearly more work is needed to achieve these objectives, but the groundwork is already in place.

The task of fleshing out the BSR circuitry is still in progress. Will the application of the methods described in this thesis speed up the progress? Although it is too early to tell how this will all work out, these methods should make it easier to devise the crucial experiments and to resolve some of the puzzles.

REFERENCES

Anderson, R., & Miliaressis, E. (1994). Does the MFB convey functionally different reward signals? *Behavioural Brain Research, 60,* 55-61.

Andersson, P.-B., Perry, V. H., & Gordon, S. (1991a). The CNS acute inflammatory response to excitotoxic neuronal cell death. *Immunology Letters, 30,* 177-182.

Andersson, P.-B., Perry, V. H., & Gordon, S. (1991b). The kinetics and morphological characteristics of the macrophage-microglial response to kainic acid-induced neuronal degeneration. *Neuroscience, 42,* 201-214.

Araki, M., McGeer, P. L., & Kimura, H. (1988). The efferent projections of the rat lateral habenular nucleus revealed by the PHA-L anterograde tracing method. *Brain Research, 441,* 319-330.

Arvanitogiannis, A., Flores, C., & Shizgal, P. (1997). Fos-like immunoreactivity in the caudal diencephalon and brainstem following lateral hypothalamic self-stimulation. *Behavioural Brain Research, 88,* 275-279.

Arvanitogiannis, A., Flores, C., Pfaus, J. G., & Shizgal, P. (1996a). Increased ipsilateral expression of Fos following lateral hypothalamic self-stimulation. *Brain Research, 720,* 148-154.

Arvanitogiannis, A., Waraczynski, M., & Shizgal, P. (1996b). Effects of excitotoxic lesions of the basal forebrain on MFB self-stimulation. *Physiology and Behavior, 59,* 795-806.

Barone, F. C., Wayner, M. J., Scharoun, S. L., Guevara-Aguilar, R., & Aguilar-Baturoni, H. U. (1981). Afferent connections to the lateral hypothalamus: a horseradish peroxidase study in the rat. *Brain Research Bulletin, 7,* 75-88.

Baum, W. M., & Rachlin, H. (1969). Choice as time allocation. *Journal of the Experimental Analysis of Behavior, 12,* 861-874.

Bielajew, C., & Shizgal, P. (1982). Behaviorally derived measures of conduction velocity in the substrate for rewarding medial forebrain bundle stimulation. *Brain Research, 237,* 107-119.

Bielajew, C., & Shizgal, P. (1986). Evidence implicating descending fibers in self-stimulation of the medial forebrain bundle. *The Journal of Neuroscience, 6,* 919-929.

Bielajew, C. H. (1991). Distribution of cytochrome oxidase in response to rewarding brain stimulation: effect of different pulse durations. *Brain Research Bulletin, 26,* 379-384.

Black, I. B., Adler, J. E., Dreyfus, C. F., Friedman, W. F., LaGamma, E. F., & Roach, A. (1987). Biochemistry of information storage in the nervous system. *Science, 236,* 1263-1268.

Blaha, C. D., & Phillips, A. G. (1990). Applications of in vivo electrochemistry to the measurement of changes in dopamine release during intracranial self-stimulation. *Journal of Neuroscience Methods, 34,* 125-133.

Bo, L., Dawson, T. M., Wesselingh, S., Mork, S., Choi, S., Kong, P. A., Hanley, D., & Trapp, B. D. (1994). Induction of nitric oxide synthase in demyelinating regions of multiple sclerosis brains. *Annals of Neurology, 36,* 778-786.

Boye, S. M., & Rompre, P. P. (1996). Mesencephalic substrate of reward: axonal connections. *Journal of Neuroscience, 16,* 3511-3520.

Bullitt, E. (1990). Expression of c-fos-like protein as a marker for neuronal activity following noxious stimulation in the rat. *Journal of Comparative Neurology, 296,* 517-530.

Carr, K. D. (1996). Feeding, drug abuse, and the sensitization of reward by metabolic need. *Neurochemical Research, 21*(11), 1455-1467.

Carr, K. D., & Papadouka, V. (1994). The role of multiple opioid receptors in the potentiation of reward by food restriction. *Brain Research, 639,* 253-260.

Carr, K. D., & Wolinsky, T. D. (1993). Chronic food restriction and weight loss produce opioid facilitation of perifornical hypothalamic self-stimulation. *Brain Research, 607,* 141-148.

Coffey, P. J., Perry, V. H., Allen, Y., Sinden, J., & Rawlins, J. N. P. (1988). Ibotenic acid induced demyelination in the central nervous system: A consequence of a local inflammatory response. *Neuroscience letters., 84,* 178-184.

Coffey, P. J., Perry, V. H., & Rawlins, J. N. P. (1990). An investigation into the early stages of the inflammatory response following ibotenic acid-induced neuronal degeneration. *Neuroscience, 35,* 121-132.

Colle, L. M., & Wise, R. A. (1987). Opposite effects of unilateral forebrain ablations on ipsilateral and contralateral hypothalamic self-stimulation. *Brain Research, 407,* 285-293.

Colle, L. M., & Wise, R. A. (1988). Effects of nucleus accumbens amphetamine on lateral hyothalamic brain stimulation reward. *Brain Research, 459,* 361-368.

Conover, K. L., & Shizgal, P. (1994a). Competition and summation between rewarding effects of sucrose and lateral hypothalamic stimulation in the rat. *Behavioral Neuroscience, 108*(3), 537-548.

Conover, K. L., & Shizgal, P. (1994b). Differential effects of postingestive feedback on the reward value of sucrose and lateral hypothalamic stimulation in the rat. *Behavioral Neuroscience, 108*(3), 559-572.

Conover, K. L., Woodside, B., & Shizgal, P. (1994). Effects of sodium depletion on competition and summation between rewarding effects of salt and lateral hypothalamic stimulation in the rat. *Behavioral Neuroscience, 108*(3), 549-558.

Davison, M., & McCarthy, D. (1988). *The Matching Law.* Hillsdale, NJ: Lawrence Erlbaum Associates.

Demmer, J., Dragunow, M., Lawlor, P. A., Mason, S. E., Leah, J. D., Abraham, W. C., & Tate, W. P. (1993). Differential expression of immediate early genes after hippocampal long-term potentiation in awake rats. *Molecular Brain Research, 17,* 279-286.

Deutch, A. Y., Lee, M. C., Gillham, M. H., Cameron, D. A., Goldstein, M., & Iadarola, M. J. (1991). Stress selectively increases Fos protein in dopamine neurons innervating the prefrontal cortex. *Cerebral Cortex, 1,* 273-292.

Dragunow, M., & Faull, R. (1989). The use of c-fos as a metabolic marker in neuronal pathway tracing. *Journal of Neuroscience Methods, 29,* 261-265.

Dragunow, M., & Robertson, H. A. (1987). Kindling stimulation induces c-fos protein in granule cells of the rat dentate gyrus. *Nature, 329,* 441-442.

Dusart, I., Marty, S., & Peschanski, M. (1992). Demyelination, and remyelination by schwann cells and oligodendrocytes after kainate-induced neuronal depletion in the central nervous system. *Neuroscience, 51,* 137-148.

Edmonds, D. E., & Gallistel, C. R. (1974). Parametric analysis of brain stimulation reward in the rat: III. Effect of performance variables on the reward summation function. *Journal of Comparative and Physiological Psychology, 87,* 876-883.

Esposito, R. U., Porrino, L. J., Seeger, T. F., Crane, A. M., Everist, H. D., & Pert, A. (1984). Changes in local cerebral glucose utilization during rewarding brain stimulation. *Proceedings of the National Academy of Sciences USA, 81,* 635-639.

Flores, C., Arvanitogiannis, A., & Shizgal, P. (1997). Fos-like immunoreactivity in forebrain regions following self-stimulation of the lateral hypothalamus and the ventral tegmental area. *Behavioural Brain Research, 87,* 239-251.

Frank, R. A., & Stutz, R. M. (1984). Self-deprivation: A review. *Psychological Bulletin, 96,* 384-393.

Gallin, W. J., & Greenberg, M. E. (1995). Calcium regulation of gene expression in neurons: the mode of entry matters. *Current Opinion in Neurobiology, 5,* 367-374.

Gallistel, C. R. (1978). Self-stimulation in the rat: Quantitative characteristics of the reward pathway. *Journal of Comparative and Physiological Psychology, 92,* 977-998.

Gallistel, C. R., & Beagley, G. (1971). Specificity of brain stimulation reward in the rat. *Journal of Comparative and Physiological Psychology, 76,* 199-205.

Gallistel, C. R., Boytim, M., Gomita, Y., & Klebanoff, L. (1982). Does pimozide block the reinforcing effect of brain stimulation? *Pharmacology Biochemistry and Behavior, 17,* 769-781.

Gallistel, C. R., & Freyd, G. (1987). Quantitative determination of the effects of catecholaminergic agonists on the rewarding efficacy of brain stimulation. *Pharmacology Biochemistry and Behavior, 26,* 731-741.

Gallistel, C. R., Gomita, Y., Yadin, E., & Campbell, K. A. (1985). Forebrain origins and terminations of the medial forebrain bundle metabolically activated by rewarding stimulation or by reward-blocking doses of pimozide. *The Journal of Neuroscience, 5,* 1246-1251.

Gallistel, C. R., & Karras, D. (1984). Pimozide and amphetamine have opposing effects on the reward summation function. *Pharmacology Biochemistry and Behavior, 20,* 73-77.

Gallistel, C. R., & Leon, M. (1991). Measuring the subjective magnitude of brain stimulation reward by titration with rate of reward. *Behavioral Neuroscience, 105,* 913-925.

Gallistel, C. R., Leon, M., Lim, B. T., Sim, J. C., & Waraczynski, M. (1996). Destruction of the medial forebrain bundle caudal to the site of stimulation reduces rewarding efficacy but destruction rostrally does not. *Behavioral Neuroscience, 110*(4), 1-25.

Gallistel, C. R., Shizgal, P., & Yeomans, J. S. (1981). A portrait of the substrate for self-stimulation. *Psychological Review, 88,* 228-273.

Gomita, Y., & Gallistel, C. R. (1982). Effects of reinforcement-blocking doses of pimozide on neural systems driven by rewarding stimulation of the MFB: A 14C-2-deoxyglucose analysis. *Pharmacology Biochemistry and Behavior, 17,* 841-845.

Gratton, A., Hoffer, B. J., & Gerhardt, G. A. (1988). Effects of electrical stimulation of brain reward sites on release of dopamine in rat: an in vivo electrochemical study. *Brain Research Bulletin, 21,* 319-324.

Greatrex, R. M., & Phillipson, O. T. (1982). Demonstration of synaptic input from prefrontal cortex to the habenula in the rat. *Brain Research, 238,* 192-197.

Hallanger, A. E., & Wainer, B. H. (1988). Ascending Projections from the Pedunculopontine Tegmental Nucleus and the Adjacent Mesopontine Tegmentum in the Rat. *The Journal of Comparative Neurology, 274,* 483-515.

Hastings, M. H., Winn, P., & Dunnett, S. B. (1985). Neurotoxic amino acid lesions of the LH: a parametric comparison of the effects of ibotenate, N-methyl-D, L-aspartic acid, and quisqualate in the rat. *Brain Research, 360,* 248-256.

Herkenham, M., & Nauta, W. J. (1977). Afferent connections of the habenular nuclei in the rat. A horseradish peroxidase study with a note on the fiber-of passage problem. *Journal of Comparative Neurology, 173,* 123-146.

Herkenham, M., & Nauta, W. J. (1979). Efferent connections of the habenular nuclei in the rat. *Journal of Comparative Neurology, 187,* 19-47.

Herrnstein, R. J. (1961). Relative and absolute strength of response as a function of frequency of reinforcement. *Journal of the Experimental Analysis of Behavior, 4,* 267-272.

Herrnstein, R. J. (1970). On the law of effect. *Journal of the Experimental Analysis of Behavior, 13,* 243-266.

Hill, C. S., & Treisman, R. (1995). Transcription regulation by extracellular signals: mechanisms and specificity. *Cell, 80,* 199-211.

Hoebel, B. G. (1965). Hypothalamic lesions by electrocauterization: Disinhibition of feeding and self-stimulation. *Science, 149,* 452-453.

Hoebel, B. G. (1968). Inhibition and disinhibition of self-stimulation and feeding: hypothalamic contol and postingestional factors. *Journal of Comparative and Physiological Psychology, 66,* 89-100.

Hoebel, B. G. (1969). Feeding and self-stimulation. *Annals of the New York Academy of Sciences, 157,* 758-778.

Hoebel, B. G., & Teitelbaum, P. (1962). Hypothalamic control of feeding and self-stimulation. *Science, 135,* 375-377.

Hoebel, B. G., & Thompson, R. D. (1969). Aversion to lateral hypothalamic stimulation caused by intragastric feeding or obesity. *Journal of Comparative and Physiological Psychology, 68,* 536-543.

Hsu, S. M., Raine, L., & Fanger, H. (1981). The use of anti-avidin antibody and avidin-botin-peroxidase complex in immunoperoxidase technics. *American Journal of Clinical Pathology, 75,* 816-821.

Hughes, P., & Dragunow, M. (1995). Induction of immediate early genes and the control of neurotransmitter-regulated gene expression within the nervous system. *Pharmacological Reviews, 47,* 133-175.

Hunt, S. P., Pini, A., & Evans, G. (1987). Induction of c-fos-like protein in spinal cord neurons following sensory stimulation. *Nature, 328,* 632-634.

Janas, J., & Stellar, J. R. (1987). The effects of knife-cut lesions of the medial forebrain bundle in self-stimulating rats. *Behavioral Neuroscience, 101*, 832-845.

Johnson, P. I., & Stellar, J. R. (1994). NMDA-induced lesions of the nucleus accumbens and/or ventral pallidum fail to attenuate lateral hypothalamic self-stimulation reward. *Brain Research, 646*, 73-84.

Kadekaro, M., Crane, A. M., & Sokoloff, L. (1985). Differential effects of electrical stimulation of sciatic nerve on metabolic activity in spinal cord and dorsal root ganglion in the rat. *Proceedings of the National Academy of Sciences USA, 82*, 6010-6013.

Kerppola, T. K., & Curran, T. (1991a). DNA bending by Fos and Jun: the flexible hinge model. *Science, 254*, 1210-1214.

Kerppola, T. K., & Curran, T. (1991b). Fos-Jun heterodimers and Jun homodimers bend DNA in opposite directions: implications for transcription factor cooperativity. *Cell, 66*, 317-326.

Kofman, O., McGlynn, S. M., Olmstead, M. C., & Yeomans, J. S. (1990). Differential effects of atropine, procaine and dopamine in the rat ventral tegmentum on lateral hypothalamic rewarding brain stimulation. *Behavioural Brain Research, 38*, 55-68.

Koprowski, H., Zheng, Y. M., & Heber-Katz, E. (1993). In vivo expression of inducible nitric oxide synthase in experimentally induced neurologic diseases. *Proceedings of the National Academy of Sciences USA, 90,* 3024-3027.

Kouzarides, T., & Ziff, E. (1988). The role of the leucine zipper in the fos-jun interaction. *Nature, 336,* 646-651.

Krukoff, T. L. (1993). Expression of c-fos in studies of central, autonomic and sensory systems. *Molecular Neurobiology, 7,* 247-263.

Li, Y. Q., Takada, M., & Mizuno, N. (1993a). Demonstration of habenular neurons which receive afferent fibers from the nucleus accumbens and send their axons to the midbrain periaqueductal gray. *Neuroscience Letters, 158,* 55-58.

Li, Y. Q., Takada, M., Shinonaga, Y., & Mizuno, N. (1993b). The sites of origin of dopaminergic afferent fibers to the lateral habenular nucleus in the rat. *Journal of Comparative Neurology, 333,* 118-133.

Ma, Q.-P., Zhou, Y., & Han, J.-S. (1993a). Electroacupuncture accelerated the expression of c-fos protooncogene in dopaminergic neurons in the ventral tegmental area of the rat. *International Journal of Neuroscience, 70,* 217-222.

Ma, Q.-P., Zhou, Y., & Han, J.-S. (1993b). Noxious stimulation accelerated the expression of c-fos protooncogene in cholecystokininergic and dopaminergic neurons in the ventral tegmental area. *Peptides, 14,* 561-566.

Macfarlane, D. B. (1954, March 12, 1954). McGill opens vast new research field with brain "pleasure area" discovery. *The Montreal Star,* pp. 1-2.

Malette, J., & Miliaressis, E. (1995). Interhemispheric links in brain stimulation reward. *Behavioural Brain Research, 68,* 117-137.

Margules, D. L., & Olds, J. (1962). Identical "feeding" and "rewarding" systems in the lateral hypothalamus of rats. *Science, 135,* 374-375.

Mark, T. A., & Gallistel, C. R. (1993). Subjective reward magnitude of medial forebrain stimulation as a function of train duration and pulse frequency. *Behavioral Neuroscience, 107,* 389-401.

McFarland, D. J., & Sibley, R. M. (1975). The behavioural final common path. *Philosophical Transactions of the Royal Society of London B, 270,* 265-293.

McGregor, I. S., & Hunt, G. E. (1996). Rewarding brain stimulation induces only sparse c-fos immunoreactivity in dopaminergic neurons. *Society for Neuroscience Abstracts, 22,* 686.

Miliaressis, E., Emond, C., & Merali, Z. (1991). Re-evaluation of the role of dopamine in intracranial self-stimulation using in vivo microdialysis. *Behavioural Brain Research, 46,* 43-48.

Miliaressis, E., Rompré, P. P., Laviolette, P., Philippe, L., & Coulombe, D. (1986). The curve-shift paradigm in self-stimulation. *Physiology and Behavior, 37,* 85-91.

Mitrovic, B., Ignarro, L. J., Montestruque, S., Smoll, A., & Merrill, J. E. (1994). Nitric oxide as a potential pathological mechanism in demyelination: Its differential effects on primary glial cells in vitro. *Neuroscience, 61,* 575-585.

Moghaddam, B., & Bunney, B. S. (1989). Ionic components of microdialysis perfusing solution alters the pharmacological responsiveness and basal outflow of striatal dopamine. *Journal of Neurochemistry, 53,* 652-654.

Morgan, J. I., Cohen, D. R., Hempstead, J. L., & Curran, T. (1987). Mapping patterns of c-fos expression in the central nervous system after seizure. *Science, 237,* 192-197.

Morgan, J. I., & Curran, T. (1986). Role of ion flux in the control of c-fos expression. *Nature, 322,* 552-555.

Morgan, J. I., & Curran, T. (1991). Stimulus-transcription coupling in the nervous system: Involvement of the inducible protooncogenes fos and jun. *Annual Review of Neuroscience, 14,* 421-451.

Morris, S. M., JR., & Billiar, T. R. (1994). New insights into the regulation of inducible nitric oxide synthesis. *American Journal of Physiology, 266,* E829-E839.

Mundl, W. J. (1980). A constant-current stimulator. *Physiology and Behavior, 24,* 991-993.

Murray, B., & Shizgal, P. (1991). Anterolateral lesions of the medial forebrain bundle increase the frequency threshold for self-stimulation of the lateral hypothalamus and ventral tegmental area in the rat. *Psychobiology, 19,* 135-146.

Murray, B., & Shizgal, P. (1996a). Attenuation of medial forebrain bundle reward by anterior lateral hypothalamic lesions. *Behavioural Brain Research, 75,* 33-47.

Murray, B., & Shizgal, P. (1996b). Behavioral measures of conduction velocity and refractory period for reward-relevant axons in the anterior LH and VTA. *Physiology and Behavior, 59,* 643-652.

Murray, B., & Shizgal, P. (1996c). Physiological measures of conduction velocity and refractory period for putative reward-relevant MFB axons arising in the rostral MFB. *Physiology and Behavior, 59,* 427-437.

Nakahara, D., Ozaki, N., Miura, Y., Miura, H., & Nagatsu, T. (1989). Increased dopamine and serotonin metabolism in rat nucleus accumbens produced by intracranial self-stimulation of medial forebrain bundle as measured by in vivo microdialysis. *Brain Research, 495,* 178-181.

Newsome, W. T., & Salzman, D. C. (1993). The neuronal basis of motion perception. *Ciba Foundation Symposium, 174,* 217--246.

Nieuwenhuys, R., Geeraedts, L. M. G., & Veening, J. G. (1982). The medial forebrain bundle of the rat. I. General information. *Journal of Comparative Neurology, 206,* 49-81.

Olds, J. (1958). Self-stimulation of the brain. *Science, 127,* 315-324.

Olds, J., & Milner, P. M. (1954). Positive reinforcement produced by electrical stimulation of septal area and other regions of rat brain. *Journal of Comparative and Physiological Psychology, 47,* 419-427.

Olds, J., & Olds, M. E. (1964). The mechanisms of voluntary behavior. In R. G. Heath (Ed.), *The role of pleasure in behavior* (pp. 23-53). New York, NY: Harper & Row.

Olds, M. E., & Olds, J. (1963). Approach-avoidance analysis of rat diencephalon. *Journal of Comparative Neurology, 120,* 259-295.

Parent, A., Gravel, S., & Boucher, R. (1981). The origin of forebrain afferents to the habenula in rat, cat and monkey. *Brain Research Bulletin, 6,* 23-38.

Paxinos, G., & Watson, C. (1986). *The rat brain in stereotaxic coordinates.* (2nd ed.). Sydney: Academic Press.

Pettit, H. O., & Justice, J. B. (1989). Dopamine in the nucleus accumbens during cocaine self-administration as studied by in vivo microdialysis. *Pharmacology Biochemistry and Behavior, 34,* 899-904.

Phillips, A. G. (1984). Brain reward circuitry: A case for separate systems. *Brain Research Bulletin, 12,* 195-201.

Porrino, L. J., Esposito, R. U., Seeger, T. F., Crane, A. M., Pert, A., & Sokoloff, L. (1984). Metabolic mapping of the brain during rewarding self-stimulation. *Science, 224,* 306-309.

Porrino, L. J., Huston-Lyons, D., Bain, G., Sokoloff, L., & Kornetsky, C. (1990). The distribution of changes in local cerebral energy metabolism associated with brain stimulation reward to the medial forebrain bundle of the rat. *Brain Research, 511,* 1-6.

Rompré, P. P., & Shizgal, P. (1986). Electrophsiological characteristics of neurons in forebrain regions implicated in self-stimulation of the medial forebrain bundle in the rat. *Brain Research, 364,* 338-349.

Routtenberg, A., & Lindy, J. (1965). Effects of the availability of rewarding septal and hypothalamic stimulation on bar pressing for food under conditions of deprivation. *Journal of Comparative and Physiological Psychology, 60,* 158-161.

Sagar, S. M., Sharp, F. R., & Curran, T. (1988). Expression of c-fos protein in the brain: metabolic mapping at the cellular level. *Science, 244,* 1328-1331.

Salzman, C. D., Britten, K. H., & Newsome, W. T. (1990). Cortical microstimulation influences perceptual judgements of motion direction. *Nature, 346,* 174-177.

Salzman, C. D., Murasugi, C. M., Britten, K. H., & Newsome, W. T. (1992). Microstimulation in visual area MT: effects of direction discrimination performance. *The Journal of Neuroscience, 12,* 2331-2355.

Saper, C. B., Swanson, L. W., & Cowan, W. M. (1979). An autoradiographic study of the efferent connections of the lateral hypothalamic area in the rat. *Journal of Comparative Neurology, 183,* 689-706.

Schwarcz, R., Hokfelt, T., Fuxe, K., Jonsson, G., Goldstein, M., & Terenius, T. (1979). Ibotenic acid-induced neuronal degeneration: a

morphological and neurochemical study. *Experimental Brain Research, 37,* 199-216.

Sharp, F. R., Sagar, S. M., & Swanson, R. A. (1993). Metabolic mapping with cellular resolution: c-fos vs. 2-deoxyglucose. *Critical Reviews in Neurobiology, 7,* 205-228.

Sheng, M., & Greenberg, M. E. (1990). The regulation and function of c-fos and other immediate early genes in the nervous system. *Neuron, 4,* 477-485.

Shizgal, P. (1997). Neural basis of utility estimation. *Current Opinion in Neurobiology, 7*(2), 198-208.

Shizgal, P., Bielajew, C., Corbett, D., Skelton, R., & Yeomans, J. (1980). Behavioral methods for inferring anatomical linkage between rewarding brain stimulation sites. *Journal of Comparative and Physiological Psychology, 94,* 227-237.

Shizgal, P., & Conover, K. (1996). On the neural computation of utility. *Current Directions in Psychological Science, 5*(2), 37-43.

Shizgal, P., Conover, K., & Arvanitogiannis, A. (1996). Performance for brain stimulation reward as a function of the rate and magnitude of reinforcement. *Society for Neuroscience Abstracts, 22,* 686.

Shizgal, P., & Matthews, G. (1977). Electrical stimulation of the rat diencephalon: Differential effects of interrupted stimulation on on- and off-responding. *Brain Research, 129,* 319-333.

Shizgal, P., & Murray, B. (1989). Neuronal basis of intracranial self-stimulation. In J. M. Liebman & S. J. Cooper (Eds.), *The neuropharmacological basis of reward* (pp. 106-163). Oxford: Oxford University Press.

Shizgal, P., & Murray, B. (1994). The behavioural adaptation of the collision test: inference of axonal linkage and estimation of conduction velocity from effects of paired-pulse stimulation. *Neuroscience Protocols, 94-010-04-01.*

Shizgal, P., Schindler, D., & Rompré, P.-P. (1989). Forebrain neurons driven by rewarding stimulation of the medial forebrain bundle in the rat: comparison of psychophysical and electrophysiological estimates of refractory periods. *Brain Research, 499,* 234-248.

Simmons, J. M., & Gallistel, C. R. (1994). Saturation of subjective reward magnitude as a function of current and pulse frequency. *Behavioral Neuroscience, 108,* 151-160.

Steininger, T. L., Rye, D. B., & Wainer, B. H. (1992). Afferent projections to the cholinergic pedunculopontine tegmental nucleus and adjacent

midbrain extrapyramidal area in the albino rat. I. Retrograde tracing studies. *Journal of Comparative Neurology, 321,* 515-543.

Stellar, J. R. (1990). Investigating the neural circuitry of brain stimulation reward, *Progress in Psychobiology and Physiological Psychology* (Vol. 14, pp. 235-294). New York: Academic Press.

Stellar, J. R., & Corbett, D. (1989). Regional neuroleptic microinjections indicate a role for nucleus accumbens in lateral hypothalamic self-stimulation reward. *Brain Research, 477,* 126-143.

Stellar, J. R., Hall, F. S., & Waraczynski, M. (1991). The effects of excitotoxin lesions of the lateral hypothalamus on self-stimulation reward. *Brain Research, 541,* 29-40.

Stellar, J. R., Kelley, A. E., & Corbett, D. (1983). Effects of peripheral and central dopamine blockade on lateral hypothalamic self-stimulation: evidence for both reward and motor deficits. *Pharmacology Biochemistry and Behavior, 18,* 433-442.

Stellar, J. R., Waraczynski, M., & Wong, K. (1988). The reward summation function in hypothalamic self-stimulation. In R. M. Church, M. L. Commons, J. R. Stellar, & A. R. Wagner (Eds.), *Quantitative analyses of behavior: Biological determinants of behavior.* (Vol. 7, pp. 31-58). Hillsdale, NJ: Lawrence Erlbaum Associates.

Sutherland, R. J., & Nakajima, S. (1981). Self-stimulation of the habenular complex in the rat. *Journal of Comparative and Physiological Psychology, 95,* 781-791.

Swanson, L. W. (1992). *Brain maps: Structure of the rat brain.* Amsterdam: Elsevier.

Tsacopoulos, M., & Magistretti, P. J. (1996). Metabolic coupling between glia and neurons. *The Journal of Neuroscience, 16,* 877-885.

Tulving, E. (1985). How many memory systems are there? *American Psychologist, 40,* 385-398.

Valenstein, E. S. (1973). *Brain Control.* New York: Wiley.

Veening, J. G., Swanson, L. W., Cowan, W. M., Nieuwenhuys, R., & Geeraedts, L. M. G. (1982). The medial forebrain bundle of the rat. II. An autoradiographic study of the major descending and ascending components. *Journal of Comparative Neurology, 206,* 82-108.

Villalobos, J., & Ferssiwi, A. (1987). The differential descending projections from the anterior central and posterior regions of the lateral hypothalamic area: an autoradiographic study. *Neuroscience Letters, 81,* 95-99.

Waraczynski, M., Conover, K., & Shizgal, P. (1992). Rewarding effectiveness of caudal MFB stimulation is unaltered following DMH lesions. *Physiology and Behavior, 52,* 211-218.

Waraczynski, M. A. (1988). Basal forebrain knife cuts and medial forebrain bundle self-stimulation. *Brain Reseasrch, 438,* 8-22.

Waraczynski, M. A., Ng Cheong-Ton, M., & Shizgal, P. (1990). Failure of amygdaloid lesions to increase the threshold for self-stimulation of the lateral hypothalamus and ventral tegmental area. *Behavioural Brain Research, 40,* 159-168.

Waraczynski, M. A., & Shizgal, P. (1995). Self-stimulation of the MFB following parabrachial lesions. *Physiology and Behavior, 58,* 559-566.

Waxman, S. G. (1977). Conduction in myelinated, unmyelinated, and demyelinated fibers. *Archives in Neurology, 34,* 585-589.

Winn, P. (1991). Excitotoxins as tools for producing brain lesions. In P. M. Conn (Ed.), *Lesions and Transplantation* (Vol. 7, pp. 16-27). San Diego, CA: Academic Press.

Wisden, W., Errington, M. L., Williams, S., Dunnett, S. B., Waters, C., Hitchcock, D., Evans, G., Bliss, T. V. P., & Hunt, S. P. (1990). Differential expression of immediate early genes in the hippocampus and spinal cord. *Neuron, 4,* 603-614.

Wise, R. A. (1980). Action of drugs of abuse on brain reward systems. *Pharmacology, Biochemistry and Behavior, 13, Suppl. 1,* 213-223.

Wise, R. A. (1996). Addictive drugs and brain stimulation reward. *Annual Review of Neuroscience, 19,* 319-340.

Wise, R. A., & Rompré, P.-P. (1989). Brain dopamine and reward. *Annual Review of Psychology, 40,* 191-225.

Yao, D.-L., Komoly, S., Zhang, Q.-L., & Webster deF, H. (1994). Myelinated axons demonstrated in the CNS and PNS by anti-neurofilament immunoractivity and luxol fast blue counterstaining. *Brain Pathology, 4,* 97-100.

Yeomans, J. S. (1975). Quantitative measurement of neural post-stimulation excitability with behavioral methods. *Physiology and Behavior, 15,* 593-602.

Yeomans, J. S. (1979). The absolute refractory periods of self-stimulation neurons. *Physiology & Behavior, 22,* 911-919.

Yeomans, J. S. (1982). The cells and axons mediating medial forebrain bundle reward. In B. G. Hoebel & D. Novin (Eds.), *The neural basis of feeding and reward* (pp. 405-417). Brunswick, ME: Haer Institute.

Yeomans, J. S. (1988). Mechanisms of brain-stimulation reward. *Progress in Psychobiology and Physiological Psychology, 13,* 227-265.

Yeomans, J. S., Kofman, O., & McFarlane, V. (1985). Cholinergic involvement in lateral hypothalamic rewarding brain stimulation. *Brain Research, 329,* 19-26.

Yeomans, J. S., Mathur, A., & Tampakeras, M. (1993). Rewarding brain stimulation: role of tegmental cholinergic neurons that activate dopamine neurons. *Behavioral Neuroscience, 197,* 1077-1087.